Theoretical and experimental investigation of shield effects in microstrip

Dumbell, Keith David

Award date:
1989

Awarding institution:
University of Bath

THEORETICAL & EXPERIMENTAL

INVESTIGATION OF SHIELD EFFECTS IN MICROSTRIP

Submitted by Keith David Dumbell
for the degree of PhD
of the University of Bath
1989.

ProQuest LLC
789 East Eisenhower Parkway
P.O. Box 1346
Ann Arbor, MI 48106-1346

ACKNOWLEDGEMENTS

This work was initiated by Professor T.E.Rozzi and Dr. J.P.McGeehan [1] of the University of Bath. Continuing supervision has been provided by Professor T.E.Rozzi & Dr. S.R.Pennock. I would like to express my gratitude to all of the above for their encouragement and guidance.

Further, I am grateful to the technical staff at the University of Bath for their assistance with the practical work and all of my colleagues particularly for their assistance with computation.

Funding was provided by the MoD (contract RU33/2) and I hope that the material presented herein justifies their support for this research.

[1] Since starting this research J.P McGeehan has been appointed to the chair of Communications at the University of Bristol.

SUMMARY

The shielded microstrip transmission line has been investigated rigorously and the parameters of single strips arbitrarily placed on the substrate and twin strips symmetrically placed have been both investigated theoretically and verified experimentally. Further, the more complex geometry including overlay dielectrics has been programmed and some interesting results presented.

The knowledge of the modes of the continuous line have been used to determine the effects of the step discontinuity in microstrip. The theoretical technique presented is new and capable of dealing with asymmetrically placed strips and cascades - a technique for the computation of the higher order modes scattererd at the step is given. The experimental techniques used to verify these results have married the well known techniques of calibration with the recently available time domain techniques which for the first time enable the parameters of the step to be measured directly.

Whilst the theoretical techniques used may be unsuitable for direct programming of CAD packages, they do provide a means for revising the widely used curve fit formulae which are shown to be in error.

CONTENTS

LIST OF SYMBOLS

Where possible unified symbols have been used throughout and are defined here. However, changes may have been necessary and symbols may be redefined in the text.

$\underline{a}_x$,$\underline{a}_y$,$\underline{a}_z$: Unit vectors in the specified direction.

$\underline{e}_i$,$\underline{h}_i$: Transverse electric/magnetic fields of mode i. (superscript may define the guide).

k ,k_0 ,k_n : Wavenumbers.

n : Summation variable of spectral components.

$\underline{n}$: Unit normal to surface.

$\underline{\underline{s}}$: Reciprocity multiplyer for guided wave.

u ,v : Alternative coordinate system.

v_p ,v_c : Phase velocity and velocity of light in free space.

x ,y ,z : Rectangular coordinates.

C ,C_0 : Static capacitance of transmission line per unit length with/without dielectric.

C_p ,C_{pq} : Mode coupling coefficients.

E_x ,E_y ,E_z : Electric field components for either of the regions. (superscript may define the region).

G ,$\underline{\underline{G}}$: Greens functions.

G_{xx} ,G_{xz} / G_{zx} ,G_{zz} : Scaled Impedance terms.

H_x ,H_y ,H_z : Magnetic field components for either of the regions. (superscript may define the region).

H_{xx} ,H_{xz} / H_{zx} ,H_{zz} : Scaled Admittance terms.

I : Total longitudinal current.

I_n : Arbitrary constant of the index.

$I1 - I7$: Standard integrals.

J_i : Bessel Functions (of order i).

J_x , J_z : x,z directed current density on the microstrip.

K_{xx}, K_{xz}, K_{zx}, K_{zz} : Element of the matrix of coefficients.

L : Inductance per unit length.

N_x , N_z : Co-ordinate transformation scaling factors.

P : Power (determined by the complex Poynting vector).

P_i : Legendre polynomials (of order i).

R : Reading of ideal network analyser.

S : Guiding cross section.

S_{11}, S_{12}, S_{11}, S_{12} : Scattering parameters.

T_i : Chebyshev polynomials (of order i).

V : Potential.

V_n : Arbitrary constant of the index.

X_n , Y_n : The n'th characteristic equation of the LSE,LSM modes of the slab loaded guide.

Xl_n, Yl_n : The n'th characteristic equation of the LSE,LSM modes of the layered slab loaded guide.

Y_{TE}, Y_{TM} : Wave admittance for TE,TM modes. (superscript may specify the region).

Y_e , Y_h : Input admittance of short circuit transformed along a length of TE,TM transmission line. (superscript may specify the region).

$Y_e(in)$: Input admittance of short circuit layered region (TE).

$Y_h(in)$: Input admittance of short circuit layered region (TM).

Y_{in} : Input admittance.

Y_{xx} ,Y_{xz} / Y_{zx} ,Y_{zz} : Admittance elements.

Z_0 : Characteristic impedance.

Z_{xx} ,Z_{xz} / Z_{zx} ,Z_{zz} : Impedance elements.

α : Attenuation constant.

β : Phase constant.

γ : Propagation constant.

ε ,ε_0 ,ε_r : Permittivity and free space value/ relative value.

$\varepsilon(eff)$: Effective permittivity.

η_n : Neumann's number.

∂ : Partial derivative.

δ_n : Kronecker Delta.

θ_n : Angular measurement.

ω : Angular frequency.

μ ,μ_0 ,μ_r : Permeability and free space value/ relative value.

ρ : Charge density.

λ : Wavelength.

ψ ,ψ_e ,ψ_h : Scalar potentials.

$\underline{\xi}$,$\underline{\xi}_1$: Transverse electric field distributions.

$\underline{\Psi}_i$: Transverse electric field basis functions.

Φ : Variational expression.

Γ : Gamma function.

Γ ,Γ_1 ,Γ_2 : Value for reflection of standards.

$\underline{\Pi}_e$,$\underline{\Pi}_h$: Herzian potentials of electric/magnetic type.

Δ : Coefficient implying small value.

∇_t : Differential operator in the transverse plane.

∇_t^2 : Two dimensional Laplacian operator.

INTRODUCTION

The subject of this thesis is the shielded microstrip transmission line. The simplest of the structures considered is shown below.

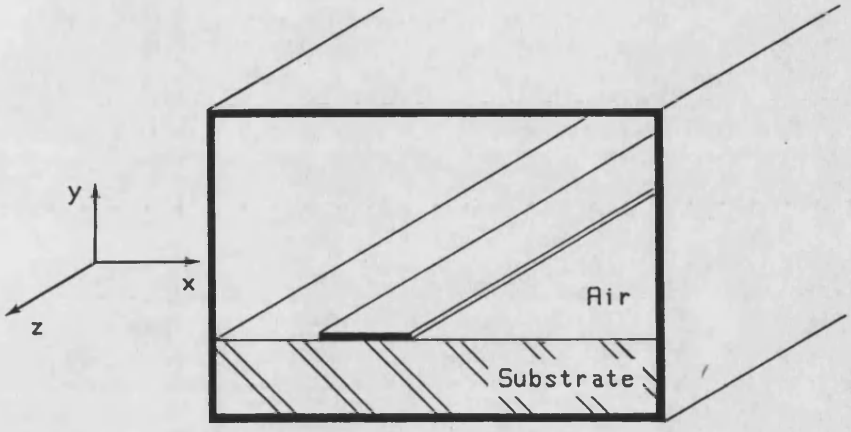

There are variations on this basic structure such as the covered microstrip which may be considered to be an infinitely wide version of the above and also the open microstrip when all of the shielding in the above is removed. The physical properties of these is fundamentally different because of the existence of radiating modes and as such are beyond the scope of this work. However, certain mathematical similarities do exist and the development of the present analysis frequently uses techniques devised for these and other related structures particularly finline.

The basic principles for the analysis of the continuous line are well known although it is only recently that the existence of complex modes in this structure have been reported. This thesis thus begins by analysing the continuous line (chapter 3) using the information derived from the mass of information available; a summary of which is presented in chapters 1 & 2. Properties of asymmetric microstrip lines are considered as well as the effect of dielectric overlay.

Although the analysis used is readily available, little attention seems to be paid to these effects in computer aided design packages for example Super Compact[1] allows only the cover height to be varied and Touchstone[2] neglects the effect of shielding all together. This is surprising since all commercially available microwave devices will be packaged in some form of casing both to protect them both from electromagnetic interference and other environmental problems.

To ensure that the analysis is proceeding along the right tracks a test jig has been developed (chapter 4) to measure the parameters of the line. In the first instance all that is possible is the determination of the propagation parameters of the line, based on the resonance principle.

The challenge, once the elementary properties of the line have been determined and verified experimentally, is to correctly characterise the discontinuities that occur. Typical discontinuities which occur are the open circuit, the gap, the step in width and also the cascaded step. The main investigation has focused on the step in width (chapter 5). Although this may appear to be very restricted it is clear that a correct understanding of this discontinuity, which is in principle the junction between two dissimilar guiding structures may be applied directly to the other discontinuities merely by replacing the eigenmodes of one of the guides with those of the new structure. Indeed it may be shown that, for the theoretical technique presented, with the minimal of computational effort,it is possible to analyse the discontinuity that arises between a single line feed to a coupled line which arises frequently in coupler design and filter elements.

---

[1] Super Compact is a trade name of Compact Software

[2] Touchstone is a trade name of EESOF.

As a further challenge an attempt has been made to characterise the step experimentally (chapter 6). The easiest discontinuity to verify is clearly the open circuit since this may be determined using two open circuited resonators. The step discontinuity presents many problems, however; no such simple techniques are possible and most attempts to use calibration, for example, have failed to overcome the considerable de-embedding errors which arise during measurement. Thus a new technique has had to be devised.

This technique,which is essentially a calibration to the microstrip plane, incorporates a time domain analysis in the first instance to compensate for the inadequacy of the matched terminal loads that are available and secondly to minimise the effects of connector non-repeatability. By using this method the full two port parameters of the step have been determined. Although once again the attention has focussed on this one specific case it is shown that the analysis is quite general and could be used not only for the alternative microstrip discontinuities but could equally well be adopted for other forms of transmission line.

CHAPTER ONE

REVIEW OF THE STATIC METHOD OF ANALYSIS

The fundamental mode of a two conductor transmission line, which includes microstrip, is essentially a transverse electromagnetic wave (TEM): the assumptions being that the medium surrounding the conductors is homogeneous and that any losses in the system are assumed to be negligible [1]. Even if this is not so it may still be possible to approximate the true mode of propagation to a TEM mode. This is most important since this type of mode may be determined from an equivalent two dimensional electrostatic problem which may be approached by considering either Laplace's or Poisson's equation in the transverse plane.

The parameters of the transmission line may thus be determined. For conductors in a homogeneous medium, the phase velocity 'v_p' may be written in terms of the material constants and may also be given in terms of the capacitance per unit length 'C' and the inductance per unit length 'L' from transmission line theory [2]:-

$$v_p = \frac{v_c}{\sqrt{\mu_r \varepsilon_r}} \qquad \left\{ = \frac{1}{\sqrt{LC}} \right\} \tag{1.1}$$

where v_c is the velocity of light in vacuum. The characteristic impedance 'Z_0' may therefore, be expressed as:-

$$Z_0 = \left(v_p \, C \right)^{-1} \qquad \left\{ = \sqrt{\frac{L}{C}} \right\} \tag{1.2}$$

For conductors in a non-homogeneous medium the above may be modified by defining the effective permittivity '$\varepsilon_r(\text{eff})$' as:-

$$\varepsilon_r(\text{eff}) = \frac{C}{C_0} \tag{1.3}$$

where C_0 is the capacitance of the equivalent line in free space.

This definition may be interpreted as that value of relative permittivity of a fictitious dielectric which when completely surrounding the conductors gives the same value of capacitance as the non-homogeneous medium. This value of effective permittivity may now be used instead of ε_r in (1.1) to give an approximation for the phase velocity which will, however, be exact in the limit of low frequency.

Similar expressions may also be determined for a symmetric pair of lines assuming that the lines either have equal charges (even mode) or opposite charges (odd mode). This is a specific case of a system of N conductors which, in general, will have N-1 basic modes of operation [1].

Depending on the geometry of the conductor system there are certain preferred methods for evaluating the capacitance of the transmission line and hence the line parameters. A few of these methods are outlined in the next few sections.

1.1 Conformal Mapping.

In general, the solution of Laplace's equation in the x,y plane will not be easy unless the conductors follow the constant co-ordinate curves. However, the potential in the x,y co-ordinate system, will under conformal mapping to a new co-ordinate system, still satisfy Laplace's equation [3]. Thus a conformal mapping may be used so as to simplify the boundary conditions.

Cohn analysed the stripline illustrated in fig.(1.1a). Here the upper and lower plates are assumed to be held at zero potential and may be assumed to extend to infinity. Because of symmetry only one quadrant need be considered. The area may be mapped to the half plane and subsequently to a closed rectangle having electric/magnetic boundaries. The evaluation of the capacitance of this rectangle is straightforward whilst the appropriate dimensions are a function of the conformal mapping and are given in terms of elliptic integrals. Additionally Cohn [4] considered coupled stripline 'fig.(1.1b)'. Again the symmetry, which is different for the odd & even modes, leads to an analysis similar to the above.

The capacitance of a strip over an infinite conducting ground plane may be determined from that of a parallel plate capacitor an analysis of which is given in [5]. Symmetry of the parallel plate capacitor allows an electric wall to be placed midway between the plates giving the same boundary value problem as the open microstrip line. The result in both cases is given in terms of elliptic integrals.

Wheeler [6] saw the need for an approximate technique giving 'slide rule accuracy'. Using several approximations he arrives at a result in terms of hyperbolic/exponential functions. In a later contribution [7] he also considered the case of microstrip over a dielectric introducing the approximate 'filling factor'.

1.2 Variational Method.

The variational method, which has a variety of forms, was first introduced by Schwinger in the analysis of waveguide discontinuities [8]. The features of this technique, as applied to two conductor transmission lines are described below.

If the region surrounding a conductor system, see fig.(1.2), is homogeneous then the potential 'ϕ' in this region will satisfy Laplace's equation:-

$$\nabla_t^2 \phi = \frac{\partial^2 \phi}{\partial x^2} + \frac{\partial^2 \phi}{\partial y^2} = 0 \qquad (1.4)$$

and subject to this relationship, the energy stored in the electric field per unit length is given by:-

$$W_e = \frac{1}{2} \varepsilon \iint \left(\left(\frac{\partial \phi}{\partial x} \right)^2 + \left(\frac{\partial \phi}{\partial y} \right)^2 \right) dx\, dy = \frac{1}{2} C V^2 \qquad (1.5)$$

having zero first order variation in the functional form of ϕ. Thus a variational expression for the capacitance of the line is:-

$$C = \varepsilon \frac{\iint \left(\nabla_t \phi \cdot \nabla_t \phi \right) dx\, dy}{V^2} \qquad (1.6)$$

The calculated value of C, when an approximate value for $\nabla_t \phi$ is used, is always too large i.e. it is an upper bound to the true value. Note that $\nabla_t \phi$ may be derived from an assumed aperture electric field or an assumed charge distribution. In practice it is possible to define a functional form for the approximate solution which has several parameters and a more accurate solution is obtained by treating each of these parameters as independent variables and minimising (1.6) with respect to these parameters i.e. differentiating with respect to each of the parameters in turn and equating the results to zero.

The dual of this approach uses the Green's function technique to give a lower bound to the capacitance. For the electrostatic problem characterised by Poisson's equation:-

$$\nabla_t^2 \psi = \frac{1}{\varepsilon} \rho(x',y') \qquad (1.7)$$

it is possible to define a Green's function given by:-

$$\nabla_t^2 G = - \frac{1}{\varepsilon} \delta(x - x')\delta(y - y') \qquad (1.8)$$

so that by superposition the potential, and in particular the potential 'V' on one conductor, may be written as:-

$$\psi(x,y) = \int G(x,y|x',y')\, \rho(x',y')\, dl' \quad \left\{ = V \ (x,y \text{ on } S) \right\} \qquad (1.9)$$

From this relationship the line capacitance may be determined:-

$$\frac{1}{C} = \frac{\int\int G(x,y|x',y')\rho(x,y)\rho(x',y') \ dl \ dl'}{\left[\int \rho(x,y) \ dl \right]^2} \qquad (1.10)$$

The expression may be shown to be stationary for arbitrary first order variations in the functional form of ρ and further since the Green's function is symmetric the integral will always be positive and hence the calculated value of capacitance, when an approximation to ρ is used will always be less than the true value i.e. the analysis gives a lower bound to the true value. Note again that here the charge distribution may be determined from an assumed aperture electric field.

This approach has been applied to stripline [1],but the flexibility of the technique allows more complicated systems to be considered. For example, Yamahita & Mittra [9] have analysed the open microstrip line by assuming a charge density distribution of the form $|x|$. Later Yamashita [10] also considered the effect of covering, recognising the importance of correctly representing the charge distribution.

The actual charge distribution 'ρ(x)' on an isolated conducting strip of width w may be determined by conformal mapping [11]:-

$$\rho(x) = \rho(0) \left[1 - \left[\frac{2.x}{w} \right]^2 \right]^{-1/2} \qquad (1.11)$$

The important feature of the above is that the charge becomes infinite at the edges. Yamashita used the approximation to this:-

$$\rho(x) = \rho(0) \left[1 + \left[\frac{2.x}{w} \right]^3 \right] \qquad (1.12)$$

principally because this form facilitated the numeric computation. More complicated structures could also be analysed: Yamashita & Yamazika [12] considered the effect of the strip embedded in a dielectric sheet and later Yamashita & Atsuki [13] considered the effect of shielding walls and multiple dielectric layers and gave a lower bound to the capacitance of this structure, (an analysis for the upper bound was subsequently presented by Araki & Naito [14]).

Note that in the above analyses the Green's function was taken to be the solution of Poisson's equation (1.7) where the value of ε is taken to be the value of the dielectric constant at the consideration point. The validity of this choice has subsequently been discussed by Santos [15] and later by Kobayashi [16] and it was confirmed that this does lead to the required symmetric form of Green's function.

The flexibility of these approaches are such that they have been used by Horno [17] for single strips on anisotropic substrates and by Horno & Marqués [18] for coupled microstrips on double anisotropic substrates. Further, Krage & Haddad [19] have provided an analysis for the case of coupled strips and Das & Prasad [20] have considered 'coplanar as well as non-coplanar strips of equal & unequal widths arbitrarily located between ground planes and filled with layered substrates', using this method.

1.3 Integral Equation Methods.

Recalling equation (1.9) giving the potential of one conductor in terms of the Green's function it is clear that this is a Fredholm integral equation of the first kind and there are many standard techniques for obtaining approximate solutions for this type of equation [21].

In particular, Silvester [22] has determined the Green's function for the dielectric and conductor boundary of an open microstrip using the method of images. The microstrip, which need not be considered to be infinitely thin, is then split into segments each having an unknown charge. When used in the equation (1.9) the resulting set of inhomogeneous equations may be solved by conventional matrix techniques. Yamashita & Atsuki [23] having determined the Green's function for the shielded microstrip line, for use in the variational technique, were able to consider the effect of finite strip thickness in this structure using a technique similar to Silvester's.

Bryant & Weiss [24] also considered the open microstrip line but used an alternative formulation for the Green's function specifically for a source at the air/dielectric interface to give a Fredholm integral equation of the second kind. By splitting the microstrip into segments this equation could then be solved by an iterative procedure although it was reported that convergence of this method was not always guaranteed. This method was also suitable for the evaluation of the coupled line parameters and particular emphasis was placed on this.

1.4 Finite Difference / Finite Element Techniques.

The finite difference and finite element techniques are essentially numerical methods for evaluating the cross sectional field distribution and hence the parameters of the transmission line.

An upper bound for the line capacitance may be determined from the variational expression (1.6). The corresponding lower bound may be determined , it has been found, by using the duality of the magneto-static potential. Both upper and lower bounds for the line capacitance have been determined by Sinnott [25] using the finite difference technique and by Shepherd & Daly [26] using the finite element technique. A fuller description of the suitability of these techniques can be found in the references in the above papers.

References.

[1]... Collin, R.E.. "Field Theory of Guided Waves."
McGraw-Hill Book Co., New York 1960.

[2]... Edwards, T.C.. "Foundations for Microstrip Circuit Design."
John Wiley & Sons Ltd., 1981.

[3]... Churchill, R.V.. "Introduction to Complex Variables & Applications."
McGraw-Hill Book Company Inc., New York 1948.

[4]... Cohn, S.B.. "Shielded Coupled-Strip Transmission Line."
IEEE Trans. MTT-3, No. 5, October 1955, pp. 29-38.

[5]... Palmer, H.B.. "The Capacitance of a Parallel Plate Capacitor by the Schwartz Christoffel Transformation."
Trans. Amer. Inst. Elect. Engrs., Vol-56, 1937, pp. 363-366.

[6]... Wheeler, H.. "Properties of Parallel Wide Strips by Conformal Mapping."
IEEE Trans. MTT-12, May 1964, pp. 280-289.

[7]... Wheeler, H.. "Transmission Line Properties of Parallel Strip Separated by a Dielectric Sheet."
IEEE Trans. MTT-13, No. 2, March 1965, pp. 172-185.

[8]... Saxon, D.S.. "Notes on Lectures by Julian Schwinger."
Mass. Inst. Technology, February 1945.
Schwinger, J.. "Discontinuities in Waveguides."
MIT lecture notes,edited by Saxon, D.S.. Gordon & Breach 1968.

[9]... Yamashita, E. & Mittra, R.. "Variational Methods for the analysis of Microstrip Lines."
IEEE Trans. MTT-16, No. 4, April 1968, pp. 251-256.

[10].. Yamashita, E.. "Variational Method for the analysis of Microstip-Like Transmission Lines."
IEEE Trans. MTT-16, No. 8, August 1968, pp. 529-535.

[11].. Hallen, E.. "Electromagnetic Theory."
London: Chapman & Hall, 1962.

[12].. Yamashita, E. & Yamazika. "Parallel strip Line Embedded in or Printed on a dielectric Sheet."
IEEE Trans. MTT-16, No.11, November 1968, pp. 972-973.

[13].. Yamashita, E. & Atsuki, K.. "Strip Line with Rectangular outer conductor and Three Dielectric Layers."
IEEE Trans. MTT-18, No. 5, May 1970, pp. 238-244.

[14].. Araki, K. & Naito, Y.. "Upper bound Calculations on Capacitance of Microstrip Line using Variational Method & Spectral Domain Approach.
IEEE Trans. MTT-26, No. 7, July 1978, pp. 506-512.

[15].. Santos dos, A.F. & Vieira, V.R.. "The Green's Function for Poisson's Equation in a two dielectric Region."
IEEE trans. MTT-20, No.11, November 1972, pp. 777.

[16].. Kobayashi, M.. "Green's Function in a Region with inhomogeneous Isotropic dielectric Media."
IEEE Trans. MTT-23, No. 9, September 1975, pp. 762-765.

[17].. Horno, M.. "Quasi Static Characteristics of Microstrip on Arbitrary Anisotropic Substrate."
Proc. IEEE Vol.86, pp. 1033-1034 Aug. 1980.

[18].. Horno, M. & Marqués, R.. "Coupled Microstrips on Double Anisotropic Substrates."
IEEE Trans. MTT-32, No. 4, April 1984, pp. 467-470.

[19].. Krage, M.K. & Haddad, G.I.. "Characteristics of Coupled Mode Transmission Lines II:- Evaluation of Coupled Line Parameters.
IEEE Trans. MTT-18, No. 4, April 1970, pp. 222-228.

[20].. Das, B.N. & Prasad, K.V.S.V.R.. "A Generalised Formulation for Electromagnetically Coupled StripLines."
IEEE Trans. MTT-32, No.11, November 1984.

[21].. Moiseiwitsch, B.L.. "Integral Equations."
Longman Inc., New York 1977.

[22].. Silvester, P.. "TEM wave Propagation of Microstrip Transmission Lines and of Coupled Pairs of Microstrip Lines."
Proc. Inst. Elec. Eng., Vol.-115, Jan 1968, pp.43-48.

[23].. Yamashita, E. & Atsuki, K.. "Analysis of Thick Strip Transmission Lines."
IEEE Trans. MTT-19,No. 1, January 1971, pp. 120-122.

[24].. Bryant, T.G. & Weiss, J.A.. "Parameters of Microstrip Transmission Lines and of Coupled Pairs of Microstrip Lines."
IEEE Trans. MTT-16, No.12, December 1968, pp. 1021-1027.

[25].. Sinnott, D.H.. "Upper & Lower bounds on the Characteristic Impedance of TEM mode Transmission Lines with Curved Dielectric Boundaries."
IEEE Trans. MTT-16, No.11, November 1968, pp. 971-972.

[26].. Shepherd, P.R. & Daly, P.. "Modelling and Measurement of Microstrip Transmission-Line Structures."
IEEE Trans. MTT-33, No.12, December 1985, pp. 1501-1506.

Figures. Page.

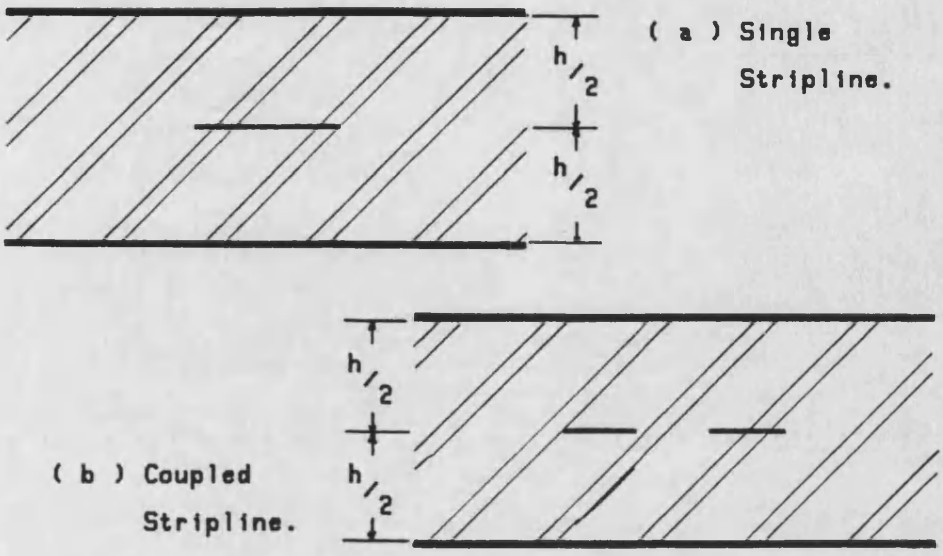

Single & Coupled Striplines.

Fig.(1.1)

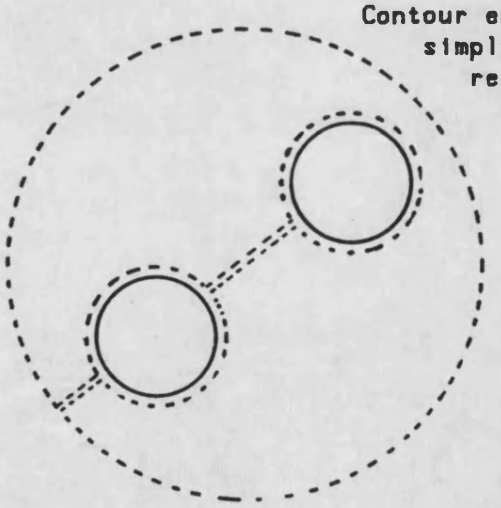

Laplace's scalar potential for a two conductor system.

Fig.(1.2)

CHAPTER TWO

DEVELOPMENT OF THE FULL WAVE ANALYSIS

The presence of the dielectric in a microstrip transmission line allows the fundamental mode to be TEM only at zero frequency. The effective permittivity thus becomes a function of the frequency and may be defined in terms of its phase velocity:-

$$\varepsilon_r(eff) = \left(\frac{v_c}{v_p}\right)^2 \qquad (2.1)$$

In order to determine the phase velocity for different frequencies it is essential to provide a full wave analysis for the microstrip line to account for the hybrid nature of the field.

Further, the fundamental mode is not the only mode of propagation on the line. Here it is necessary to distinguish between the case of an open line and the shielded structure; for the open line there will be a continuous spectrum of radiating modes in addition to the fundamental mode whilst for the shielded line there will be a discrete spectrum of higher order modes in addition to the fundamental.

Although the two structures described above are physically dissimilar, the mathematical techniques used for the analysis of these structures are alike in many respects. Further, analogies may be drawn between the case of slotline and open microstrip and between finline and boxed microstrip such that the present analysis for the microstip line originates from developments in the analysis of all of the above.

As for the static analysis of the previous chapter, there are several preferred methods of analysis and these will be reviewed.

2.1 Finite Difference / Finite Element Methods.

Whereas, assuming quasi-TEM operation, these numerical methods provided only an alternative to the already established methods of derivation of the microstrip line parameters, the finite difference / finite element methods were the first methods used in describing the hybrid nature of both the fundamental mode and higher order modes of microstrip.

For example, Hornsby & Gopinath [1] determined the parameters of the fundamental mode using finite difference methods. The method was also capable of evaluating the parameters of higher order modes as indeed was shown by Corr & Davis [2] using a graded finite difference mesh although problems of spurious modes have been reported.

Meanwhile finite element techniques were used by Daly [3] and both fundamental & higher order modes were determined although, it would appear that one of the modes was in error.

2.2 Integral Equation Methods.

There are many variations which come under the general context of an integral equation technique. Consider first the method used by Denlinger [4] in the solution of the open microstrip line. Here the field is expanded as a linear combination of TE-to-z and TM-to-z mode fields (a technique common to most methods) which are required to satisfy the boundary conditions at the air/substrate interface:-

$$E_x^{(1)}(x,0) = E_x^{(2)}(x,0) \qquad (2.2a)$$

$$E_z^{(1)}(x,0) = E_z^{(2)}(x,0) \qquad (2.2b)$$

$$-H_x^{(1)}(x,0) + H_x^{(2)}(x,0) = J_z \qquad (2.2c)$$

$$H_z^{(1)}(x,0) - H_z^{(2)}(x,0) = J_x \qquad (2.2d)$$

where J_x and J_z are the longitudinal and transverse current densities at the interface. Imposing the following conditions on the strip:-

$$E_z(x,0) = 0 \qquad (\ x \text{ on strip}\ ) \qquad (2.3a)$$

$$\frac{dH_z(x,0)}{dy} = 0 \qquad (\ x \text{ on strip}\ ) \qquad (2.3b)$$

results in a pair of coupled integral equations in terms of J_x & J_z. The form of J_z is at first taken to be the singular form derived from the charge distribution given by (1.11):-

$$J_z = J_{zo}\left[1 - \left[\frac{2.x}{w}\right]^2\right]^{-1/2} \qquad (2.4)$$

and later is derived from the approximate form for the charge distribution used by Yamashita (1.12):-

$$J_z = J_{zo}\left[1 + \left[\frac{2.x}{w}\right]^3\right] \qquad (2.5)$$

which facilitates the computation.

For the transverse current distribution use is made of the conservation of charge relationship. An approximation to J_x was determined using data for the charge distribution on the strip with and without the substrate present which was evaluated using the method of Bryant & Weiss [1,24]. An analytical expression which closely describes this distribution was found:-

$$J_x = J_{xo} \begin{cases} \sin\left\{\frac{\pi}{0.7\,w}\,x\right\} & |x| \leq 0.8\,\frac{w}{2} \\ \cos\left\{\frac{\pi}{0.2\,w}\,x\right\} & 0.8\,\frac{w}{2} < |x| \leq \frac{w}{2} \end{cases} \qquad (2.6)$$

the fourier transform of which may be simply determined. Upon assuming these distributions in the coupled integral equations the resulting pair of homogeneous equations could be solved by setting the determinant of the matrix of coefficients of the unknown current amplitudes (J_{xo}, J_{zo}) equal to zero.

A much more mathematically involved technique was used by Mittra & Itoh [5] using a singular integral equation technique for the shielded structure. As before the technique requires the solution of a set of homogeneous simultaneous equations but where the accuracy of the technique may be systematically improved by increasing the number of independent parameters in 'the expansion'.

Although excellent results are obtained for both the fundamental and higher order modes of the shielded line it is not clear how the physical fields relate to the mathematical expressions i.e. the technique requires 'some intricate mathematical manipulations'. One further drawback of the method is the need to evaluate certain integrals numerically. Neither of these problems, however, are present in the method used by Krage & Haddad [6].

In this method, in which coupled strips were also considered, the fields are expanded in terms of the currents on the strip which, it is noted, admit to expansions in terms of a complete set of basis functions over the interval of the strip. The coefficients in this expansion may then be determined by requiring that the tangential components of electric field be zero at equally spaced points on the strip. The resulting set of homogeneous equations so formed would have a non-trivial solution if and only if the determinant of the matrix of coefficients is zero, so that the propagation constants, for which the above condition is true, may then be determined by iteration.

The form of expansion for the transverse current 'J_x' was chosen so that the current was zero at the strip edges:-

$$J_x = \sum_{m=0}^{M} a_m \sin\left\{\frac{m.\pi}{(w/2)}\, x\right\} \qquad (2.7)$$

and the transverse current 'J_z' chosen to be:-

$$J_z = \sum_{m=0}^{N} b_m P_m\left\{\frac{2.x}{w}\right\} \qquad (2.8)$$

where P_m are the Legendre polynomials. Typically, the order of the expansions were taken to be 2,4 for the x,z directed currents respectively. Even then it was found that the procedure may fail to give a zero determinant where a root should occur and was attributed to the inadequacy of the set of expanding functions to correctly account for the singularity in the current at the edge of the strip.

This effect was considered by Yamashita & Atsuki [7]. Here the electromagnetic field is expanded in terms of the currents and electric fields at the air/dielectric interface.

However, the method of solution is based on considering the interface to be divided into regions where the transverse electric field is defined to be constant over the individual subregions in the aperture and likewise for the longitudinal current on the strip. By enforcing the conditions that the current must be zero in the aperture and the transverse electric field zero over the strip, the resulting set of homogeneous simultaneous equations give a non-trivial solution only for the correct assumed value of propagation constant.

The method may be improved by increasing the number of regions and further by dividing the regions unequally with a greater density in the vicinity of the edge of the strip in order to take account of the singularity in the electromagnetic field. The adaptation of the technique to other types of planar striplines was demonstrated.

2.3 Galerkin's Method.

Before explaining the procedure based on Galerkin's method it is necessary to clarify the use of the Spectral Domain Approach. In general the analysis for laterally open structures must be performed using the Fourier Transform of field components with respect to x. If the structure to be analysed is not open, then the Fourier transform may be interpreted as the finite Fourier Transform. A clarification is given by Jansen [8] in his review paper.

Galerkin's method, which is essentially a method of moments [9], was first proposed for use for the microstrip problem by Itoh & Mittra [10] having successfully used a similar technique for slotline [11]. The basic method for formulating the electromagnetic problem is similar to the method used by Denlinger, however, rather than applying the final boundary conditions in the space domain, the condition is imposed in the Fourier Transform domain instead.

The method of analysis may be more clearly explained by considering a later contribution for the shielded structure by the same authors [12] using a method which is essentially that used today. It is important to note that instead of imposing conditions (2.3) the following requirements are made:-

$$E_x(x,0) = 0 \qquad (x \text{ on strip}) \tag{2.9a}$$

$$E_z(x,0) = 0 \qquad (x \text{ on strip}) \tag{2.9b}$$

This change is important because it gives rise to an integral representation which is self-adjoint.

The Fourier Transforms of the longitudinal electric field and the transverse electric field in the plane of the air/dielectric interface are related to the Fourier Transforms of the x,z directed currents in the strip typically in the form:-

$$\begin{bmatrix} Z_{xx} & Z_{xz} \\ Z_{zx} & Z_{zz} \end{bmatrix} \begin{bmatrix} \tilde{J}_x \\ \tilde{J}_z \end{bmatrix} = \begin{bmatrix} \tilde{E}_x \\ \tilde{E}_z \end{bmatrix} \qquad (2.10)$$

where, for this specific example the fourier transform donoted by (~) is taken to be:-

$$\tilde{A} = \int_{-a/2}^{a/2} A \cdot \exp\left\{ j \frac{n.\pi}{a} x \right\} \qquad (2.11)$$

with the microstrip enclosure symmetric about the x axis and having width a. The current components are now expanded as a set of known basis functions as follows:-

$$\tilde{J}_x = \sum_{m=0}^{M} a_m \tilde{J}_{xm} \qquad \tilde{J}_z = \sum_{m=0}^{M} b_m \tilde{J}_{zm} \qquad (2.12)$$

where a_m and b_m are, as yet, undetermined weighting coefficients. These basis functions are chosen so that their inverses are non-zero on the strip but zero elsewhere.

After using these expansion in (2.10) the innerproducts of the individual basis functions 'J_{xm}' and 'J_{zm}'may be taken. Since the transverse electric field must be zero over the region of the strip and since the current will be zero elsewhere the result of this operation will be a system of homogeneous equations.

These equations may now be written:-

$$0 = \sum_{m=0}^{M} a_m K_{xx}(i,m,\gamma) + \sum_{m=0}^{N} b_m K_{xz}(i,m,\gamma) \qquad (i=0,..,M) \qquad (2.13a)$$

$$0 = \sum_{m=0}^{M} a_m K_{zx}(i,m,\gamma) + \sum_{m=0}^{N} b_m K_{zz}(i,m,\gamma) \qquad (i=0,..,N) \qquad (2.13b)$$

where the elements of the matrix of coefficients are given as:-

$$K_{xx}(i,m,\gamma) = \sum_{n} \tilde{J}_{xi} \; Z_{xx}(n,\gamma) \; \tilde{J}_{xm} \qquad (2.14a)$$

$$K_{xz}(i,m,\gamma) = \sum_{n} \tilde{J}_{xi} \; Z_{xz}(n,\gamma) \; \tilde{J}_{zm} \qquad (2.14b)$$

$$K_{zx}(i,m,\gamma) = \sum_{n} \tilde{J}_{zi} \; Z_{zx}(n,\gamma) \; \tilde{J}_{xm} \qquad (2.14c)$$

$$K_{zz}(i,m,\gamma) = \sum_{n} \tilde{J}_{zi} \; Z_{zz}(n,\gamma) \; \tilde{J}_{zm} \qquad (2.14d)$$

The summation arises as a consequence of the shielding whereas for the laterally open structure this would be an integration. One can verify, on applying Parseval's theorem, that the right hand sides of equations (2.10) are indeed eliminated by this procedure. The simultaneous equations may now be solved by setting the determinant of the matrix of coefficients equal to zero.

This method is essentially that used by Jansen [13] in his analysis of the covered microstrip. In this contribution particular emphasis was placed on the computational considerations of the evaluation of the matrix equation. There are three particular features which are of significance. First, the currents / electric fields are normalised so as to make the elements of the matrix to be evaluated entirely real and symmetrical. Secondly, an integral relationship is introduced between the basis functions representing the x & z components of the strip current and thirdly, the representations chosen for the

currents take account of the singularity occuring at the strip edges. The extra efficiency of these factors enable many results to be given for both the fundamental and higher order modes and further results are given for the case of coupled strips which have also been considered.

As a specific example of how Galerkin's method could be used for other structures, consider the analysis of the bilateral Finline by Schmidt [14]. With the exception that different boundary conditions apply in the expansion of the electromagnetic field in the enclosure (a magnetic wall is assumed along the line of symmetry between the two metallisation layers) the method of analysis is analogous to that of the shielded microstrip. Indeed, for the air/dielectric interface, equations (2.10) could be said to apply. However, for the finline structure the following are determined:-

$$\begin{bmatrix} Y_{xx} & Y_{xz} \\ Y_{zx} & Y_{zz} \end{bmatrix} \begin{bmatrix} \tilde{E}_x \\ \tilde{E}_z \end{bmatrix} = \begin{bmatrix} \tilde{J}_x \\ \tilde{J}_z \end{bmatrix} \qquad (2.15)$$

application of Galerkin's method now requires an expansion of the electric field in the slot viz.:-

$$\tilde{E}_x = \sum_{m=0}^{M} c_m \tilde{E}_{xm} \qquad \tilde{E}_z = \sum_{m=0}^{M} d_m \tilde{E}_{zm} \qquad (2.16)$$

& the propagation constants may be evaluated as before.

2.3.1 Equivalent Transmission Line Model.

In his analysis of generalised printed transmission lines Itoh [15] resolves the similarities in all of the previous formulations. Using the equivalent transmission line in the y direction by expanding the general field as a combination of TE-to-y and TM-to-y fields and also using the spectral domain approach he recognised that from:-

$$E_y(x,y)\, e^{-j\beta z} = \frac{1}{2.\pi} \int_{-\infty}^{\infty} \tilde{E}_y \left\{ \frac{n.\pi}{a} , y \right\} e^{-j\left[\left[\frac{n.\pi}{a}\right]x + \beta z\right]} \tag{2.16}$$

that the field components are a superposition of inhomogeneous (in y) waves propagating at an angle θ_n to the z axis where θ_n is given by:-

$$\theta_n = \cos^{-1}\left[\frac{\beta}{\left[\frac{n.\pi}{a}\right]^2 + \beta^2}\right] \tag{2.17}$$

For each θ_n waves may be decomposed in TM-to-y (E_y,E_v,H_u) and TE-to-y (H_y,E_u,H_v) where the co-ordinates u and v are as shown in fig.(2.1). The J_v current creates only the TM fields and J_u the TE fields so that it is possible to draw an equivalent circuit for the TM and TE fields as in fig.(2.2). Using conventional transmission line theory for the equivalent circuits it is possible to equate the electric field and currents on the interface which may then be transformed back to the original co-ordinates.

This method provides a simple and compact way of deriving the relationship between the interface tangential electric fields and the interface current distribution. An example of how this technique may be used to consider the effect of dielectric overlay is considered in chapter 3 and should clarify the technique.

2.4 Complex Modes.

To complete the introductory sections it must be noted that in addition to the propagating and evanescent modes there is an additional case to be considered; that of a pair of complex modes having complex conjugate propagation constants.

Although the existence of these types of modes have been known for other related structures (see for example Omar & Schünemann [16]) it is only recently that they have been reported for the case of microstrip by Huang & Itoh [17] and Railton & Rozzi [18].

The main feature of these modes is the way in which the energy is stored in the mode. Whereas for the evanescent modes the energy stored will be either wholly inductive or capacitive, for the complex modes the energy stored oscillates from being of one type to the other. A more complete discussion may be obtained from [16] for the case of Finline.

References.

[1]... Hornsby, J.K. & Gopinath, A.. "A Numerical Analysis of a Dielectric-loaded Waveguide with a Microstrip Line - Finite Difference Methods."
IEEE Trans. MTT-17, No. 9, September 1969, pp. 684-690.

[2]... Corr, D.G. & Davies, J.B.. "Computer Analysis of the Fundamental & Higher Order Modes in Single and Coupled Microstrip."
IEEE Trans. MTT-20, No.10, October 1972, pp. 669-677.

[3]... Daly, P.. "Hybrid Mode Analysis by Finite Element Methods."
IEEE Trans. MTT-19, No. 1, January 1971, pp. 19-25.

[4]... Denlinger, E.J.. "A Frequency Dependent Solution for Microstrip Transmission Lines."
IEEE Trans. MTT-19, No. 1, January 1971, pp. 30-39.

[5]... Mittra, R. & Itoh, T.. "A New Technique for the Analysis of the Dispersion Characteristics of Microstrip Lines."
IEEE Trans. MTT-19, No. 1, January 1971, pp. 47-56.

[6]... Krage, M.K. & Haddad, G.I.. "Frequency-Dependent Characteristics of Microstrip Transmission Lines."
IEEE Trans. MTT-20, No.10, October 1972, pp. 678-688.

[7]... Yamashita, E. & Atsuki, K.. "Analysis of Microstrip-Like Transmission Lines by Nonuniform Discretization of Integral Equations."
IEEE Trans. MTT-24, No. 4, April 1976, pp. 195-200.

[8]... Jansen, R.H.. "The Spectral-Domain Approach for Microwave Integrated Circuits."
IEEE Trans. MTT-33, No.10, October 1985, pp. 1043-1056.

[9]... Harrington, R.F.. "Field Computation by Moment Methods."
New York, Macmillan 1968.

[10].. Itoh, T. & Mittra, R.. "Dispersion Characteristics of Slot Lines."
Electronics Letters, Vol. 7, No.13, July 1971.

[11].. Itoh, T. & Mittra, R.. "Spectral-Domain Approach for Calculating the Dispersion Characteristics of Microstrip Lines."
IEEE Trans. MTT-21, No. 7, July 1973, pp. 496-499.

[12].. Itoh, T. & Mittra, R.. "A Technique for Computing Dispersion Characteristics of Shielded Microstrip Lines."
IEEE Trans. MTT-22, No.10, October 1974, pp. 896-898.

[13].. Jansen, R.H.. "High-Speed Computation of Single and Coupled Microstrip Parameters Including Dispersion, High-Order Modes, Loss and Finite Strip Thickness."
IEEE Trans. MTT-26, No. 2, February 1978, pp. 75-82.

[14].. Schmidt, L-P. & Itoh, T.. "Spectral Domain Analysis of Dominant and Higher Order Modes in Fin-Lines."
IEEE Trans. MTT-28, No. 9,September 1980.

[15].. Itoh, T.. "Spectral Domain Immittance Approach for Dispersion Characteristics of Generalized Printed Transmission Lines.
IEEE Trans. MTT-28, No. 7, July 1980, pp. 733-736.

[16].. Omar, A.S. & Schünemann, K.. "Formulation of the Singular Integral Equation Technique for Planar Transmission Lines."
IEEE Trans. MTT-33, No.12, December 1985, pp. 1313-1322.

[17].. Huang, W-X. & Itoh, T.. "Complex Modes in Lossless Shielded Microstrip Lines."
IEEE Trans. MTT-36, No. 1, January 1988, pp. 163-165.

[18].. Railton, C.J. & Rozzi, T.. "Complex Modes in Boxed Microstrip."
IEEE Trans. MTT-36, No. 5, May 1988, pp. 865-874.

Figures. Page.

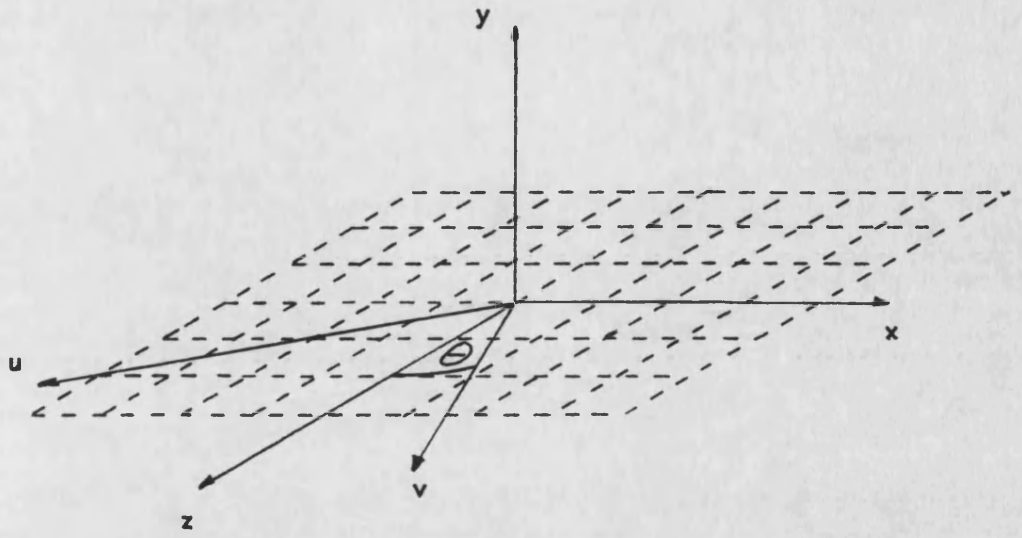

Co-ordinate transformation for TE & TM equivalent circuits.

Fig.(2.1)

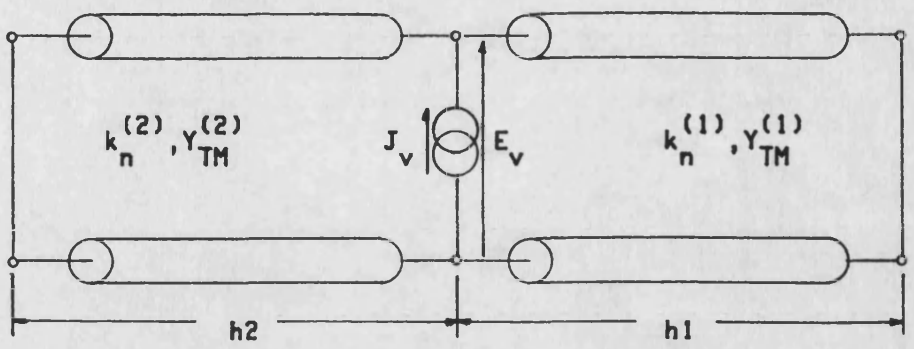

(a) Equivalent TM circuit for single layer shielded microstrip.

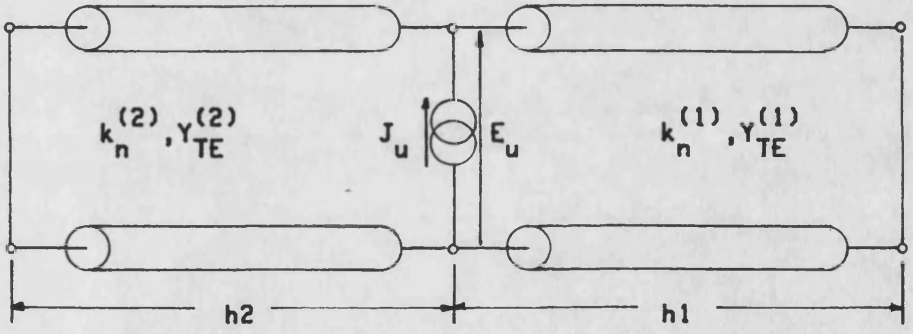

(b) Equivalent TE circuit for single layer shielded microstrip.

Fig.(2.2)

CHAPTER THREE

SHIELDED MICROSTRIP FORMULATION

The aim of this chapter is to provide a rigorous method to determine the modes of a shielded microstrip transmission line using the techniques outlined in the previous chapters together with the work done in the electrical engineering department at the University of Bath [1],[2],[3].

The propagation constants of the modes of the continuous line may be determined using a variational approach instead of the extensively used Galerkin's method although the final results may be shown to be equivalent. Once the modes have been identified their field distributions may be determined which then enables a test for mode orthogonality and also enables the power flow to be calculated. The characteristic impedance, for the fundamental mode, is also defined and evaluated.

Numerous results are presented for varying parameters such as strip width, asymmetry and dielectric overlay as well as results for symmetric twin strips.

3.1. The Electromagnetic Field in Shielded Microstrip.

The electromagnetic field in the individual layers of the shielded microstrip transmission line of fig.(3.1) may be represented as a superposition of TM-to-y and TE-to-y fields which may be derived from an electric 'Π_e' and magnetic type 'Π_h' of Hertzian potential [1,1]:-

$$\underline{\Pi}_e = \underline{a}_y \, \psi_e(x,y) \, e^{-\gamma z} \tag{3.1}$$

$$\underline{\Pi}_h = \underline{a}_y \, \psi_h(x,y) \, e^{-\gamma z} \tag{3.2}$$

where propagation is assumed to be in the positive z direction with a propagation constant γ, and a time dependence $e^{j\omega t}$ which is suppressed throughout the analysis. The terms ψ_e and ψ_h are scalar functions of the co-ordinates x and y. The field components may thus be written in terms of these potentials:-

$$\begin{bmatrix} E_x \\ E_y \\ E_z \end{bmatrix} = \begin{bmatrix} \partial_x \partial_y \\ k^2 + \partial_y^2 \\ -\gamma \partial_y \end{bmatrix} \psi_e + \begin{bmatrix} -j\omega\mu_0\gamma \\ 0 \\ -j\omega\mu_0 \partial_x \end{bmatrix} \psi_h \tag{3.3}$$

$$\begin{bmatrix} H_x \\ H_y \\ H_z \end{bmatrix} = \begin{bmatrix} j\omega\varepsilon\gamma \\ 0 \\ j\omega\varepsilon\partial_x \end{bmatrix} \psi_e + \begin{bmatrix} \partial_x \partial_y \\ k^2 + \partial_y^2 \\ -\gamma \partial_y \end{bmatrix} \psi_h \tag{3.4}$$

where the symbol ∂ indicates partial differentiation with respect to the subscipted co-ordinate. The analysis is similar to the derivation of the Longitudinal Section Electric (LSE) & Longitudinal Section Magnetic (LSM) modes of a slab loaded waveguide. However, unlike these LSE and LSM modes which do not have an E_y or H_y component respectively and may, therefore, be derived from one potential alone, the presence of the strip in shielded microstrip gives rise to modes having all six components and thus both potentials must be defined for each layer.

The scalar functions ψ_e & ψ_h must be written as some general expansion of the co-ordinates x & y. First, since the tangential electric field at the bounding walls must be zero we may assume a suitable sinusoidal expansion :-

$$\psi_e = \sum_{n=1}^{\infty} f_{en}(y)\,\phi_{sn} \qquad \phi_{sn} = \sqrt{\left(\frac{2}{a}\right)} \sin\left\{\frac{n.\pi}{a}\,x\right\} \tag{3.5}$$

$$\psi_h = \sum_{n=0}^{\infty} f_{hn}(y)\,\phi_{cn} \qquad \phi_{cn} = \sqrt{\left(\frac{\eta_n}{a}\right)} \cos\left\{\frac{n.\pi}{a}\,x\right\}$$

$$\eta_n = \begin{cases} 1 & n = 0 \\ 2 & n \neq 0 \end{cases} \tag{3.6}$$

The normalising factors have been introduced to make the functions orthonormal over the interval x = 0 to x = a. Substituting the above into the homogeneous vector Helmholtz equation, which the Hertzian potentials must satisfy [1,1], results in the following second order differential equations:-

$$\partial_y^2 f_{en}(y) + k_n^2 f_{en}(y) = 0 \tag{3.7}$$

$$\partial_y^2 f_{hn}(y) + k_n^2 f_{hn}(y) = 0 \tag{3.8}$$

where:-

$$k_n^2 = k^2 - \left[\frac{n.\pi}{a}\right]^2 + \gamma^2 \tag{3.9}$$

Solving these equations in the absence of any boundary conditions the following choice may be made:-

$$f_{en}(y) = A_{en} \cos\left\{k_n.(y-y(\text{upper}))\right\} + B_{en} \cos\left\{k_n.(y-y(\text{lower}))\right\} \tag{3.10}$$

$$f_{hn}(y) = A_{hn} \sin\left\{k_n.(y-y(\text{upper}))\right\} + B_{hn} \sin\left\{k_n.(y-y(\text{lower}))\right\} \tag{3.11}$$

Here y(upper) & y(lower) are the y co-ordinates of the interfaces.

Using the knowledge that the tangential electric field at the top and bottom of the structure will be zero we may write suitable expansions specifically relating to one region only. For region (1):-

$$\psi_e^{(1)} = \sum_{n=1}^{\infty} I_n^{(1)} \phi_{sn} \cos\left\{ k_n^{(1)} .(y - h_1) \right\} \qquad (3.12)$$

$$\psi_h^{(1)} = \sum_{n=0}^{\infty} V_n^{(1)} \phi_{cn} \sin\left\{ k_n^{(1)} .(y - h_1) \right\} \qquad (3.13)$$

$$k_n^{(1)2} = \varepsilon_1 k_0^2 - \left[\frac{n.\pi}{a}\right]^2 + \gamma^2 \qquad (3.14)$$

whilst for region (2) the above apply with (1) replaced with (2), $(y - h_1)$ replaced by $(y - -h_2)$ and ε_1 replaced by ε_2.

Note that the above expressions for ψ_e and ψ_h have been simplified because of the requirement that the tangential electric field be zero on the top and bottom conductors. If this had not been so, as occurs with an intermediate layer, no such simplification would have been possible and twice as many arbitrary constants would appear in the expansions. When considering the overlay later in this chapter, this property that the tangential electric field at one interface may be expressed in terms of one set of arbitrary constants whilst the tangential electric field at the other interface is given in terms of another independent set of constants, gives rise to a greatly simplified analysis and accounts for the choice of (3.10) & (3.11).

In the following analysis, it is necessary to equate the fields at the interface of the the layers and this may only be done if it is assumed that the strip is infinitely thin since the use of Hertzian potentials applies only to homogeneous source free regions.

In practice, however, as the frequency increases the skin depth of a copper conductor,for example,(approx. 1μm. at 4 GHz.) becomes many times smaller than practical strip thickness (typically 35-70 μm.). This gives rise to the possibility of variations of current density as a function of y. Nevertheless, since the assumptions are an accurate description of the system at both the lower frequencies and given that the expressions for the current in the strip may be interpreted as the total current flowing in both the upper and lower surfaces, the assumption of an infinitely thin strip will be maintained.

For the purpose of simplification, it will be assumed that the loss in the system is so small that its effect on the propagation will be of little effect. It is conventional to take account of such small effects as a final stage in any analysis by assuming a perturbation from the ideal case [2,8]. Such loss mechanisms that could be dealt with in this manner include both the dielectric and conductor loses although there are additional problems associated with the conductor losses on account of the secondary effect of surface roughness and the effect of the singularity which arises in the ideal case being different to that which will exist in practice.

Using these assumptions, it is possible to eliminate some of the variables V_n & I_n in both the air and substrate regions from the knowledge of field behaviour at boundaries. To this end, the fields in both regions are expanded in full.

The three components of the electric field in the layers may now be determined by substitution of the potentials (3.12) & (3.13) into the component equations of (3.3):-

$$\tilde{E}_x^{(1)}(cn,y) = - I_n^{(1)}\, k_n^{(1)} \left[\frac{n.\pi}{a}\right] \sin\left\{k_n^{(1)}.(y - h_1)\right\} - V_n^{(1)}\, j\omega\mu_0 \left[\gamma\right] \sin\left\{k_n^{(1)}.(y - h_1)\right\} \qquad (3.15)$$

$$\tilde{E}_y^{(1)}(sn,y) = I_n^{(1)} \left[\left[\frac{n.\pi}{a}\right]^2 - \gamma^2\right] \cos\left\{k_n^{(1)}.(y - h_1)\right\} \qquad (3.16)$$

$$\tilde{E}_z^{(1)}(sn,y) = I_n^{(1)}\, k_n^{(1)} \left[\gamma\right] \sin\left\{k_n^{(1)}.(y - h_1)\right\} + V_n^{(1)}\, j\omega\mu_0 \left[\frac{n.\pi}{a}\right] \sin\left\{k_n^{(1)}.(y - h_1)\right\} \qquad (3.17)$$

Note that in the above I_0 is taken as zero and the symbol ($\tilde{}$) is used to imply the discrete Fourier sine or cosine transform given by:-

$$\tilde{A}(sn) = \int_0^a A(x)\, \phi_{sn}\, dx \qquad \tilde{A}(cn) = \int_0^a A(x)\, \phi_{cn}\, dx \qquad (3.18)$$

The corresponding equations for region (2) may be obtained by replacing (1) with (2) and replacing $(y - h_1)$ with $(y - -h_2)$.

The continuity of the tangential electric field at the boundary:-

$$\tilde{E}_x^{(1)}(cn,+0) = \tilde{E}_x^{(2)}(cn,-0) \qquad (3.19)$$

$$\tilde{E}_z^{(1)}(sn,+0) = \tilde{E}_z^{(2)}(sn,-0) \qquad (3.20)$$

enables the following equivalences to be derived:-

$$I_n^{(1)}\, k_n^{(1)} \sin\left\{k_n^{(1)}.-h_1\right\} = I_n^{(2)}\, k_n^{(2)} \sin\left\{k_n^{(2)}.+h_2\right\} \qquad (3.21)$$

$$V_n^{(1)} \sin\left\{k_n^{(1)}.-h_1\right\} = V_n^{(2)} \sin\left\{k_n^{(2)}.+h_2\right\} \qquad (3.22)$$

Note that continuity of the tangential electric field is independent of the presence of any metallisation at the interface.

The three components of the magnetic field in the layers may be derived in exactly the same way as for the electric field components using the component equations (3.4):-

$$\tilde{H}_x^{(1)}(sn,y) = I_n^{(1)}\, j\omega\varepsilon_0\varepsilon_1 \left[\gamma\right] \cos\left\{k_n^{(1)}.(y - h_1)\right\} - V_n^{(1)}\, k_n^{(1)} \left[\frac{n.\pi}{a}\right] \cos\left\{k_n^{(1)}.(y - h_1)\right\} \quad (3.23)$$

$$\tilde{H}_y^{(1)}(cn,y) = V_n^{(1)} \left[\left[\frac{n.\pi}{a}\right]^2 - \gamma^2\right] \sin\left\{k_n^{(1)}.(y - h_1)\right\} \quad (3.24)$$

$$\tilde{H}_z^{(1)}(cn,y) = I_n^{(1)}\, j\omega\varepsilon_0\varepsilon_1 \left[\frac{n.\pi}{a}\right] \cos\left\{k_n^{(1)}.(y - h_1)\right\} - V_n^{(1)}\, k_n^{(1)} \left[\gamma\right] \cos\left\{k_n^{(1)}.(y - h_1)\right\} \quad (3.25)$$

Again the corresponding equations for the other region may be determined by replacing (1) with (2), $(y - h_1)$ with $(y - -h_2)$ and ε_1 with ε_2.

The next step in the analysis is to equate the current in the strip to the difference in the magnetic field at either side of the air / dielectric interface. Here, as mentioned previously, the definition is based upon a laminar flow of current but is also correct when there is current flow on either surface of a perfectly conducting sheet where the current considered is the total of that on the two surfaces.

The relationship between the tangential magnetic field subject to a surface current density $\underline{J}_s$ is given by:-

$$\underline{n} \times (\underline{H}^{(1)} - \underline{H}^{(2)}) = \underline{J}_s \quad (3.26)$$

where $\underline{n}$ is the unit normal to the air / dielectric interface directed from region (2) into region (1).

Expanding equation (3.26) it is possible to obtain two separate component equations:-

$$\tilde{J}_x(cn) = \tilde{H}_z^{(1)}(cn,+0) - \tilde{H}_z^{(2)}(cn,-0) \qquad (3.27a)$$

$$\tilde{J}_z(sn) = -\tilde{H}_x^{(1)}(sn,+0) + \tilde{H}_x^{(2)}(sn,-0) \qquad (3.27b)$$

Thus using the relationships already derived this becomes:-

$$\tilde{J}_x(cn) = j\omega\varepsilon_0\left[\frac{n.\pi}{a}\right]X_n\, I_n^{(1)}\, k_n^{(1)}\, \sin\left\{k_n^{(1)}.-h_1\right\} - [\gamma]\, Y_n\, V_n^{(1)}\, \sin\left\{k_n^{(1)}.-h_1\right\} \qquad (3.28a)$$

$$\tilde{J}_z(sn) = -j\omega\varepsilon_0\,[\gamma]\, X_n\, I_n^{(1)}\, k_n^{(1)}\, \sin\left\{k_n^{(1)}.-h_1\right\} + \left[\frac{n.\pi}{a}\right]Y_n\, V_n^{(1)}\, \sin\left\{k_n^{(1)}.-h_1\right\} \qquad (3.28b)$$

Here the following abbreviations have been used:-

$$X_n = \frac{\varepsilon_1}{k_n^{(1)}.\tan\left\{k_n^{(1)}.-h_1\right\}} - \frac{\varepsilon_2}{k_n^{(2)}.\tan\left\{k_n^{(2)}.+h_2\right\}} \qquad (3.29)$$

$$Y_n = k_n^{(1)}.\cot\left\{k_n^{(1)}.-h_1\right\} - k_n^{(2)}.\cot\left\{k_n^{(2)}.+h_2\right\} \qquad (3.30)$$

Note that relationships (3.29) & (3.30) give the transcendental equations of the LSE and LSM modes of the slab waveguide when equated to zero. Rearranging equations (3.28):-

$$I_n^{(1)}\, k_n^{(1)}\, \sin\left\{k_n^{(1)}.-h_1\right\} = \frac{\tilde{J}_x(cn)\,\frac{n.\pi}{a} + \tilde{J}_z(sn)\,\gamma}{j\omega\varepsilon_0\, X_n\left[\left[\frac{n.\pi}{a}\right]^2 - \gamma^2\right]} \qquad (3.31)$$

$$V_n^{(1)}\, \sin\left\{k_n^{(1)}.-h_1\right\} = \frac{\tilde{J}_x(cn)\,\gamma + \tilde{J}_z(sn)\,\frac{n.\pi}{a}}{Y_n\left[\left[\frac{n.\pi}{a}\right]^2 - \gamma^2\right]} \qquad (3.32)$$

Use of these identities allows the electric field in the layers to be expressed in terms of the current density at the interface.

Specifically, for the electric field at the interface:-

$$\begin{bmatrix} -\tilde{E}_x(cn) \\ \tilde{E}_z(sn) \end{bmatrix} = j\omega\mu_0 \begin{bmatrix} G_{xx}(n,\gamma) & G_{xz}(n,\gamma) \\ G_{xz}(n,\gamma) & G_{zz}(n,\gamma) \end{bmatrix} \begin{bmatrix} \tilde{J}_x(cn) \\ \tilde{J}_z(sn) \end{bmatrix} \qquad (3.33)$$

where the terms in the above are:-

$$G_{xx} = N_x N_x \frac{1}{-k_0^2 X_n} + N_z N_z \frac{1}{Y_n} \qquad (3.34a)$$

$$G_{xz} = N_x N_z \frac{1}{-k_0^2 X_n} + N_x N_z \frac{1}{Y_n} \qquad (3.34b)$$

$$G_{zz} = N_z N_z \frac{1}{-k_0^2 X_n} + N_x N_x \frac{1}{Y_n} \qquad (3.34c)$$

and the terms N_x and N_z are given by the following:-

$$N_x^2 = \frac{\left[\frac{n.\pi}{a}\right]^2}{\left[\frac{n.\pi}{a}\right]^2 - \gamma^2} \qquad N_z^2 = \frac{\gamma^2}{\left[\frac{n.\pi}{a}\right]^2 - \gamma^2} \qquad (3.35)$$

By inversion of the above the transverse current density may be expressed as a function of the transverse electric field:-

$$\begin{bmatrix} -\tilde{J}_x(cn) \\ \tilde{J}_z(sn) \end{bmatrix} = \frac{1}{j\omega\mu_0} \begin{bmatrix} H_{xx}(n,\gamma) & H_{xz}(n,\gamma) \\ H_{xz}(n,\gamma) & H_{zz}(n,\gamma) \end{bmatrix} \begin{bmatrix} \tilde{E}_x(cn) \\ \tilde{E}_z(sn) \end{bmatrix} \qquad (3.36)$$

The terms in the above are given by:-

$$H_{xx} = -k_0^2 N_x N_x X_n + N_z N_z Y_n \qquad (3.37a)$$

$$H_{xz} = -k_0^2 N_x N_z X_n + N_x N_z Y_n \qquad (3.37b)$$

$$H_{zz} = -k_0^2 N_z N_z X_n + N_x N_x Y_n \qquad (3.37c)$$

Additional equivalences may also be derived for example, recalling the method used by Yamashita [2,7], requires the J_x & E_z to be expressed as functions of J_z & E_x.

3.2 Solution for modes of the continuous line.

The set of inhomogeneous algebraic equations (3.33) may be solved in a procedure based on Galerkin's method. First the currents J_x & J_z are expanded as a truncated set of known basis functions J_{xm} & J_{zm}:-

$$\tilde{J}_x(cn) = \sum_{m=0}^{M} a_m \tilde{J}_{xm}(cn) \qquad \tilde{J}_z(sn) = \sum_{m=0}^{M} b_m \tilde{J}_{zm}(sn) \tag{3.38}$$

where a_m and b_m are, as yet, undetermined weighting coefficients. These basis functions are chosen so that their inverses are non-zero on the strip but zero elsewhere. After using these expansions in (3.33) the innerproducts with the individual basis functions may be taken resulting in the sets of homogeneous equations:-

$$0 = \sum_{m=0}^{M} a_m K_{xx}(i,m,\gamma) + \sum_{m=0}^{N} b_m K_{xz}(i,m,\gamma) \qquad (i=0,1,..,M) \tag{3.39}$$

$$0 = \sum_{m=0}^{M} a_m K_{zx}(i,m,\gamma) + \sum_{m=0}^{N} b_m K_{zz}(i,m,\gamma) \qquad (i=0,1,..,N) \tag{3.40}$$

where :-

$$K_{xx}(i,m,\gamma) = \sum_{n=0}^{\infty} \tilde{J}_{xi}(cn)\, G_{xx}(n,\gamma)\, \tilde{J}_{xm}(cn) \tag{3.41a}$$

$$K_{xz}(i,m,\gamma) = \sum_{n=1}^{\infty} \tilde{J}_{xi}(cn)\, G_{xz}(n,\gamma)\, \tilde{J}_{zm}(sn) \tag{3.41b}$$

$$K_{zx}(i,m,\gamma) = \sum_{n=1}^{\infty} \tilde{J}_{zi}(sn)\, G_{zx}(n,\gamma)\, \tilde{J}_{xm}(cn) \tag{3.41c}$$

$$K_{zz}(i,m,\gamma) = \sum_{n=1}^{\infty} \tilde{J}_{zi}(sn)\, G_{zz}(n,\gamma)\, \tilde{J}_{zm}(sn) \tag{3.41d}$$

The sets of homogeneous simultaneous equations (3.39) & (3.40) may be solved for characteristic values of the propagation constant by requiring that the determinant of the matrix of coefficients be zero.

This method has received much attention with the accuracy achieved using only approximate expansion functions being attributed to the self-adjointness of the integral operators arising from (3.33). This property suggests that a variational procedure using the Rayleigh-Ritz may be possible.

Therefore, consider the method used by Rumsey [4] in his analysis of the dielectric filled slotted waveguide which has been shown to apply to boxed microstrip by Hassan [5]. As a prerequisite to his analysis Rumsey determined the implications of reciprocity for a guided wave which, he observed, were distinctly different to that of a resonant structure. He then formulated a variational expression:-

$$\begin{aligned} \Phi(\gamma) &= \int \underline{J} \cdot \underline{\underline{s}}\, \underline{E}\, dl \qquad \underline{\underline{s}} = \begin{bmatrix} 1 & 0 & 0 \\ 0 & 1 & 0 \\ 0 & 0 & -1 \end{bmatrix} \\ &= 0 \end{aligned} \tag{3.42}$$

In the above, the integral is taken around a closed contour in the cross section of the guiding structure and is stationary for small variations in the assumed value of $\underline{E}$. Thus from fig.(3.2) and choosing either contour 1 or 2 to use in the above gives:-

$$\Phi(\gamma) = \int_0^a \left(J_x\, E_x(x,0) - J_z\, E_z(x,0) \right) dx \tag{3.43}$$

Thus from the knowledge of the field components at the interface the above expression can be written in one of two forms. Consider first the expansion in terms of the tangential electric field:-

$$\begin{aligned} \Phi(\gamma) = &- \sum_{n=0}^{\infty} \left(H_{xx}(n,\gamma)\, \tilde{E}_x(cn)\, \tilde{E}_x(cn) \right) \\ &- 2 \sum_{n=1}^{\infty} \left(H_{xz}(n,\gamma)\, \tilde{E}_x(cn)\, \tilde{E}_z(cn) \right) \\ &- \sum_{n=1}^{\infty} \left(H_{zz}(n,\gamma)\, \tilde{E}_z(sn)\, \tilde{E}_z(sn) \right) \end{aligned} \tag{3.44}$$

which may be determined using equation (3.36).

Now the transforms of the electric fields admit to expansions in terms of a truncated set of suitable basis functions:-

$$\tilde{E}_x(cn) = \sum_{m=0}^{M} c_m \tilde{E}_{xm}(cn) \qquad \tilde{E}_z(sn) = \sum_{m=0}^{M} d_m \tilde{E}_{zm}(sn) \tag{3.45}$$

Upon substituting these expansions into (3.45) the c_m's & d_m's may be treated as independent variables and the Rayleigh-Ritz variational principle may be used to minimise $\Phi(\gamma)$ with respect to these parameters. To achieve this the equation is differentiated with respect to each of c_m's & d_m's in turn:-

$$\frac{\partial\Phi(\gamma)}{\partial c_i} = -2 \sum_{m=0}^{M} c_m \sum_{n=0}^{\infty} H_{xx}(n,\gamma)\, \tilde{E}_{xm}(cn)\, \tilde{E}_{xi}(cn) \qquad (i=0,1,..,M)$$
$$-2 \sum_{m=0}^{N} d_m \sum_{n=1}^{\infty} H_{xz}(n,\gamma)\, \tilde{E}_{zm}(sn)\, \tilde{E}_{xi}(cn) \tag{3.46}$$

$$\frac{\partial\Phi(\gamma)}{\partial d_i} = -2 \sum_{m=0}^{M} c_m \sum_{n=1}^{\infty} H_{xz}(n,\gamma)\, \tilde{E}_{xm}(cn)\, \tilde{E}_{zi}(sn) \qquad (i=0,1,..,N)$$
$$-2 \sum_{m=0}^{N} d_m \sum_{n=1}^{\infty} H_{zz}(n,\gamma)\, \tilde{E}_{zm}(sn)\, \tilde{E}_{zi}(sn) \tag{3.47}$$

Equating each of these expressions to zero results in a set of homogeneous simultaneous equations that may be solved as before.

There are some interesting properties of the above. Consider for example the case of the slab loaded waveguide without metallisation at the interface, choosing suitable one term expansion functions as:-

$$\tilde{E}_x(cn) = \begin{cases} c_q & n = q \\ 0 & n \neq q \end{cases} \qquad \tilde{E}_z(sn) = \begin{cases} d_q & n = q \\ 0 & n \neq q \end{cases} \tag{3.48}$$

The above imply a single sinusoidal component for each of the fields.

For this case the determinental equation gives the following result:-

$$X_q \quad Y_q \quad = \quad 0 \qquad (3.49)$$

Thus is is clear that for this choice of expansion, the solution is exact since the expressions $X_q = 0$ & $Y_q = 0$ correspond to the transcendental equation for the LSE_q & the LSM_q modes of this structure. The reason that the other sets of modes are excluded in this solution would appear to be attributed to mode orthogonality.

The application of this technique to using the currents as the expansion functions has been hinted at by Harrington [6] in his analysis of the slotted waveguide. He concluded that, although it was possible it would not have been efficient to expand over the larger region. For microstrip, however, the opposite is true and the equivalence of Galerkin's method and this variational technique may again be demonstrated.

3.3 Choice of Basis Functions.

Having formulated the method of solution, it is necessary to put the technique into practice. The basis functions for the longitudinal current may be taken as [2,18]:-

$$J_z = \sum_{m=0}^{N} b_m \frac{T_m\left\{\frac{2(x-ms)}{w}\right\}}{\left[1-\left[\frac{2(x-ms)}{w}\right]^2\right]^{1/2}} \qquad (ns \leq x \leq fs) \tag{3.50}$$

where T_m are the Tchebychev polynomials, ms is the x coordinate of the middle and w the width of the strip and it is assumed that J_z is zero outside of this range. The above form has the correct singularity at the strip edges and the expansion, when N is assumed to tend to infinity, forms a complete set.

To express the transverse current density recall the requirement as laid down by Jansen [2,13] that there should be an integral relationship between the current components. From the conservation of charge formula (with ρ_s representing the charge density):-

$$\frac{\partial J_x}{\partial x} + \frac{\partial J_z}{\partial z} = -j\omega\rho_s \tag{3.51}$$

it is clear that the x derivative of J_x (J_x') will have a form closely related to that of J_z. Following the method of [1] the transforms involving J_x may be integrated by parts:-

$$\begin{aligned}\tilde{J}_x(cn) &= \int_{ns}^{fs} J_x \cdot \phi_{hn}\, dx \qquad \text{(hn → sn?)} \\ &= \left[\frac{n.\pi}{a}\right]^{-1}\left[\left[J_x \cdot \phi_{sn}\right]_{ns}^{fs} - \int_{ns}^{fs} J_x' \cdot \phi_{sn}\, dx\right] \quad (n\neq 0) \\ &= \sqrt{\frac{1}{a}}\left[\left[J_x \cdot x\right]_{ns}^{fs} - \int_{ns}^{fs} J_x' \cdot x\, dx\right] \quad (n=0)\end{aligned} \tag{3.52}$$

The first terms in the above are identically equal to zero as a consequence of the current at the edge being zero.

The derivative of J_x may now be represented in the same way as J_z:-

$$J_x' = \sum_{m=1}^{M} a_m \frac{T_m \left\{ \frac{2(x-ms)}{w} \right\}}{\left[1 - \left[\frac{2(x-ms)}{w} \right]^2 \right]^{1/2}} \qquad (ns \leq x \leq fs) \qquad (3.53)$$

Note that the lower limit excludes the zero term. This is again because of the requirement that the transverse current should be zero at both the strip edges which would not be possible should this term be included. The transforms may now be evaluated using the method given in appendix A3.1.

The elements of the matrix of coefficients may now be computed. The programming of these elements, which are repeatedly required, may be speeded up by including assymptotic terms which may be evaluated independently of the propagation constant and therefore need only be calculated once at the beginning of the program: one of the significant advantages of the method used in [1] is the ability to express this summation analytically and a similar analytical method has been given by Railton[7] for the basis functions of (3.50,3.53). For the terms which comprise the coefficient matrix (3.40) for large values of the index n the following approximations may be made:-

$$\lim_{n\to\infty} \left\{ k_n^{(1)} \right\}, \quad \lim_{n\to\infty} \left\{ k_n^{(2)} \right\} = j \left[\frac{n.\pi}{a} \right] \qquad (3.54)$$

giving the following limits:-

$$\lim_{n\to\infty} \left\{ G_{xx} \right\} = \left[\frac{n.\pi}{a} \right] \frac{1}{- k_0^2 \left(\varepsilon_1 + \varepsilon_2 \right)} \qquad (3.55a)$$

$$\lim_{n\to\infty} \left\{ G_{xz} \right\} = \frac{\gamma}{- k_0^2 \left(\varepsilon_1 + \varepsilon_2 \right)} \qquad (3.55b)$$

$$\lim_{n\to\infty} \left\{ G_{zz} \right\} = \left[\frac{n.\pi}{a} \right]^{-1} \left(\frac{\gamma^2}{- k_0^2 \left(\varepsilon_1 + \varepsilon_2 \right)} - \frac{1}{2} \right) \qquad (3.55c)$$

Note that convergence of the matrix terms is guaranteed since the transform of J_x decreases as $n^{-3/2}$ and that of J_z as $n^{-1/2}$ so that all matrix terms decrease at least as fast as n^{-2}.

With the exception of the complex modes, the computation of the roots may be simplified by using the method of normalisation adopted by Jansen [2,13]; for the evanescent waves all terms are real and as such need not be altered; for the propagating waves the expressions for G_{xz} become pure imaginary whilst the other terms remain real so that normalising J_x by including a factor j will make the elements of the matrix real and will leave the determinant unaltered.

That this should be so is because of the nature of the propagating & evanescent waves. For the evanescent waves both longitudinal and transverse current components will be in phase or in antiphase whereas for the propagating waves the current components are in phase quadrature.

The modes of propagation, for which the determinant of the matrix of coefficients is zero, may now be determined. In practice the search for the roots may be simplified by evaluating the positions of the poles which occur for values of the propagation constant for which there is either a LSE or a LSM mode of the corresponding slab loaded guide. In practice there will be one mode of the microstrip corresponding to each of the LSE and LSM modes of the slab guide.

That this is so may be verified by considering the limiting case of an infinitely narrow strip.

Using (3.44) with the currents as the expansion functions and further eliminating terms involving J_x, since these must be zero, the modes of the new structure are given by the roots of the following:-

$$\Phi(\gamma) = \sum_{n=1}^{\infty} \left(G_{zz} \quad \tilde{J}_z \quad \tilde{J}_z \right) \qquad (3.56)$$

$$= 0$$

In this case the longitudinal current may only be represented in one way; as a one term expansion using the dirac delta function:-

$$J_z = b_0 \; \delta(x-x_0, y-y_0) \qquad (3.57)$$

with x_0 & y_0 corresponding to the position of the strip. Using (3.57) in (3.56) gives the modal equation:-

$$0 = b_0^2 \sum_{n=1}^{\infty} \left(G_{zz} \sin^2 \left\{ \frac{n.\pi}{a} x_0 \right\} \right) \qquad (3.58)$$

it is clear that the resulting expression is, in general, divergent. Thus the only 'roots' will occur at the poles of G_{zz} which, it has been shown, correspond to the slab guide modes.

For widths greater than zero the roots move away from the solution of the LSE and LSM modes of the slab loaded guide. As an example of this behaviour, the normalised propagation phase constants of the propagating modes have been plotted in figs.(3.3) for three different strip widths. It can be seen that the results compare well with those obtained by other methods (see Yamashita [2,7]).

The effective permittivity of the fundamental mode, which is of most importance, is also plotted in fig.(3.4) for several widths as a function of frequency. The phase constant is both a function of the width of the strip (increasing for larger widths) but also shows clearly the effects of dispersion which in general give an increasing phase constant for increasing frequency.

3.4 Field components.

Having determined the propagation constant for a mode it is possible to evaluate the field components in the enclosure for this mode.

First the current distributions must be calculated. This is possible from the set of simultaneous equations (3.40). The solution will be unique to within a scalar constant and it is therefore possible to normalise this distribution by assuming the coefficient of J_{z0} equal to unity. The remaining coefficients may be determined from the resulting inhomogeneous equations by gaussian elimination with back substitution for example.

The field components may now be evaluated. For simplification these components may be expressed in terms of the fields at the interface. Specifically the x directed electric field in region (1) is:-

$$\tilde{E}_x^{(1)}(cn,y) = E_{xn}^{(1)} \frac{\sin\left\{k_n^{(1)} (y - h1)\right\}}{\sin\left\{k_n^{(1)} (- h1)\right\}} \qquad (3.59)$$

and the z directed electric field in region (2) is:-

$$\tilde{E}_z^{(2)}(sn,y) = E_{zn}^{(2)} \frac{\sin\left\{k_n^{(2)} (y - -h2)\right\}}{\sin\left\{k_n^{(2)} (- -h2)\right\}} \qquad (3.60)$$

Although the other components of the field may be expressed directly in terms of the current distribution by far the most efficient way to evaluate these components is to use the x and z components of the electric field to evaluate the constants V_n and I_n first and then use these constants in the expressions already derived. That the electromagnetic field can be characterised by the tangential electric field at the interface alone will be of greater importance when considering the dielectric overlay later in this chapter.

However, for the simple case without overlay the field components at the interface may be determined and the results plotted to verify that they satisfy the required boundary conditions. This may be done by calculating a set number of spectral components and then using the Fast Fourier Transform [8] to obtain the field distributions. The accuracy of the method of analysis may thus be checked since some of the field components are required to be identically zero on the strip.

Fig.(3.5) shows the results for a fundamental mode. It is clear that the required singularities are produced and that the boundary conditions are satisfied. Further, it is clear that, for this case, the electromagnetic energy is maintained closely around the strip.

For comparison a higher order mode has also been considered and the plots of the interface field are shown in fig.(3.6). For this example the energy will be more equally distributed over the guiding cross section as there are significant components of the electromagnetic field away from the strip.

3.5 Power flow.

Having determined the field distributions it is possible to use these results to determine other properties of the transmission line.

The power flow 'P' in a waveguiding structure may be determined from the complex Poynting vector [1,1]:-

$$P = \frac{1}{2}\iint \left(\underline{E} \times \underline{H}^{*} \right) \cdot \underline{a}_z \; dS \qquad (3.61)$$

with the integral taken over the guiding cross section. For the microstrip with propagation along the z axis this becomes:-

$$P = \frac{1}{2}\iint \left(E_x H_y^{*} - E_y H_x^{*} \right) \partial_x \partial_y \qquad (3.62)$$

Using the previous results it is possible to integrate over the guide cross section by considering air and substrate regions separately:-

$$P = \frac{1}{2} \int_0^{h1} \int_0^{a} \left(E_x^{(1)} H_y^{(1)*} - E_y^{(1)} H_x^{(1)*} \right) \partial_x \partial_y$$

$$+ \frac{1}{2} \int_{-h2}^{0} \int_0^{a} \left(E_x^{(2)} H_y^{(2)*} - E_y^{(2)} H_x^{(2)*} \right) \partial_x \partial_y \qquad (3.63)$$

Evaluation of these integrals is greatly simplified with the normalisations adopted:-

$$P = \frac{1}{2} \sum_{n=0}^{\infty} \left(E_{xn}^{(1)} H_{yn}^{(1)*} \cdot I4(\; 0, h1, k_n^{(1)}) \right)$$

$$+ \frac{1}{2} \sum_{n=1}^{\infty} \left(E_{yn}^{(1)} H_{xn}^{(1)*} \cdot I5(\; 0, h1, k_n^{(1)}) \right)$$

$$+ \frac{1}{2} \sum_{n=0}^{\infty} \left(E_{xn}^{(2)} H_{yn}^{(2)*} \cdot -I4(\; 0,-h2, k_n^{(2)}) \right)$$

$$+ \frac{1}{2} \sum_{n=1}^{\infty} \left(E_{yn}^{(2)} H_{xn}^{(2)*} \cdot -I5(\; 0,-h2, k_n^{(2)}) \right) \qquad (3.64)$$

The expressions I4(0,h,k) & I5(0,h,k) are integrals of the y components and are both defined and evaluated in Appendix A3.3.

3.6 Mode Orthogonality.

Having determined the power flow it is now possible to extend this analysis to give an independent check of the mode solutions for the guide. The modes of a lossless waveguiding system are expected to satisfy the following orthogonality relationship[1,1]:-

$$\frac{1}{2}\iint\left(\underline{E}_p \times \underline{H}_q^*\right).\underline{a}_z \, dS = C_{pq} = \delta_{pq} P_p \qquad (3.65)$$

with the integral taken over the guiding cross section. Physically this relationship expresses the requirement that power should not couple between different modes.

As for the power flow of a single mode, (3.65) may be expanded in terms of the electric and magnetic field components in either region. The resulting expression is of the form:-

$$\begin{aligned} C_{pq} = {} & \frac{1}{2}\sum_{n=0}^{\infty}\left(E_{xpn}^{(1)} H_{yqn}^{(1)*}.\, I6(\ 0,\ h1,\ k_{pn}^{(1)},\ k_{qn}^{(1)}\ )\right) \\ & + \frac{1}{2}\sum_{n=1}^{\infty}\left(E_{ypn}^{(1)} H_{xqn}^{(1)*}.\, I7(\ 0,\ h1,\ k_{pn}^{(1)},\ k_{qn}^{(1)}\ )\right) \\ & + \frac{1}{2}\sum_{n=0}^{\infty}\left(E_{xpn}^{(2)} H_{yqn}^{(2)*}.\,-I6(\ 0,-h2,\ k_{pn}^{(2)},\ k_{qn}^{(2)}\ )\right) \\ & + \frac{1}{2}\sum_{n=1}^{\infty}\left(E_{ypn}^{(2)} H_{xqn}^{(2)*}.\,-I7(\ 0,-h2,\ k_{pn}^{(2)},\ k_{qn}^{(2)}\ )\right) \end{aligned} \qquad (3.66)$$

The expressions $I6(0,h,k_m,k_p)$ & $I7(0,h,k_m,k_p)$ are integrals of the y components and are both defined and evaluated in Appendix A3.4.

The above formulation has been checked for two different widths of strip taking the inner products of both the fundamental and the first ten higher order modes. The results, shown in tables T3.1&2, are normalised so that the magnitude of the complex Poynting vector for the individual modes is unity. Excellent results are obtained!

3.7 Characteristic Impedance.

A definition for the characteristic impedance of a two conductor transmission line when completely surrounded in a homogeneous medium has been given in chapter one. A unique definition is possible under these circumstances first because the form of the electric field is frequency independent and indeed it may be derived from an electrostatic problem and secondly, because there is no axial component of the magnetic field, the line integral of the electric field in the transverse plane from one conductor to the other will be independent of the contour chosen i.e. it is possible to define a unique potential for the line.

For microstrip, however, no such simple definition is possible. This is because the 'potential' of the inner conductor with respect to the enclosure may not be uniquely defined since the electric field is not conservative and integration of the electric field from the inner conductor to the enclosure will depend upon the contour chosen. Further, the current in the strip is not restricted to flow in the direction of propagation apart from the limiting case of an infinitely narrow strip.

The frequency dependent behaviour of the most useful definition 'for practical use in design applications' has been discussed by Hashimoto [9] and attributed to the changing form of the current densities on the strip. The definition under consideration:-

$$Z_0 = 2 \frac{P}{|I|^2} \qquad (3.67)$$

where 'I' is the total longitudinal current, is the same as that used by Denlinger [2,6] and many others.

Thus having calculated the power in the previous section it only remains to determine 'I'. This may be done by integrating the longitutinal current density 'J_z' over the strip width. From the orthogonality of the Chebyshev polynomials only the first term in the expansion of J_z need be considered. The value of this integral is derived in Appendix A3.2.

The value of the characteristic impedance using this definition has been investigated for differing strip widths and the results are shown in fig.(3.7). For low frequencies the value will be the same as that given by the static analysis. As the frequency increases, however, this value changes by a small amount initially decreasing below the static value and eventually rising above this value and continuing its upward trend. When designing practical circuits the characteristic impedance will be determined by the strip width and the graph also shows this dependence. For very narrow strips the impedance becomes arbitrarily high and the only restriction, for the maximum value, would appear to be set by maufacturing tolerances. The lower limit, on the other hand, is set by the proximity of the strip to the shielding walls.

3.8 Overlay dielectrics.

Recalling the Spectral Domain Immitance appoach used by Itoh [2,11], it is possible to identify where the immittance terms enter into the formulation and hence it is possible to extend the method to analyse more complex structures. To demonstrate how this can be done, the case of dielectric overlay as illustrated in fig.(3.1b) will be considered. For the TM modes the wave admittance 'Y_{TM}' is:-

$$Y_{TM} = \frac{j\omega\varepsilon}{jk_n} \tag{3.68}$$

whilst for the TE modes the wave admittance 'Y_{TE}' is:-

$$Y_{TE} = \frac{jk_n}{j\omega\mu_0} \tag{3.69}$$

Thus the input admittances of the short circuit above the microstrip transformed to the air dielectric interface may be determined from transmission line theory [1,1]. Denoting these admittances, without overlay, as $Y_e^{(1)}$ & $Y_h^{(1)}$ for the TM and TE modes respectively gives:-

$$Y_e^{(1)} = - \frac{j\omega\varepsilon_0\varepsilon_1}{k_n^{(1)} \tan\left\{k_n^{(1)} h1\right\}} \tag{3.70}$$

and for the TE modes:-

$$Y_h^{(1)} = \frac{k_n^{(1)} \cot\left\{k_n^{(1)} h1\right\}}{j\omega\mu_0} \tag{3.71}$$

Similar expressions may be derived for the substrate. Hence it is possible to see that the previously derived terms X_n & Y_n are proportional to the total input admittance for the TM and TE modes respectively of both air and substrate regions. To account for other layers all that is necessary is to determine what the appropriate input admittances are and hence to adjust X_n & Y_n accordingly.

For the overlay of fig.(3.1b) the equivalent circuits are drawn in fig.(3.8). The new input admittances of the layered region may now be determined from these equivalent circuits using the terms for wave admittance and the transmission line theory of [1,1]. For example the input admittance of the TM mode is given by:-

$$Y_e(in) = Y_{TM}^{(1a)} \frac{Y_e^{(1b)} + j\, Y_{TM}^{(1a)} \tan\left\{k_n^{(1a)} l_a\right\}}{Y_{TM}^{(1a)} + j\, Y_e^{(1b)} \tan\left\{k_n^{(1a)} l_a\right\}} \qquad (3.72)$$

A similar expression may be determined for the TE equivalent circuit. These expressions may now be expanded in full and the terms X_n & Y_n modified accordingly. Further details are given in appendix A3.5. Results of the effect of overlay on $\varepsilon_r(eff)$ are plotted in fig.(3.9) and the effect is to increase this value with increasing overlay.

In order to determine the characteristic impedance of the line the power flow and hence the field components in the enclosure must be determined. The method presented above enables not only the value of $\varepsilon_r(eff)$ to be determined but also the current distribution on the strip and the tangential electric field at this interface '$\underline{E}_t(y=0)$'. Thus the electric and magnetic fields in the substrate may determined immediately. For the other regions, however, it is necessary to first determine $\underline{E}_t(y=l_a)$ which may be done by once again using the transmission line model of fig.(3.8). Specifically, for the TM modes the relationship is given by the following:-

$$\frac{E_v(y=l_a)}{E_v(y=0)} = \frac{Y_{TM}^{(1a)} / \sin\left\{k_n^{(1a)} l_a\right\}}{j\, Y_e^{(1b)} + Y_{TM}^{(1a)} \cot\left\{k_n^{(1a)} l_a\right\}} \qquad (3.73)$$

Similarly, the relationship for the TE modes may be derived. Using these formulae and the appropriate transformation, $\underline{E}_t(y=l_a)$ may be determined. Results for different overlays are shown in fig.(3.10).

3.9 Asymmetric Strips.

All the techniques previously presented have been capable of dealing with asymmetric strips. In this section several results are presented both for the single layer substrate and for dielectric overlay for when the strip is off centre.

In the first instance the variation in the effective permittivity as a function of the strip offset from the centre for the simple case without overlay has been determined and the results are plotted in fig.(3.11) for several frequencies. The trend of the frequency dependence remains the same for the degree of asymmetry i.e. the effective permittivity increases with increasing frequency. However, this effect becomes less noticeable as the strip edge approaches the shielding walls. In this case, the effective permittivity approaches the arithmitic mean of the permittivity of the layers on either side of the metallisation interface. Under these circumstances, it would appear, that the electromagnetic field is closely confined to the immediate vicinity of the strip.

The characteristic impedance has also been determined for the strip above and the results are shown in fig.(3.12).Here the characteristic impedance decreases as the strip edge approaches the shielding walls. Further, the value becomes largely independent of the frequency just as for the variation in effective permittivity. In design applications it is necessary to be able to control the value of Z_0 and this is clearly possible by altering the width of the strip for different offsets. The required width variation for a particular case has been computed and the results are shown in fig.(3.13). The curve shows that the width must be decresed as the strip moves closer to the shielding walls and indeed the width need only be decreased by half to maintain constant Z_0 for 95% of the available width.

Results have been obtained for overlay of the same permittivity and thickness of the substrate. The variation of $\varepsilon_r(eff)$ as a function of the asymmetry is shown in fig.(3.14). Interestingly, the effective permittivity increases as the strip approaches the shielding walls in an opposite trend to the effect without overlay. The characteristic impedance for this system has also been determined and the results are shown in fig.(3.15). Note that although the variation with offset remains significant, the frequency variation has almost disappeared and suggests that the large part of the electromagnetic field remains in the high dielectric medium.

Following this the effect of overlay having a permittivity value of $^{2}/_{3}$ that of the substrate but of the same thickness is shown in fig.(3.16). In this case it is noted that the phase velocity is largely independent of the asymmetry of the strip. The corresponding variation in the characteristic impedance may also be determined and the results are plotted in fig.(3.17). Although it would be desirable to control the effects of asymmetry with the use of overlay it seems clear from the results presented above and other tests using other thicknesses of overlay that the variation of $\varepsilon(eff)$ and Z_0 cannot be controlled with the use of overlay alone. The analysis of the above, however, does show how the flexibility of the method of analysis can be used to investigate the general multilayer transmission line.

3.10 Twin Strip Analysis.

The analysis for the case of two strips is very similar to that for the single strip. It is possible to expand the currents on either strip as a truncated set of basis functions as in (3.39). The technique will require twice as many arbitrary constants for the same accuracy as for the single strip.

However, for the case of symmetrically placed strips of equal width it is possible to simplify the analysis by making use of the symmetry properties. There are two cases to consider; the even modes may be determined by assuming a magnetic wall exists down the centre of the guide; on the other hand the odd modes arise by considering the effect of an electric wall along the centre. The analysis thus proceeds by modifying the general case of an asymmetric strip by eliminating those components which must be zero on the magnetic / electric walls. Note that for the odd modes the 'new structure' is simply a box of half the width of the original. Indeed the results for effective permittivity of this case 'fig.(3.18)' as a function of the strip separation show an identical trend as that for the asymmetric strip fig.(3.11). Further, the characteristic impedance 'fig.(3.19)' is similar once again to that of the asymmetric strip shown in fig.(3.12).

The even modes, however, are markedly different. For separations for which the individual strips approach the electric shielding walls the trend of the effective permittivity shown in fig.(3.20) and the characteristic impedance shown in fig.(3.21) is as before for the asymmetric strip. For separations for which the individual strips approach the fictitious magnetic wall the effect is to increase the characteristic impedance whilst the effective permittivity at first increases and then dips.

This nonmonotonical behaviour has been noted by Jansen[2,13]. The effect may be explained in terms of a single strip of varying width. As the two strips become closer together, the electromagnetic field is similar to that for a single strip having the combined width of the two individual strips plus the separation. As the separation decreases so the width of this effective strip becomes narrower and it has already been noted that this parameter change leads to a lower effective permittivity.

As a final consideration for the coupled strips, the overlay model as used for the single strip has also been applied to this geometry. The requirement for design purposes is that the odd and even mode phase velocities should be equal and many ideas as to how this may be achieved have been given in the literature [1,18]. As one possibility the results of the effect of an overlay of equal thickness and permittivity as the substrate are shown in fig.(3.22) for the odd mode and fig.(3.23) for the even mode.

Overlays of different dielectric constants and having different thicknesses may also be considered and the characteristic impedances of the odd & even modes in all these cases may be computed.

References.

[1]...

"Boxed Microstrip Circuits."

Annual Report, University of Bath, October 1983 -October 1984.

[2]...

"Boxed Microstrip Circuits."

Annual Report, University of Bath, October 1984 -October 1985.

[3]...

"Boxed Microstrip Circuits."

Annual Report, University of Bath, October 1985 -October 1986.

[4]... Rumsey, V.. "Travelling Wave Slot Antennas."

J. Appl. Phys., Vol.24, November 1953, pp.1358-1365.

[5]... Hassan, E.E.. "Field Solution, Polarization, and Eigenmodes of Shielded Microstrip Transmission Line."

IEEE Trans. MTT-34, No. 8, August 1986, pp. 845-852.

[6]... Harrington, R.F.. "Propagation Along a Slotted Cylinder."

J. Appl. Phys., Vol.24, November 1953, pp.1365-1371.

[7]... Railton, C.J.. "Boxed Microstrip Circuits."

PhD. Thesis, University of Bath, 1987.

[8]... Elliot, D. & Ramamohan Rao K.. "Fast Transforms Algorithms, Analyses & Applications."

Academic Press 1982.

[9]... Hashimoto, M.. "A Rigorous Solution for Dispersive Microstrip."

IEEE Trans. MTT-33, No.11, Noivember 1985, pp. 1131-1137.

APPENDIX A3.1.

Derivation of integrals for current transforms.

The transforms of the basis functions representing the currents may be evaluated. In general these expansions have the form:-

$$I1_i = \int_{ns}^{fs} \frac{T_i\left\{\frac{2(x-ms)}{w}\right\}}{\left[1-\left[\frac{2(x-ms)}{w}\right]^2\right]^{1/2}} \sin\left\{\frac{n.\pi}{a}x\right\} dx \qquad \text{(A3.1.1)}$$

In order to evaluate this integral the following transformation may be introduced:-

$$u = \frac{2(x-ms)}{w} \qquad \left\{ x = \left\{ \frac{w}{2}u + ms \right\} \right\} \qquad \text{(A3.1.2)}$$

where the range of integration now becomes:-

$$u = -1 \ , \ x = ns \qquad \text{(A3.1.3a)}$$

$$u = +1 \ , \ x = fs \qquad \text{(A3.1.3b)}$$

also differentiating the above gives:-

$$\frac{du}{dx} = \frac{2}{w} \qquad \text{(A3.1.4)}$$

These results may now be substituted into (A3.1.1) and using trig. identities may be separated into two components:-

$$I1_i = \frac{w}{2}\cos\left\{\frac{n.\pi}{a}ms\right\}\int_{-1}^{+1} \frac{T_i\{u\}}{\left[1-u^2\right]^{1/2}} \sin\left\{\frac{n.\pi}{a}\frac{w}{2}u\right\} du$$

$$+ \frac{w}{2}\sin\left\{\frac{n.\pi}{a}ms\right\}\int_{-1}^{+1} \frac{T_i\{u\}}{\left[1-u^2\right]^{1/2}} \cos\left\{\frac{n.\pi}{a}\frac{w}{2}u\right\} du \qquad \text{(A3.1.5)}$$

From the symmetric properties of the above the results may be simplified for different values of the index i:-

(i = 0,2,4,..)

$$I1_i = w \sin\left\{ \frac{n.\pi}{a} ms \right\} \int_0^{+1} \frac{T_i\{ u \}}{\left[1 - u^2 \right]^{1/2}} \cos\left\{ \frac{n.\pi}{a} \frac{w}{2} u \right\} du \qquad \text{(A3.1.6)}$$

(i = 1,3,5,..)

$$I1_i = w \cos\left\{ \frac{n.\pi}{a} ms \right\} \int_0^{+1} \frac{T_i\{ u \}}{\left[1 - u^2 \right]^{1/2}} \sin\left\{ \frac{n.\pi}{a} \frac{w}{2} u \right\} du \qquad \text{(A3.1.7)}$$

These result may now be determined from standard integrals:-

$$\int_0^{+1} \frac{T_{2j+1}\{ u \}}{\left[1 - u^2 \right]^{1/2}} \sin\{ bu \}\, du = (-1)^j \frac{\pi}{2} J_{2j+1}\{ b \} \qquad (b > 0) \qquad \text{(RG 7.355/1)}$$

$$\int_0^{+1} \frac{T_{2j}\{ u \}}{\left[1 - u^2 \right]^{1/2}} \cos\{ bu \}\, du = (-1)^j \frac{\pi}{2} J_{2j}\{ b \} \qquad (b > 0) \qquad \text{(RG 7.355/2)}$$

where J represent the Bessel functions of the first kind. From these standard identities the required integrals may be evaluated:-

(i = 0,2,4,..)

$$I1_i = w \sin\left\{ \frac{n.\pi}{a} ms \right\} (-1)^{(i/2)} \frac{\pi}{2} J_i\left\{ \frac{n.\pi}{a} \frac{w}{2} \right\} \qquad \text{(A3.1.8a)}$$

(i = 1,3,5,..)

$$I1_i = w \cos\left\{ \frac{n.\pi}{a} ms \right\} (-1)^{((i-1)/2)} \frac{\pi}{2} J_i\left\{ \frac{n.\pi}{a} \frac{w}{2} \right\} \qquad \text{(A3.1.8b)}$$

Special attention must also be paid to the terms corresponding to n = 0. These terms have the form:-

$$I2_i = \int_{ns}^{fs} \frac{T_i\left\{\frac{2(x-ms)}{w}\right\}}{\left[1-\left[\frac{2(x-ms)}{w}\right]^2\right]^{1/2}} \quad x \quad dx \qquad \text{(A3.1.9)}$$

In order to evaluate this integral the previous transformation may be used again resulting in the following:-

$$I2_i = \frac{w}{2}\ ms \int_{-1}^{+1} \frac{T_i\{u\}}{\left[1-u^2\right]^{1/2}}\ du + \frac{w}{2}\ \frac{w}{2} \int_{-1}^{+1} \frac{T_i\{u\}}{\left[1-u^2\right]^{1/2}}\ u\ du \qquad \text{(A3.1.10)}$$

By comparison with standard identities:-

$$\int_{-1}^{+1} \frac{T_i\{u\}\,T_j\{u\}}{\left[1-u^2\right]^{1/2}} = \begin{cases} 0 & (i \neq j) \\ \pi/2 & (i = j = 0) \\ \pi & (i = j \neq 0) \end{cases} \qquad \text{(RG 7.343/1)}$$

and recall that the first few Tchebyshev polynomials are given by:-

$$T_0 = 1 \qquad \text{(RG 8.943/1)}$$

$$T_1 = x \qquad \text{(RG 8.943/2)}$$

gives the result:-

$$I2_i = \begin{cases} \frac{w}{2}\ ms\ \pi & (i = 0) \\ \frac{w}{2}^2\ \frac{\pi}{2} & (i = 1) \\ 0 & (i > 1) \end{cases} \qquad \text{(A3.1.11)}$$

APPENDIX A3.2.

Derivation of longitudinal current.

To determine the longitudinal current the following integral is required:-

$$I3_i = \int_{ns}^{fs} \frac{T_i\left\{\frac{2(x-ms)}{w}\right\}}{\left[1 - \left[\frac{2(x-ms)}{w}\right]^2\right]^{1/2}} \, dx \qquad \text{(A3.2.1)}$$

In order to evaluate this integral the transformation as for appendix A3.1 may again be used:-

$$I3_i = \int_{-1}^{+1} \frac{T_i\{ u \}}{\left[1 - u^2\right]^{1/2}} \, \frac{w}{2} \, du \qquad \text{(A3.2.2)}$$

and again from the results of appendix A3.1 this gives:-

$$I3_i = \begin{cases} \frac{w}{2}\,\frac{\pi}{2} & (i = 0) \\ 0 & (i \neq 0) \end{cases} \qquad \text{(A3.2.3)}$$

APPENDIX A3.3.

Evaluation of integrals for power flow.

The integrals I4/5 are defined by:-

$$\begin{matrix} I4 \\ I5 \end{matrix}(ha,hb,k) = \int_{ha}^{hb} \frac{\begin{matrix} \sin \\ \cos \end{matrix}\{ k (y - hb) \} \; \begin{matrix} \sin \\ \cos \end{matrix}\{ k (y - hb) \}}{\begin{matrix} \sin \\ \cos \end{matrix}\{ k (ha - hb) \} \; \begin{matrix} \sin \\ \cos \end{matrix}\{ k (ha - hb) \}} \, dy \qquad \text{(A3.3.1)}$$

Using the definition:-

$$h = hb - ha$$

the integral becomes:-

$$\begin{matrix} I4 \\ I5 \end{matrix} = \frac{1}{2} \quad \frac{h \; \begin{matrix} - \\ + \end{matrix} \; \frac{1}{k} \; \sin\{ k h \} \cos\{ k h \}}{\left[\begin{matrix} \sin \\ \cos \end{matrix}\{ k h \} \right]^2} \qquad \text{(A3.3.2)}$$

These are the required results which may now be programmed on the computer.

APPENDIX A3.4.

Evaluation of integrals for mode orthogonality.

The integrals I6/7 are defined by:-

$$\begin{matrix} I6 \\ I7 \end{matrix}(ha,hb,k_p,k_q) = \int_{ha}^{hb} \frac{\begin{matrix} \sin \\ \cos \end{matrix}\{k_p(y - hb)\} \quad \begin{matrix} \sin \\ \cos \end{matrix}\{k_q(y - hb)\}}{\begin{matrix} \sin \\ \cos \end{matrix}\{k_p(ha - hb)\} \quad \begin{matrix} \sin \\ \cos \end{matrix}\{k_q(ha - hb)\}} \, dy \qquad (A3.4.1)$$

If $|k_p| = |k_q|$ then the integrals may be determined from I4 and I5 as used in the calculation of power flow (Appendix A3.3).

Using the definition:-

$$h = hb - ha$$

the integral becomes:-

$$\begin{matrix} I6 \\ I7 \end{matrix} = \frac{\begin{matrix} - \\ + \end{matrix} k_p \begin{matrix} \cot \\ \tan \end{matrix}\{k_p h\} \quad \begin{matrix} + \\ - \end{matrix} k_q \begin{matrix} \cot \\ \tan \end{matrix}\{k_q h\}}{k_p^2 - k_q^2} \qquad (A3.4.2)$$

These are the required results which may now be used to evaluate the integrals.

APPENDIX A3.5.

Derivation of the admittance terms for the dielectric overlay.

Using equation (3.72) it is possible to derive the admittance term for the dielectric overlay:-

$$Y_{e(in)} = Y_{TM}^{(1a)} \frac{Y_e^{(1b)} + j\, Y_{TM}^{(1a)} \tan\left\{k_n^{(1a)} l_a\right\}}{Y_{TM}^{(1a)} + j\, Y_e^{(1b)} \tan\left\{k_n^{(1a)} l_a\right\}}$$

$$= - \frac{j\omega\varepsilon_0\varepsilon_a}{k_n^{(1a)} \tan\left\{k_n^{(1a)} l_a\right\}} * \left[\frac{\dfrac{\varepsilon_b}{k_n^{(1b)} \tan\left\{k_n^{(1b)} l_b\right\}} - \dfrac{\varepsilon_a}{k_n^{(1a)} \cot\left\{k_n^{(1a)} l_a\right\}}}{\dfrac{\varepsilon_a}{k_n^{(1a)} \tan\left\{k_n^{(1a)} l_a\right\}} + \dfrac{\varepsilon_b}{k_n^{(1b)} \tan\left\{k_n^{(1b)} l_b\right\}}} \right] \qquad \text{(A3.5.1)}$$

The new expression for X_n (Xl_n), by comparison with (3.29), is:-

$$Xl_n = - \frac{\varepsilon_a}{k_n^{(1a)} \tan\left\{k_n^{(1a)} l_a\right\}} * \left[\frac{\dfrac{\varepsilon_b}{k_n^{(1b)} \tan\left\{k_n^{(1b)} l_b\right\}} - \dfrac{\varepsilon_a}{k_n^{(1a)} \cot\left\{k_n^{(1a)} l_a\right\}}}{\dfrac{\varepsilon_a}{k_n^{(1a)} \tan\left\{k_n^{(1a)} l_a\right\}} + \dfrac{\varepsilon_b}{k_n^{(1b)} \tan\left\{k_n^{(1b)} l_b\right\}}} \right] - \frac{\varepsilon_2}{k_n^{(2)} \tan\left\{k_n^{(2)} h2\right\}} \qquad \text{(A3.5.2)}$$

The limiting value of this term for large values of n given by:-

$$\lim_{n\to\infty} \left\{ Xl_n \right\} = \left[\frac{n.\pi}{a}\right]^{-1} \left(\varepsilon_2 + \varepsilon_a \right) \qquad \text{(A3.5.3)}$$

is only dependent on the material on either side of the interface.

Evaluation of the other term proceeds in the same way. Thus from (3.73):-

$$Y_h(in) = Y_{TE}^{(1a)} \frac{Y_h^{(1b)} + j\, Y_{TE}^{(1a)} \tan\left\{k_n^{(1a)} l_a\right\}}{Y_{TE}^{(1a)} + j\, Y_h^{(1b)} \tan\left\{k_n^{(1a)} l_a\right\}}$$

$$= \frac{k_n^{(1a)} \cot\left\{k_n^{(1a)} l_a\right\}}{j\omega\mu_0} \; * \; \left[\frac{k_n^{(1b)} \cot\left\{k_n^{(1b)} l_b\right\} - k_n^{(1a)} \tan\left\{k_n^{(1a)} l_a\right\}}{k_n^{(1a)} \cot\left\{k_n^{(1a)} l_a\right\} + k_n^{(1b)} \cot\left\{k_n^{(1b)} l_b\right\}}\right] \qquad \text{(A3.5.4)}$$

Thus the equivalent of Y_n (Yl_n) may be determined by comparison with (3.30):-

$$Yl_n = - k_n^{(1a)} \cot\left\{k_n^{(1a)} l_a\right\} \; * \; \left[\frac{k_n^{(1b)} \cot\left\{k_n^{(1b)} l_b\right\} - k_n^{(1a)} \tan\left\{k_n^{(1a)} l_a\right\}}{k_n^{(1a)} \cot\left\{k_n^{(1a)} l_a\right\} + k_n^{(1b)} \cot\left\{k_n^{(1b)} l_b\right\}}\right] - k_n^{(2)} \cot\left\{k_n^{(2)} h2\right\} \qquad \text{(A3.5.5)}$$

The limiting value of this expression for large values of the index n is given by:-

$$\lim_{n\to\infty} \left\{Yl_n\right\} = \left[\frac{n.\pi}{a}\right] \; (-2) \qquad \text{(A3.5.6)}$$

and is independent of the thickness of the overlay or its effective permittivity. In practice, the asymptotic formulas derived will become less useful for impractical dimensions of the thicknesses and in general attention must be paid to these numerical problems.

TABLE 3.1

Magnitude of the coupling coefficients of the modes of 3.2 mm. strip.

Mode	Electric Field 0	1	2	3	4	5	6	7	8	9	10
0	1.000000	0.003E-6	0.028E-6	0.062E-6	0.047E-6	0.244E-6	0.065E-6	0.089E-6	0.003E-6	0.068E-6	0.601E-6
1	0.011E-6	1.000000	0.003E-6	0.006E-6	0.004E-6	0.019E-6	0.005E-6	0.006E-6	0.000E-6	0.005E-6	0.041E-6
2	0.032E-6	0.001E-6	1.000000	0.012E-6	0.006E-6	0.033E-6	0.008E-6	0.010E-6	0.000E-6	0.008E-6	0.068E-6
3	0.068E-6	0.001E-6	0.010E-6	1.000000	0.012E-6	0.062E-6	0.014E-6	0.018E-6	0.000E-6	0.015E-6	0.128E-6
4	0.028E-6	0.000E-6	0.003E-6	0.008E-6	1.000000	0.020E-6	0.004E-6	0.006E-6	0.000E-6	0.005E-6	0.040E-6
5	0.141E-6	0.002E-6	0.014E-6	0.032E-6	0.013E-6	1.000000	0.015E-6	0.018E-6	0.000E-6	0.015E-6	0.131E-6
6	0.028E-6	0.000E-6	0.003E-6	0.006E-6	0.002E-6	0.013E-6	1.000000	0.003E-6	0.000E-6	0.003E-6	0.024E-6
7	0.034E-6	0.000E-6	0.004E-6	0.009E-6	0.004E-6	0.022E-6	0.005E-6	1.000000	0.000E-6	0.005E-6	0.043E-6
8	0.000E-6	0.000E-6	0.001E-6	0.002E-6	0.001E-6	0.005E-6	0.001E-6	0.002E-6	1.000000	0.001E-6	0.013E-6
9	0.028E-6	0.000E-6	0.002E-6	0.006E-6	0.002E-6	0.012E-6	0.002E-6	0.003E-6	0.000E-6	1.000000	0.020E-6
10	0.235E-6	0.002E-6	0.019E-6	0.044E-6	0.016E-6	0.088E-6	0.017E-6	0.020E-6	0.001E-6	0.017E-6	1.000000

Magnetic Field.

TABLE 3.2

Magnitude of the coupling coefficients of the modes of 7.8 mm. strip.

Mode	Electric Field 0	1	2	3	4	5	6	7	8	9	10
0	1.000000	0.003E-6	0.015E-6	0.036E-6	0.026E-6	0.155E-6	0.009E-6	0.014E-6	0.058E-6	0.066E-6	0.414E-6
1	0.006E-6	1.000000	0.001E-6	0.004E-6	0.002E-6	0.014E-6	0.001E-6	0.002E-6	0.005E-6	0.006E-6	0.034E-6
2	0.014E-6	0.000E-6	1.000000	0.008E-6	0.003E-6	0.024E-6	0.002E-6	0.003E-6	0.007E-6	0.009E-6	0.056E-6
3	0.039E-6	0.000E-6	0.004E-6	1.000000	0.005E-6	0.042E-6	0.003E-6	0.007E-6	0.012E-6	0.016E-6	0.095E-6
4	0.011E-6	0.000E-6	0.002E-6	0.008E-6	1.000000	0.025E-6	0.002E-6	0.003E-6	0.008E-6	0.010E-6	0.059E-6
5	0.088E-6	0.001E-6	0.005E-6	0.022E-6	0.004E-6	1.000000	0.004E-6	0.011E-6	0.013E-6	0.018E-6	0.106E-6
6	0.006E-6	0.000E-6	0.000E-6	0.001E-6	0.001E-6	0.004E-6	1.000000	0.000E-6	0.002E-6	0.002E-6	0.013E-6
7	0.015E-6	0.001E-6	0.003E-6	0.006E-6	0.005E-6	0.026E-6	0.002E-6	1.000000	0.010E-6	0.011E-6	0.072E-6
8	0.020E-6	0.000E-6	0.002E-6	0.008E-6	0.003E-6	0.023E-6	0.002E-6	0.004E-6	1.000000	0.009E-6	0.053E-6
9	0.028E-6	0.000E-6	0.001E-6	0.005E-6	0.000E-6	0.011E-6	0.001E-6	0.003E-6	0.002E-6	1.000000	0.018E-6
10	0.159E-6	0.002E-6	0.007E-6	0.033E-6	0.004E-6	0.071E-6	0.006E-6	0.017E-6	0.014E-6	0.023E-6	1.000000

Magnetic Field.

Figures. Page.

Page.

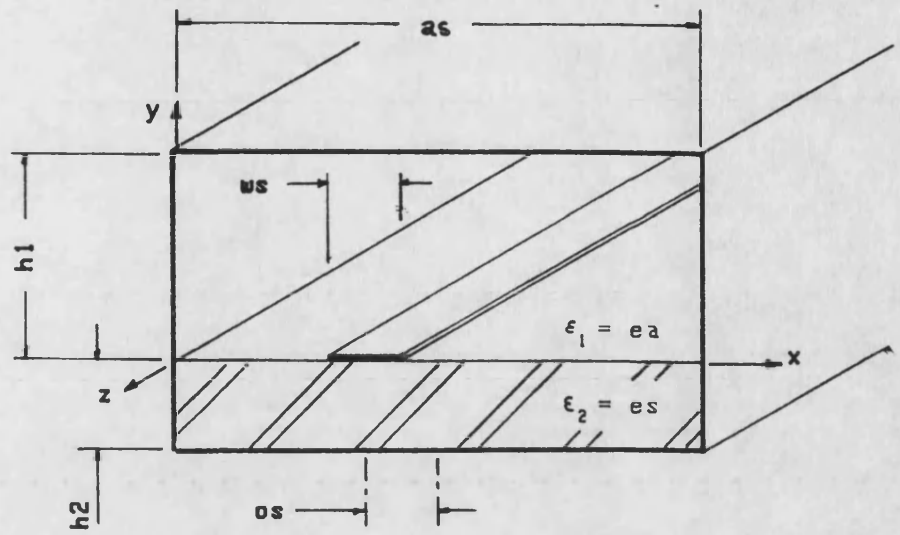

(a) Single layer shielded microstrip.

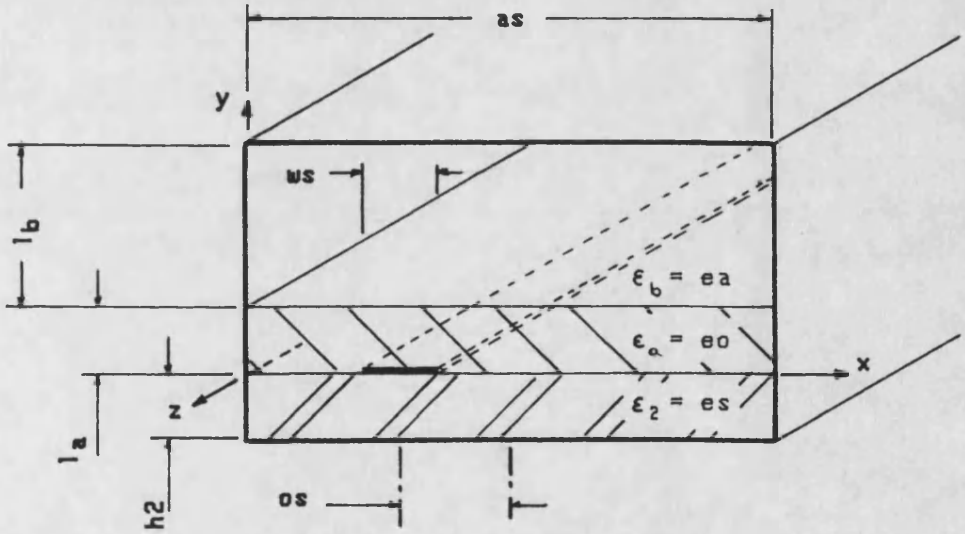

(b) Microstrip with dielectric overlay.

Fig.(3.1)

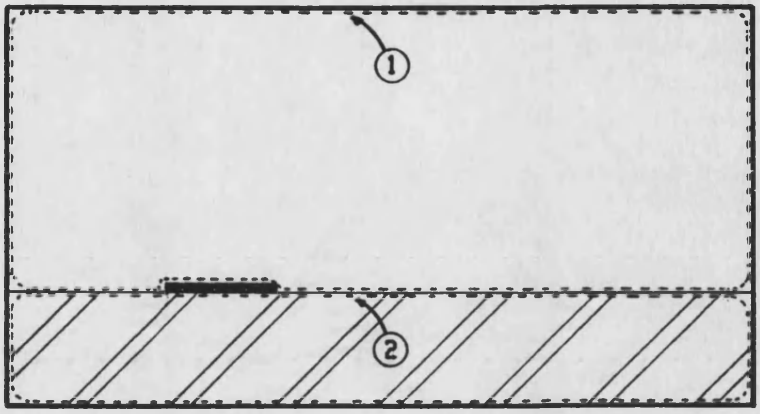

① Contour defined by the boundary of the air region.

② Contour defined by the boundary of the substrate.

Contour definitions for the variational technique.

Fig.(3.2)

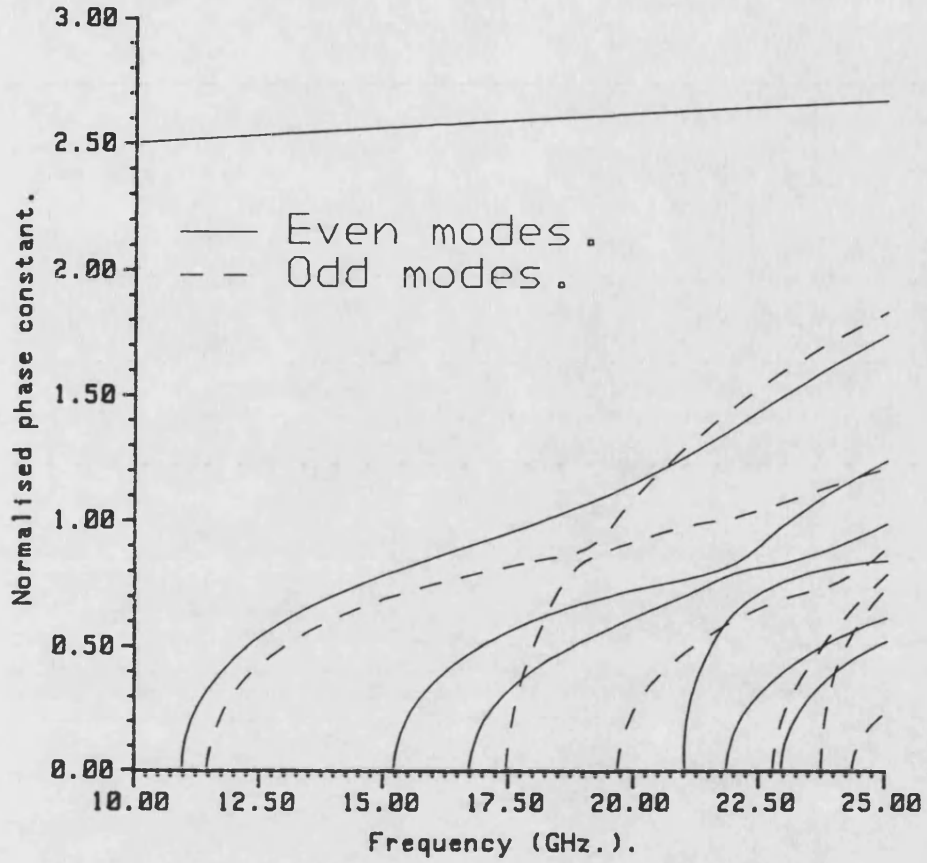

as = 12.700 mm. ws = 0.635 mm.
ha = 11.430 mm. ea = 1.000
hs = 1.270 mm. es = 8.875
symmetric strip

Theoretical data showing dependence of higher order modes on strip width.

Fig.(3.3a)

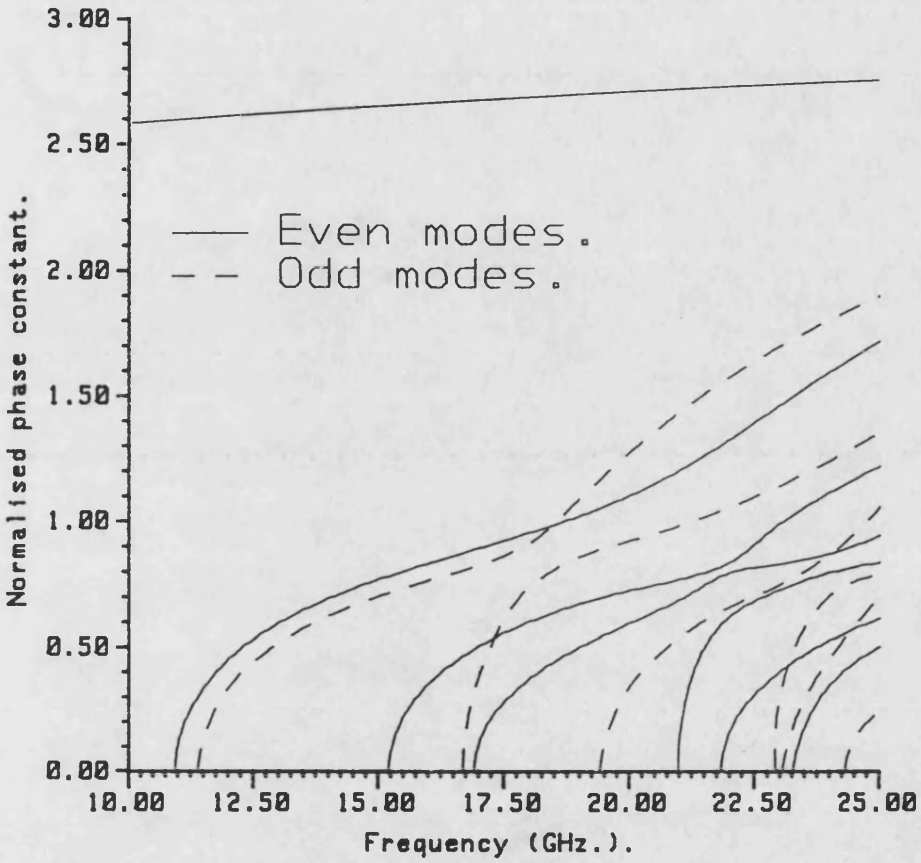

as = 12.700 mm. ws = 1.270 mm.
ha = 11.430 mm. ea = 1.000
hs = 1.270 mm. es = 8.875
symmetric strip

Theoretical data showing dependence of higher order modes on strip width.

Fig.(3.3b)

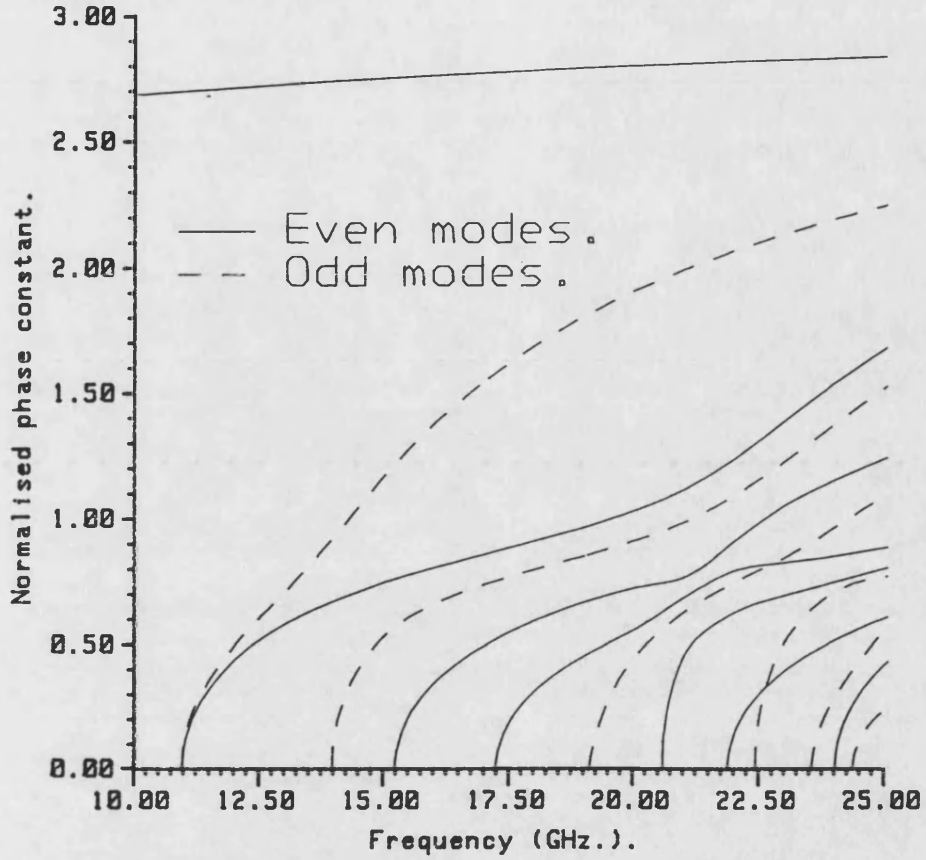

as = 12.700 mm. ws = 2.540 mm.
ha = 11.430 mm. ea = 1.000
hs = 1.270 mm. es = 8.875
symmetric strip

Theoretical data showing dependence of higher order modes on strip width.

Fig.(3.3c)

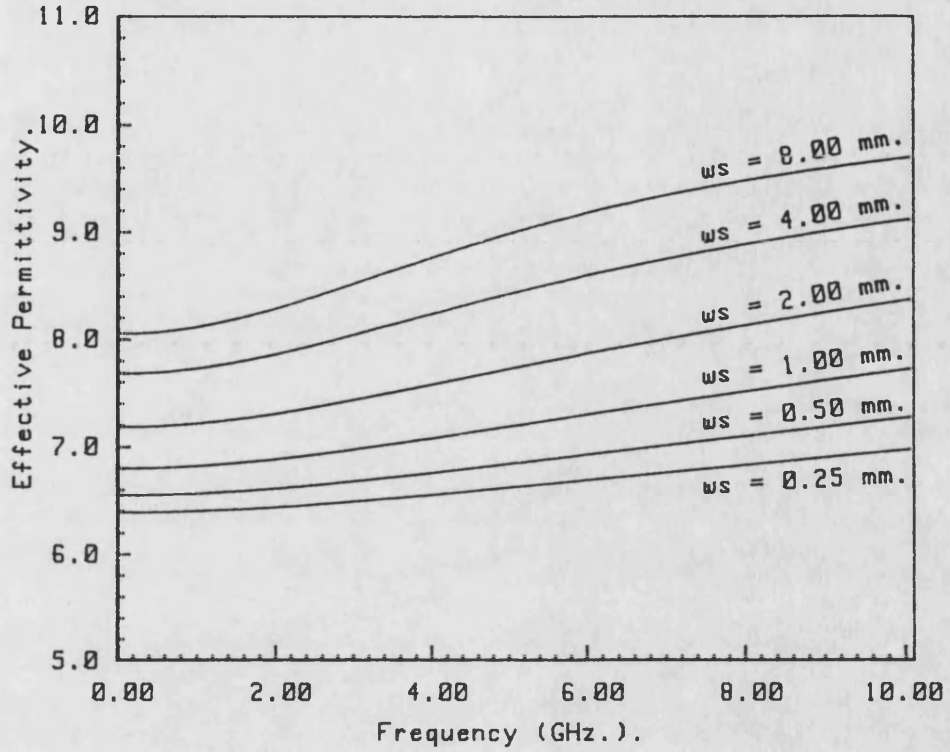

as = 12.700 mm.
ha = 11.430 mm. ea = 1.015
hs = 1.270 mm. es = 10.500

Effective permittivity variation for the symmetric strip of fig.(3.1).

Fig.(3.4)

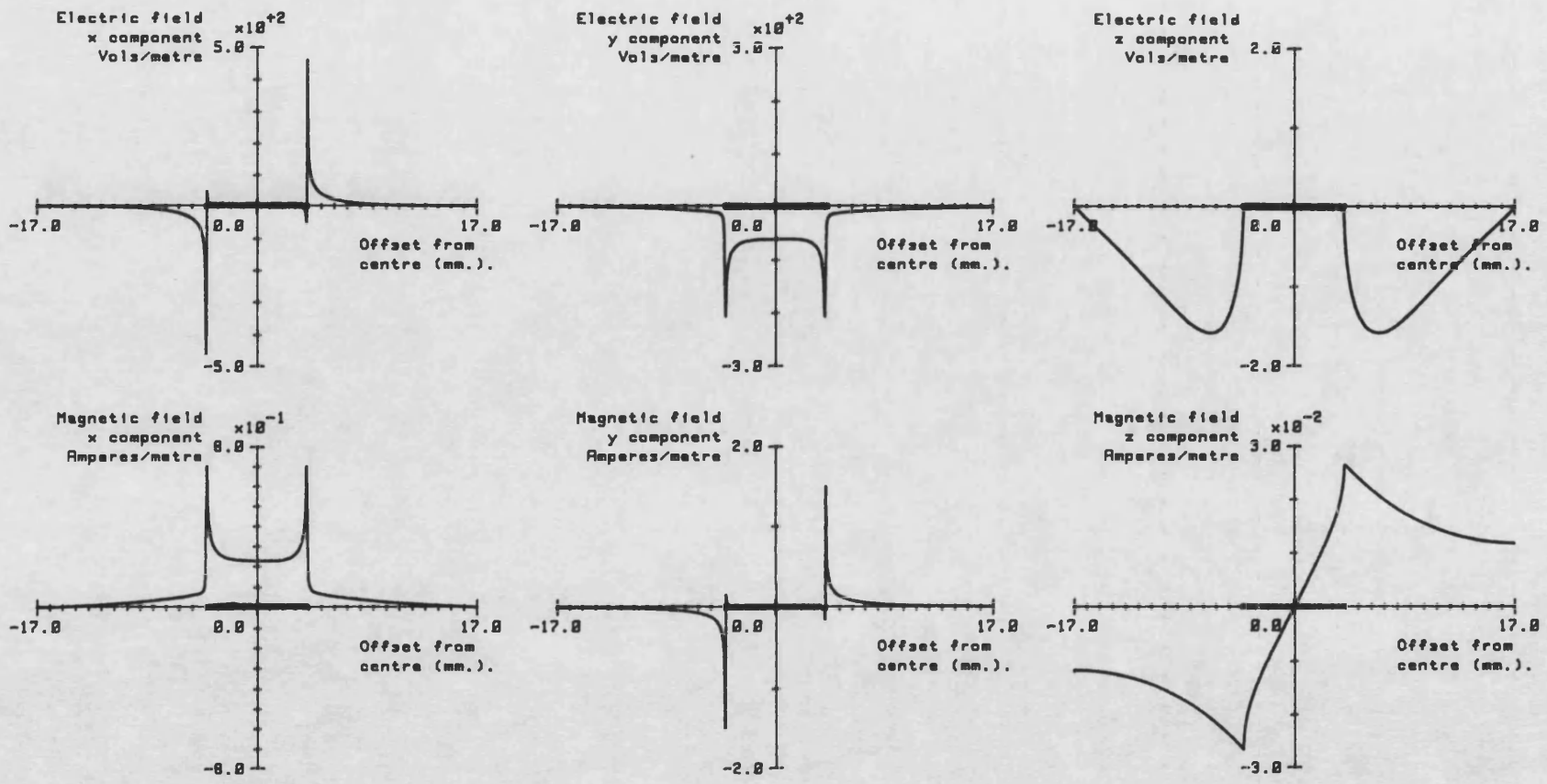

Fig.(3.5) Field plots for the fundamental mode.

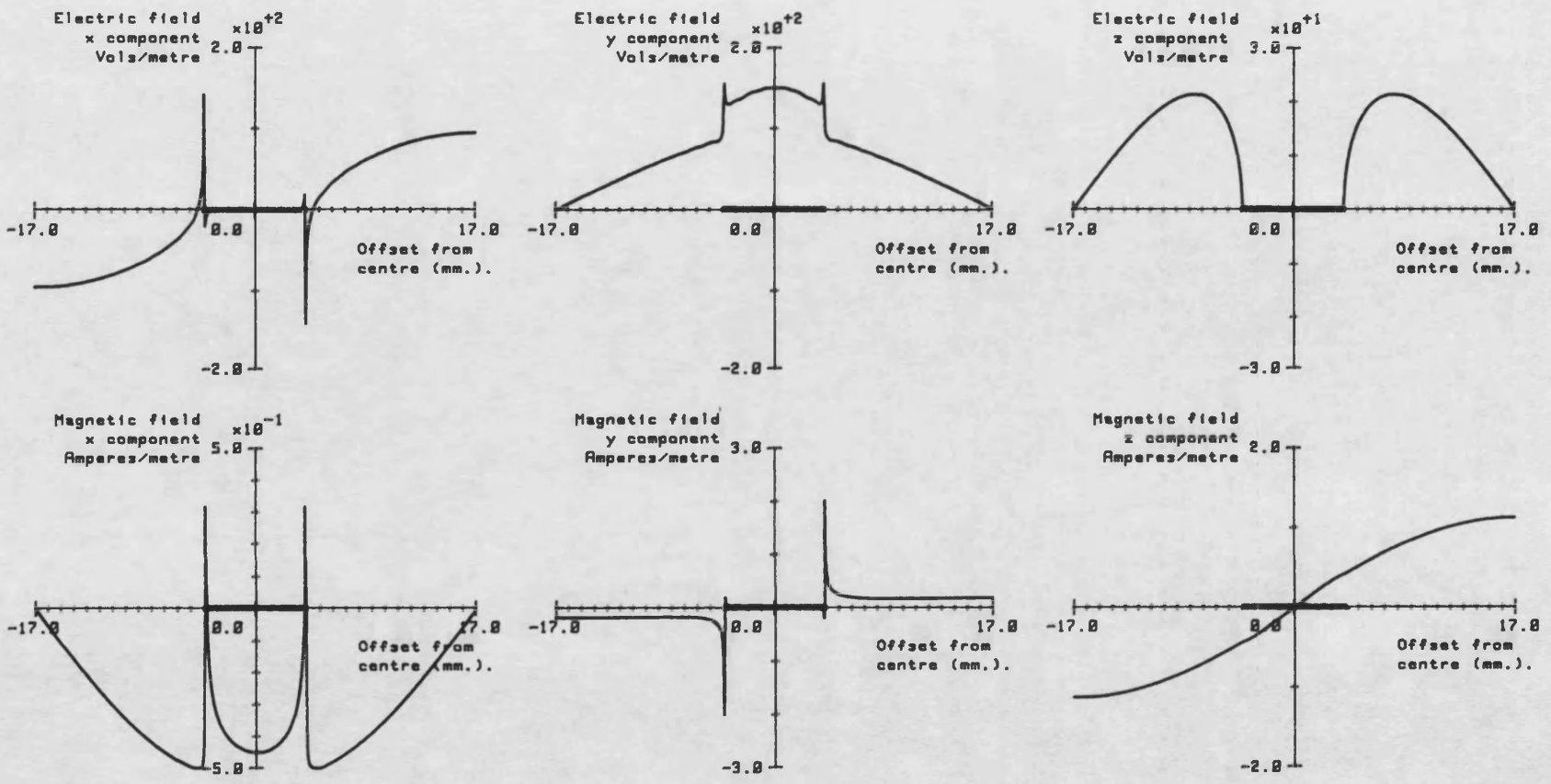

Fig.(3.6) Field plots for a higher order mode.

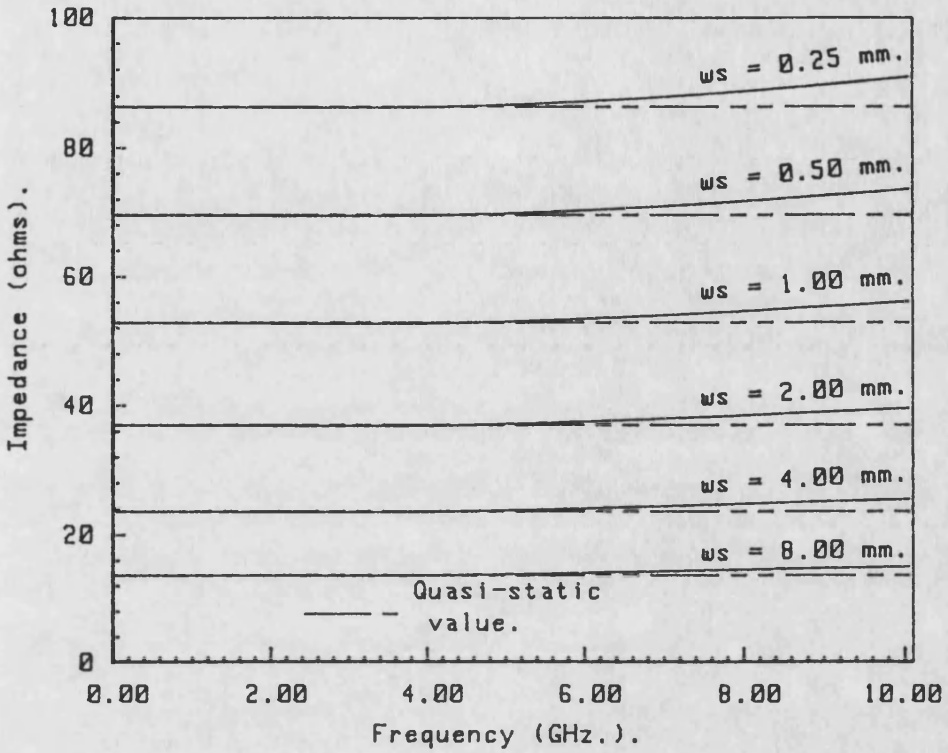

as = 12.700 mm.
ha = 11.430 mm. ea = 1.015
hs = 1.270 mm. es = 10.500

Characteristic impedance variaion for the symmetric strip of fig.(3.1a).

Fig.(3.7)

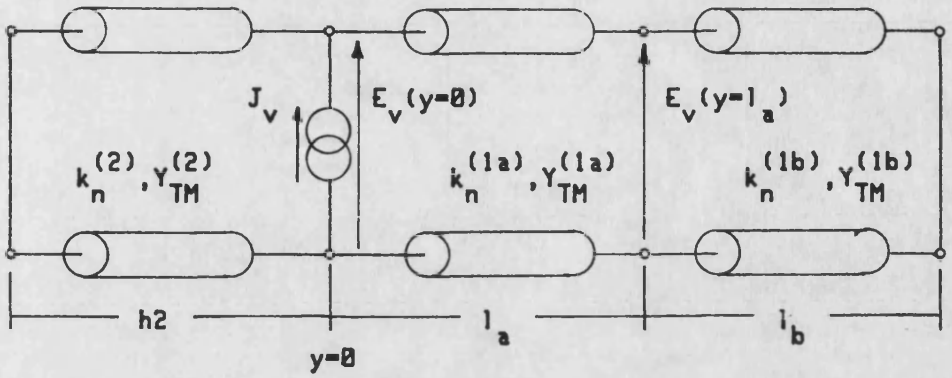

(a) Equivalent TM circuit for shielded microstrip with overlay dielectric.

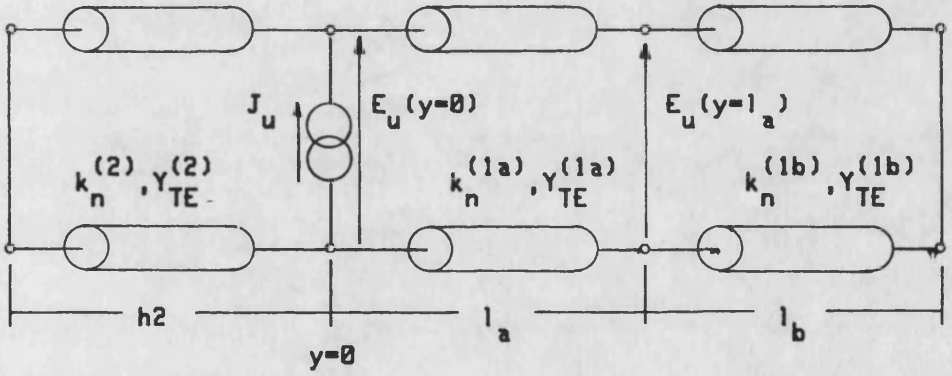

(b) Equivalent TE circuit for shielded microstrip with overlay dielectric.

Fig.(3.8)

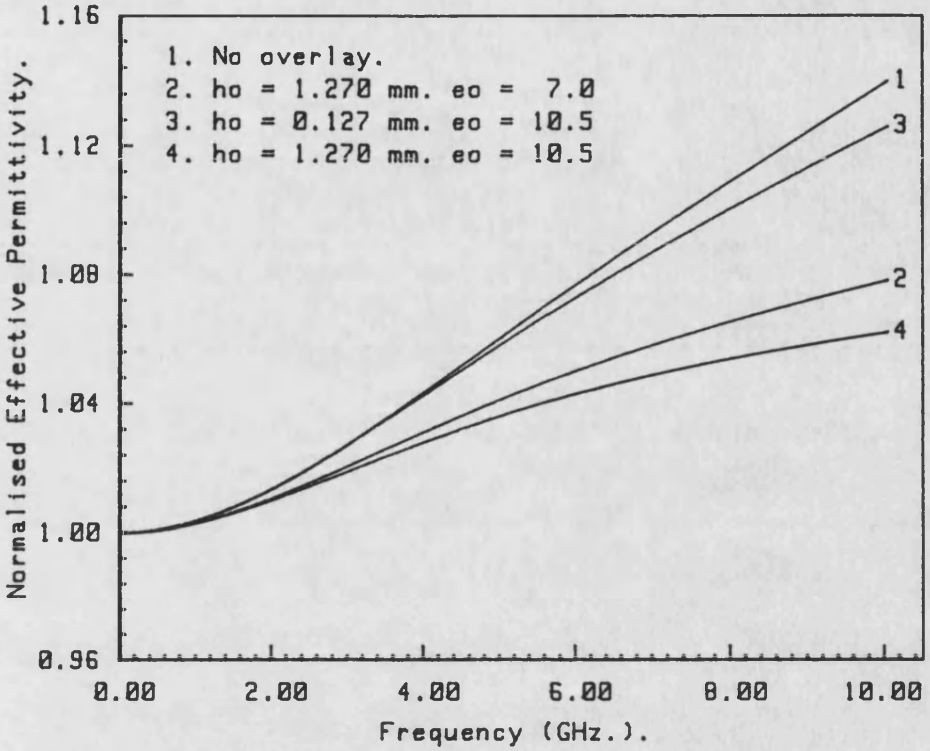

as = 12.700 mm.
ha-ho = 11.430 mm. ea = 1.015
hs = 1.270 mm. es = 10.500

Effective permittivity variation for the symmetric strip of fig.(3.1b).

Fig.(3.9)

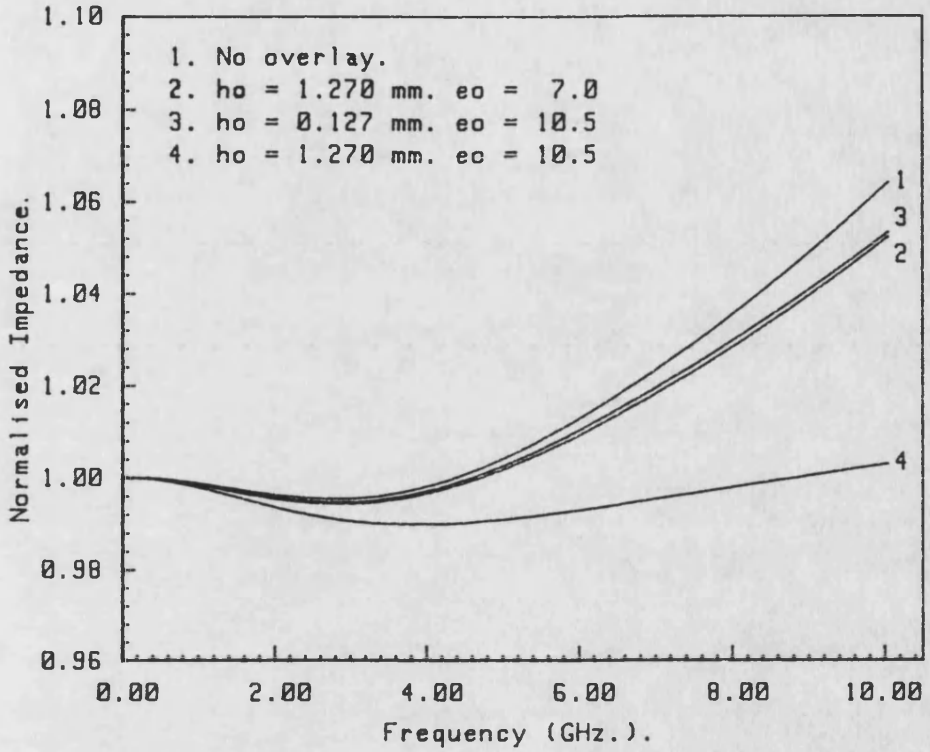

as = 12.700 mm.
ha-ho = 11.430 mm. ea = 1.015
hs = 1.270 mm. es = 10.500

Characteristic impedance variation for the symmetric strip of fig.(3.1b).

Fig.(3.10)

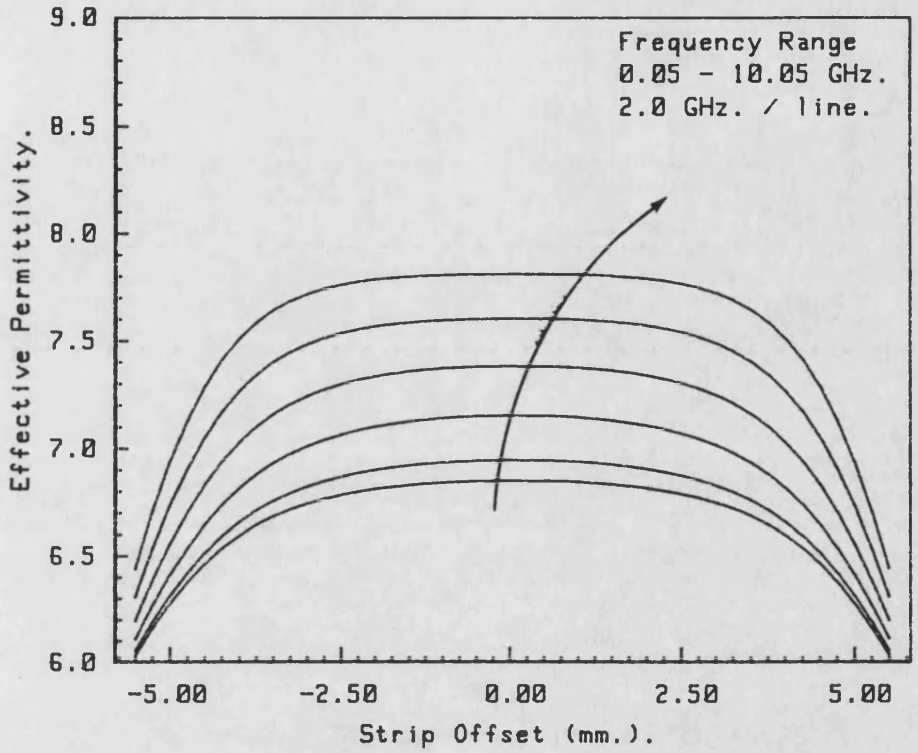

as = 12.700 mm. ws = 1.100 mm.
ha = 11.430 mm. ea = 1.015
hs = 1.270 mm. es = 10.500

Effective permittivity variation for the asymmetric strip of fig.(3.1a).

Fig.(3.11).

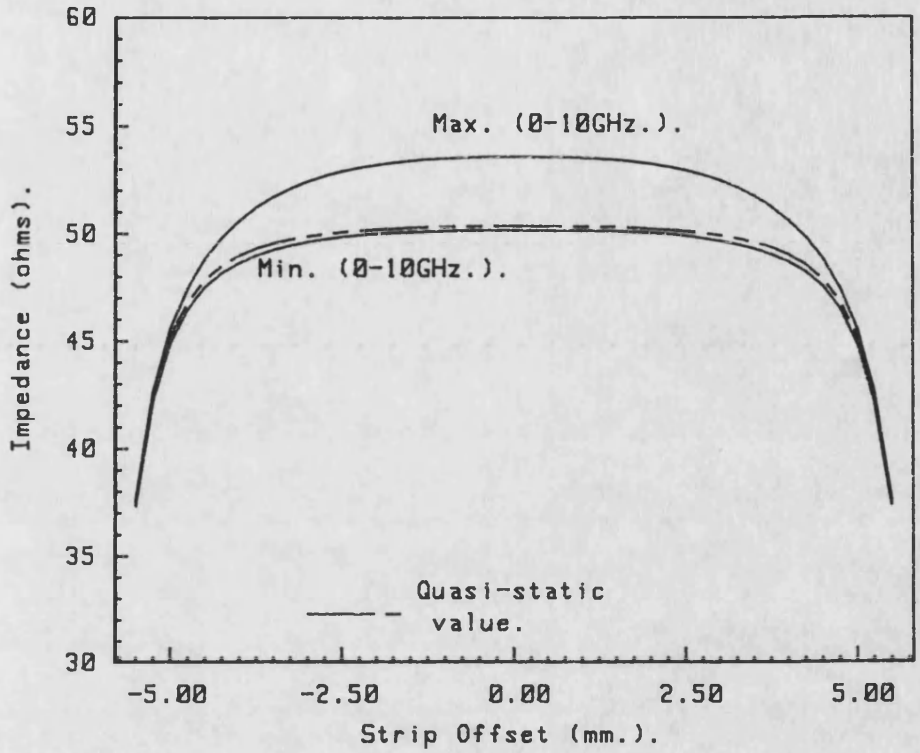

as = 12.700 mm. ws = 1.100 mm.
ha = 11.430 mm. ea = 1.015
hs = 1.270 mm. es = 10.500

Characteristic impedance variation for the asymmetric strip of fig.(3.1a).

Fig.(3.12)

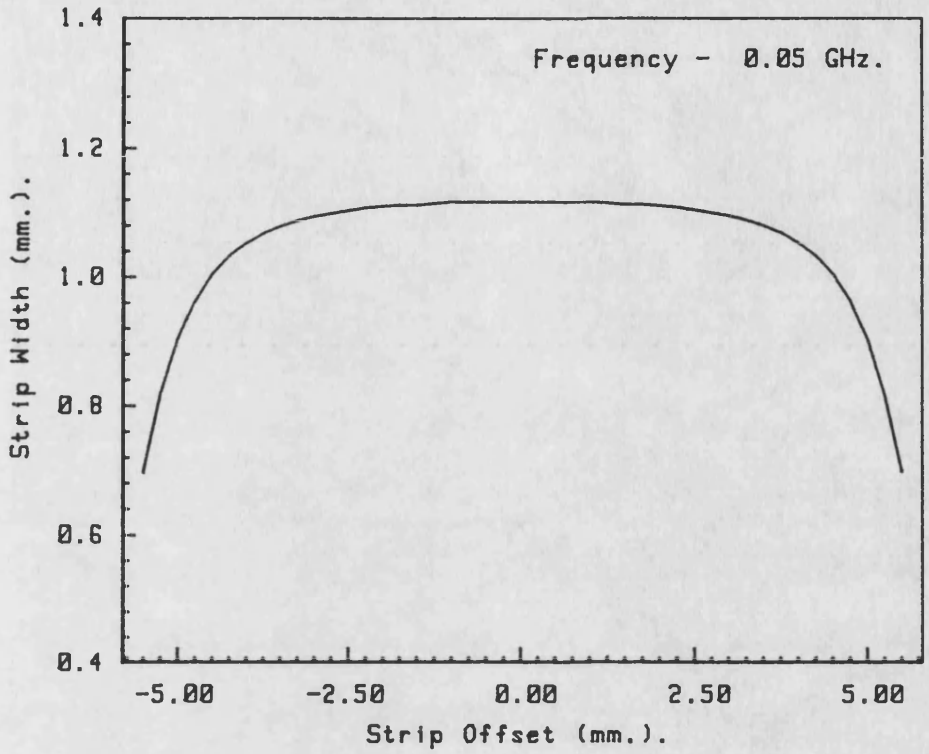

as = 12.700 mm.
ha = 11.430 mm. ea = 1.015
hs = 1.270 mm. es = 10.500

Required width to maintain a constant characteristic impedance.

Fig.(3.13)

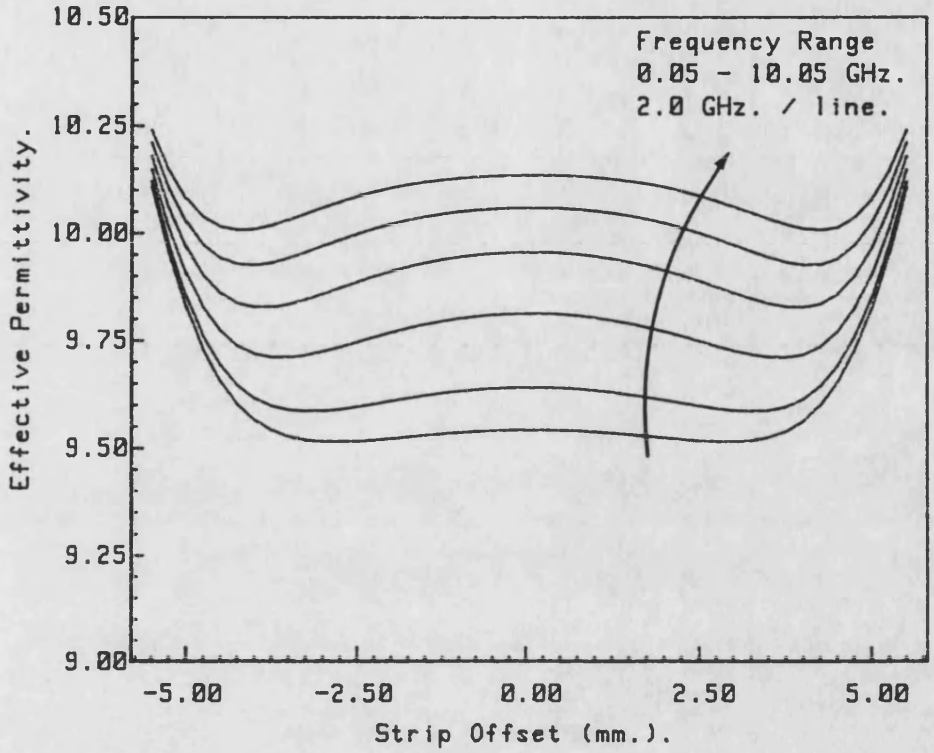

as = 12.700 mm. ws = 1.100 mm.
ha = 10.160 mm. ea = 1.015
hs = 1.270 mm. es = 10.500
ho = 1.270 mm. eo = 10.500

Effective permittivity variation for the asymmetric strip of fig.(3.1b).

Fig.(3.14)

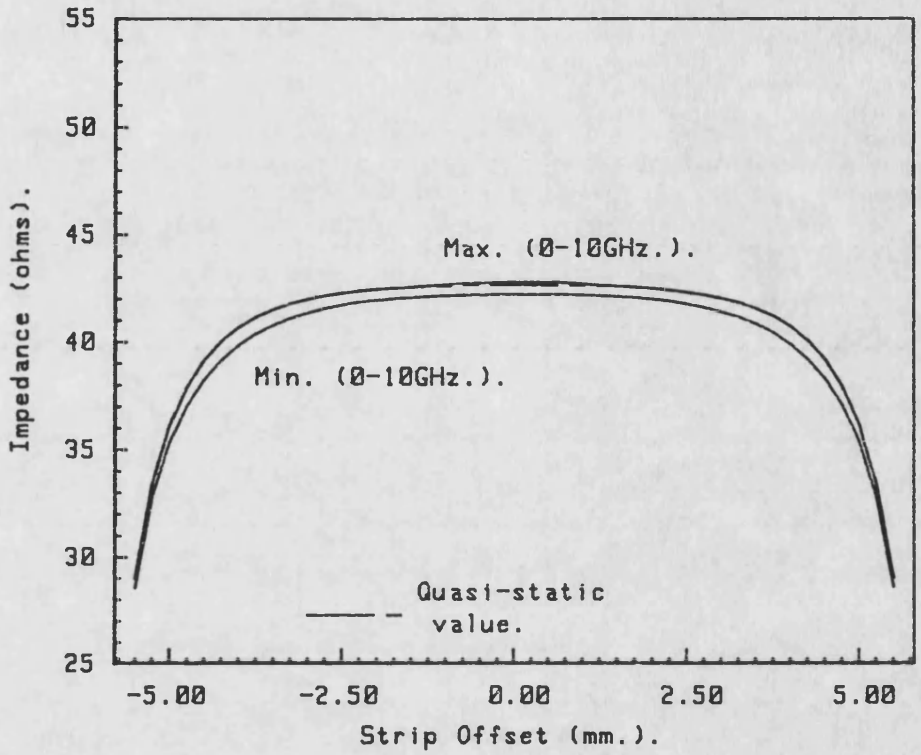

as = 12.700 mm. ws = 1.100 mm.
ha = 10.160 mm. ea = 1.015
hs = 1.270 mm. es = 10.500
ho = 1.270 mm. eo = 10.500

Characteristic impedance variation for the asymmetric strip of fig.(3.1b).

Fig.(3.15)

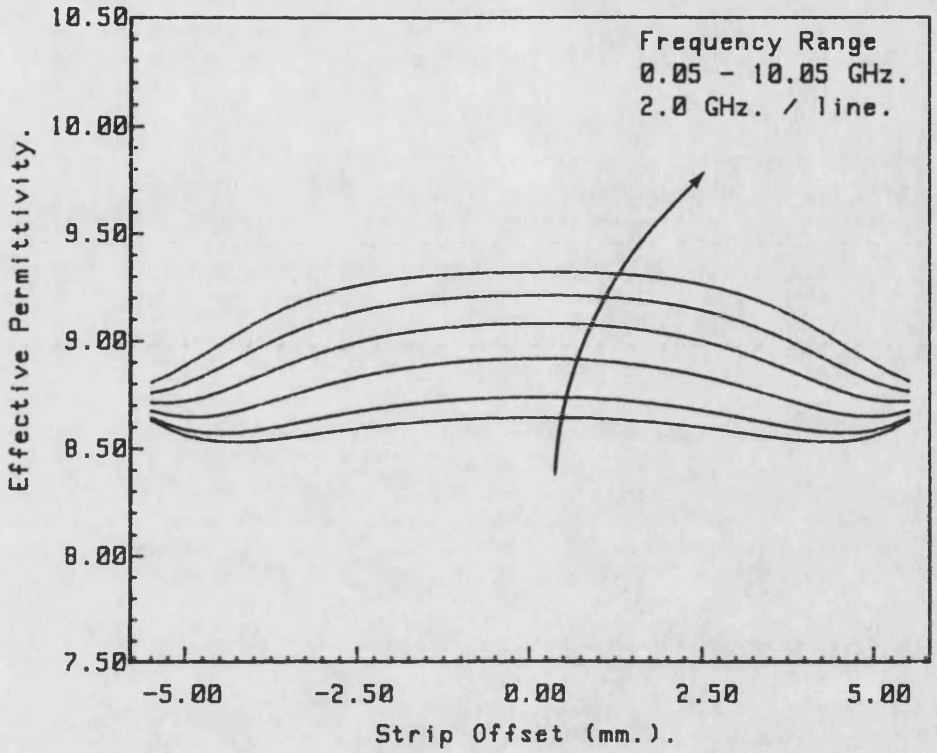

as = 12.700 mm. ws = 1.100 mm.
ha = 10.160 mm. ea = 1.015
hs = 1.270 mm. es = 10.500
ho = 1.270 mm. eo = 7.000

Effective permittivity variation for the asymmetric strip of fig.(3.1b).

Fig.(3.16)

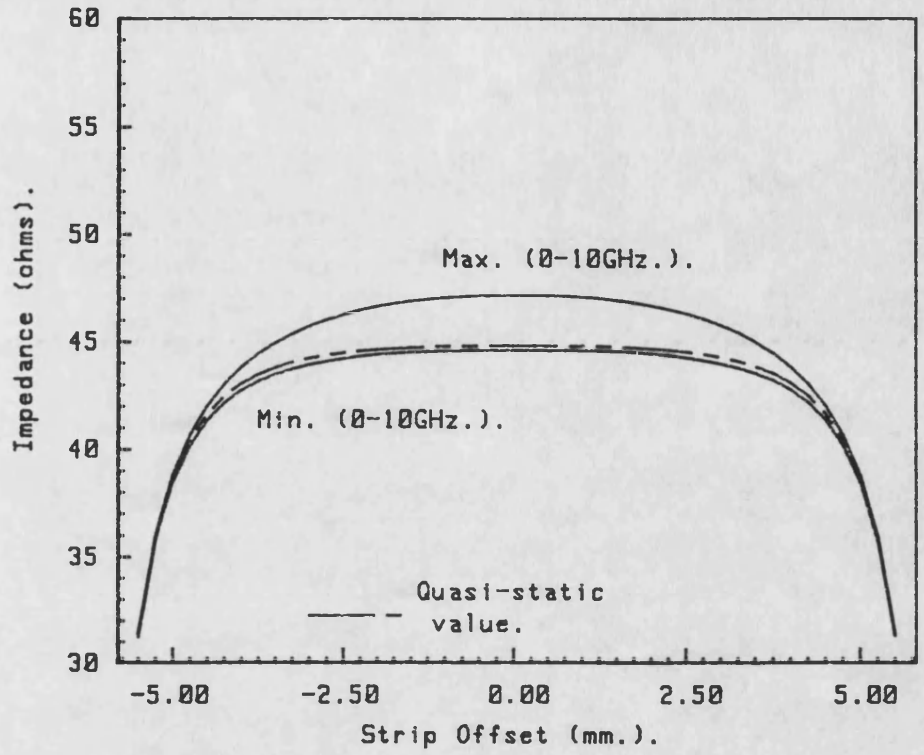

as = 12.700 mm. ws = 1.100 mm.
ha = 10.160 mm. ea = 1.015
hs = 1.270 mm. es = 10.500
ho = 1.270 mm. eo = 7.000

Characteristic impedance variation for the asymmetric strip of fig.(3.1b).

Fig.(3.17)

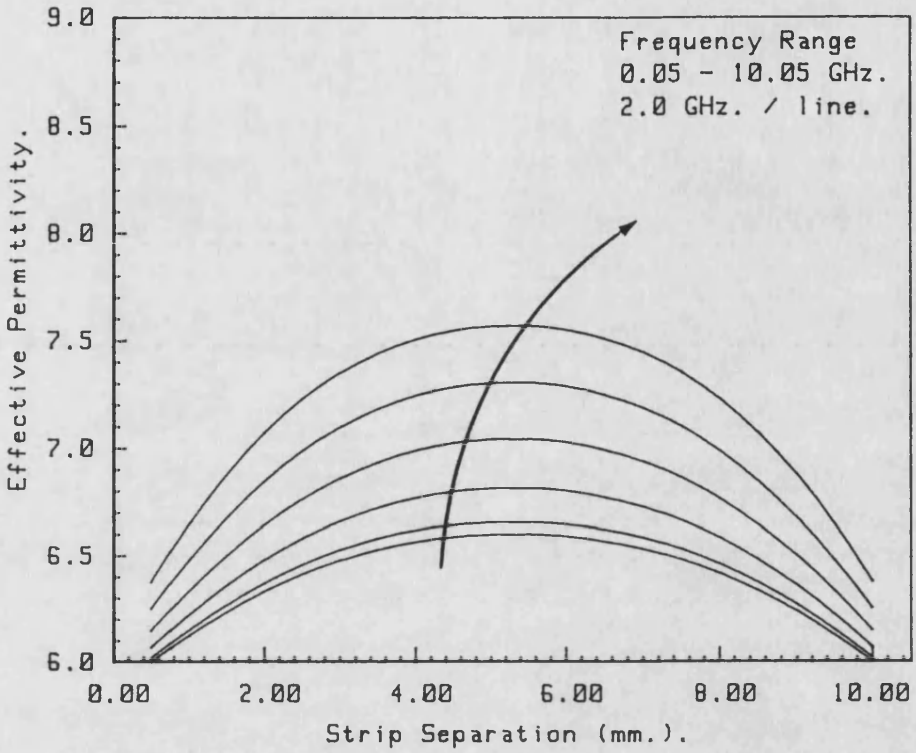

as = 12.700 mm. ws = 1.100 mm.
ha = 11.430 mm. ea = 1.015
hs = 1.270 mm. es = 10.500

Effective permittivity variation for the odd mode of symmetric twin strips.

Fig.(3.18)

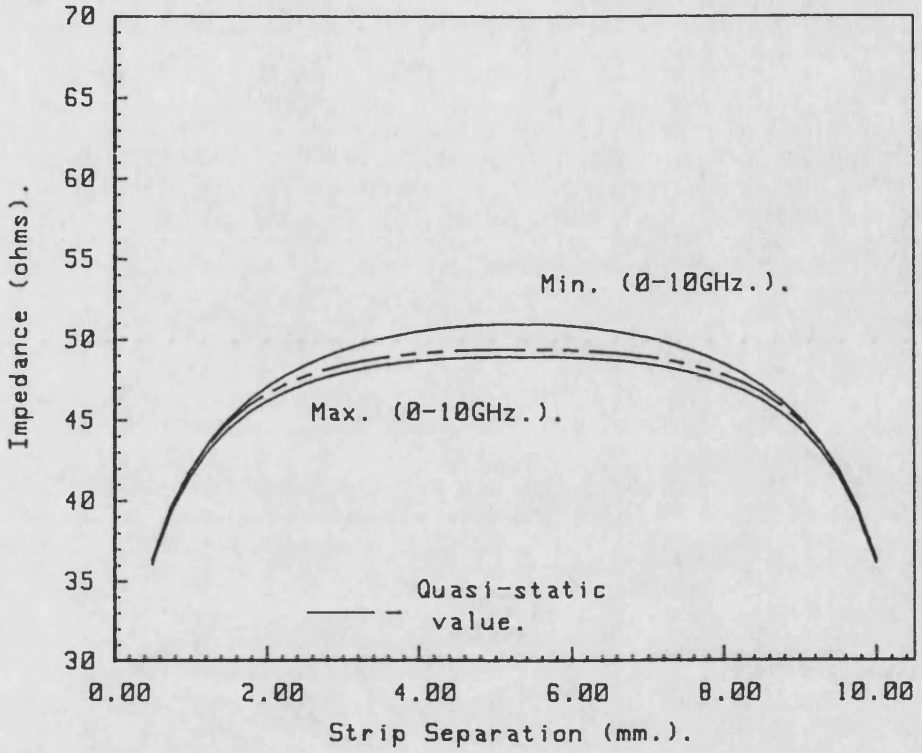

as = 12.700 mm. ws = 1.100 mm.
ha = 11.430 mm. ea = 1.015
hs = 1.270 mm. es = 10.500

Characteristic impedance variation for the odd mode of symmetric twin strips.

Fig.(3.19)

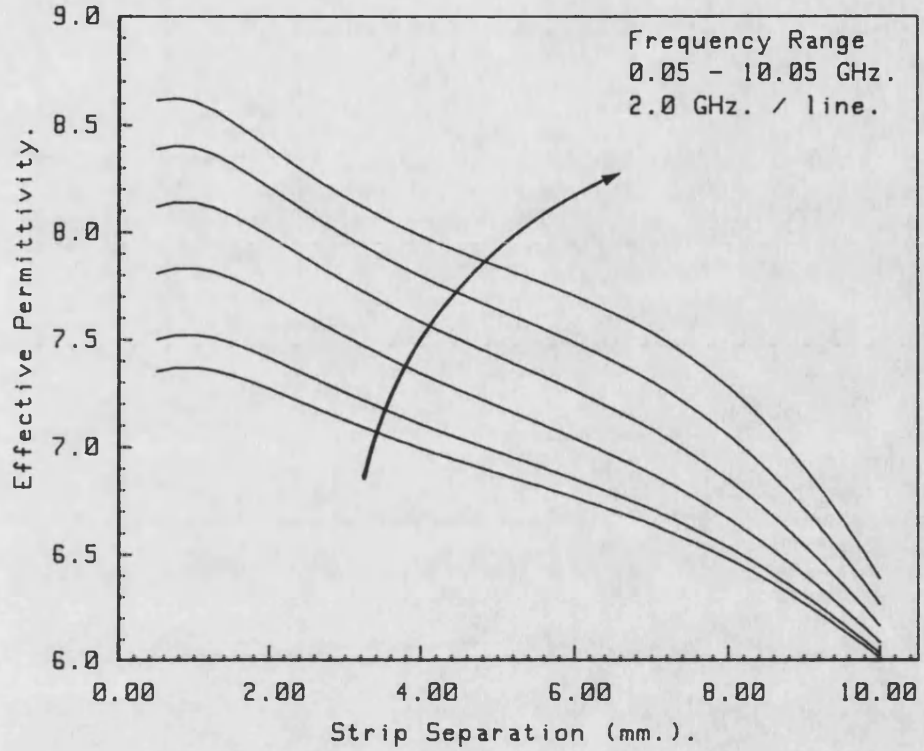

as = 12.700 mm. ws = 1.100 mm.
ha = 11.430 mm. ea = 1.015
hs = 1.270 mm. es = 10.500

Effective permittivity variation for the even mode of symmetric twin strips.

Fig.(3.20)

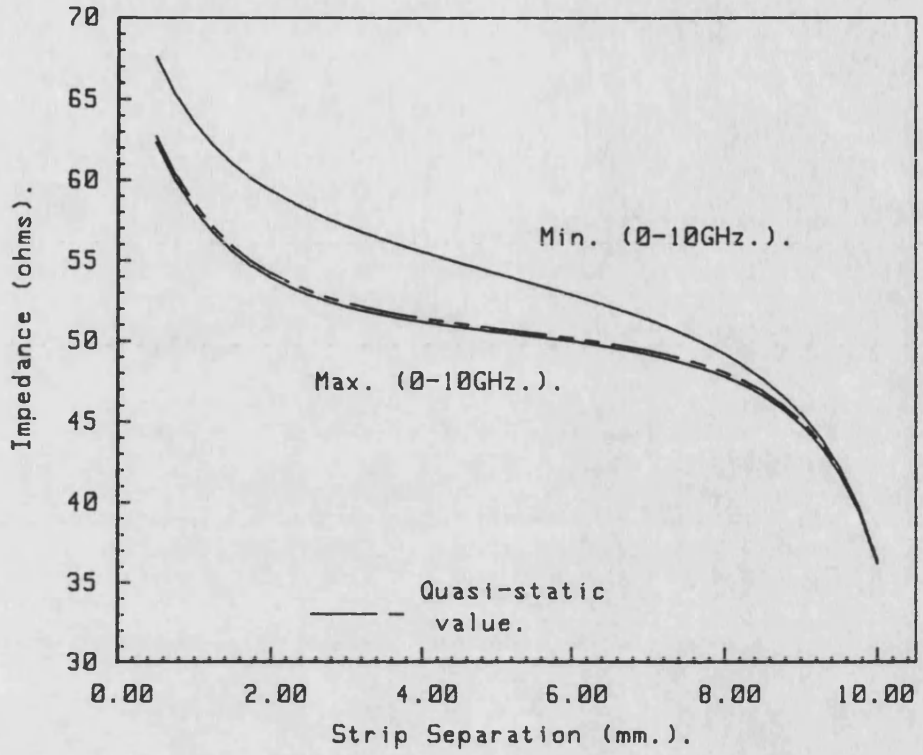

as = 12.700 mm. ws = 1.100 mm.
ha = 11.430 mm. ea = 1.015
hs = 1.270 mm. es = 10.500

Characteristic impedance variation for the even mode of symmetric twin strips.

Fig.(3.21)

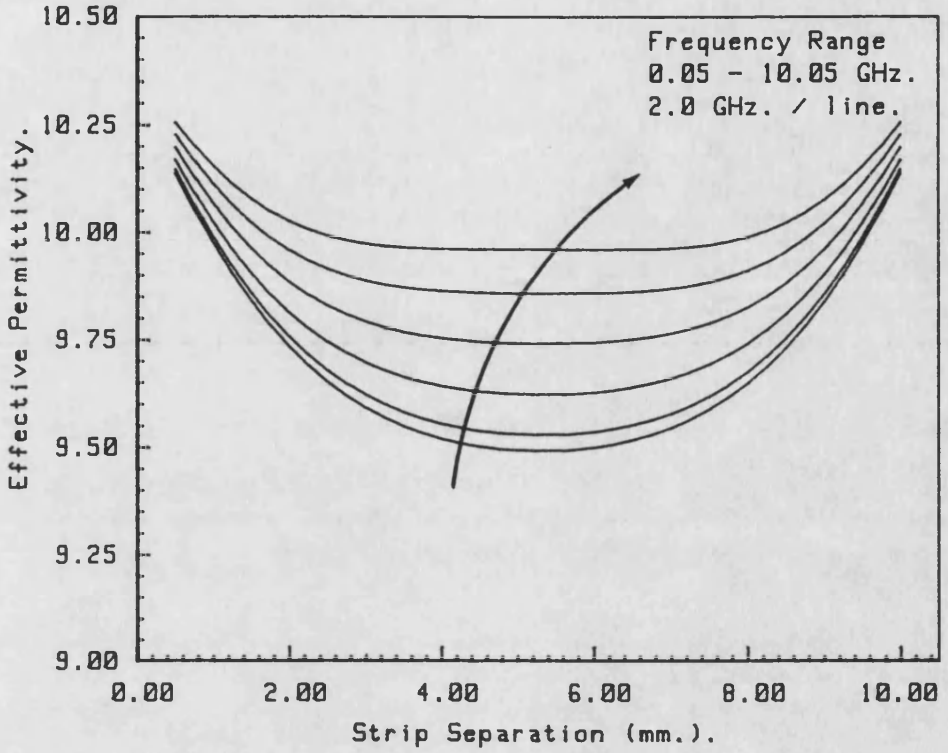

as = 12.700 mm. ws = 1.100 mm.
ha = 10.160 mm. ea = 1.015
hs = 1.270 mm. es = 10.500
ho = 1.270 mm. eo = 10.500

Effective permittivity for the odd mode of symmetric twin strips with overlay.

Fig.(3.22)

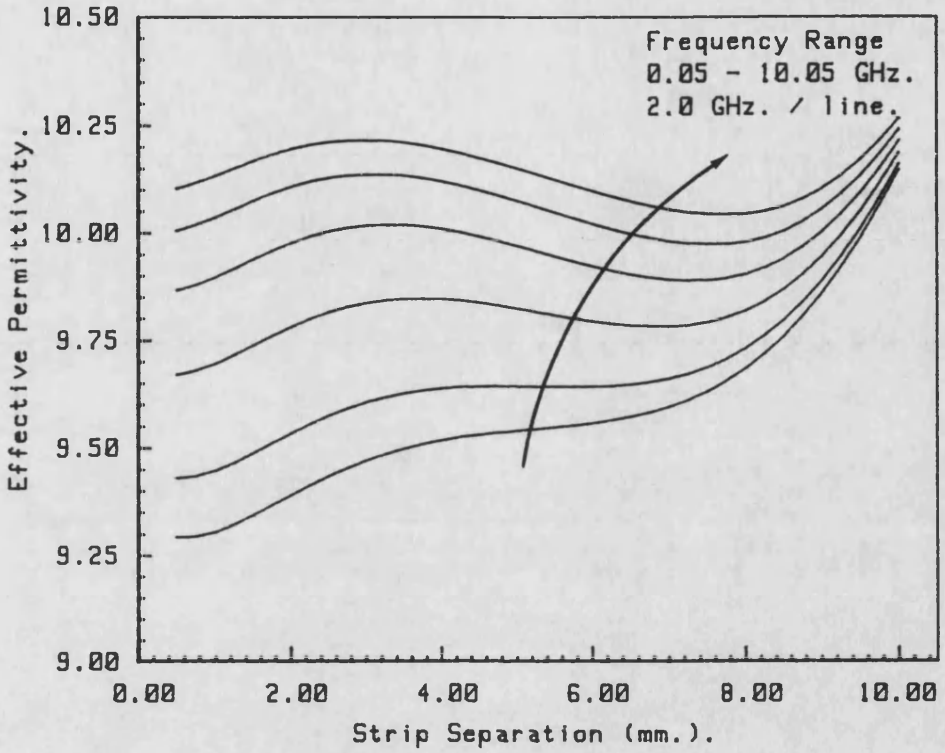

as = 12.700 mm. ws = 1.100 mm.
ha = 10.160 mm. ea = 1.015
hs = 1.270 mm. es = 10.500
ho = 1.270 mm. eo = 10.500

Effective permittivity for the even mode of symmetric twin strips with overlay.

Fig.(3.23)

CHAPTER FOUR

ELEMENTARY EXPERIMENTAL TECHNIQUES

Having theoretically analysed the continuous shielded microstrip transmission line it is important to verify these calculations, not because the mathematical techniques are in any doubt but because it is important to verify that the approximations used do not affect the final results significantly. This must be done before proceeding with the analysis of discontinuities which requires the understanding of both the fundamental and the higher order modes.

Measurements on open microstrip lines are frequently performed with the use of probes (see for example Dahale & Cullen [1]). However, although there have been attempts to use probes inside shielding no satisfactory method has been provided. Such an investigation has not, therefore, been pursued.

In its place a system of test jigs has been designed for fixed box dimensions for which different sizes of substrate may be placed having different dielectric constants and various microstrip layouts, suitable for both resonance and calibration techniques. The value of effective permittivity for the fundamental mode may be determined using resonance procedures. Further, it will be shown that this method also enables the evaluation of the phase velocities of the higher order modes provided that they are propagating. Using this technique it is also possible to investigate twin strips and offset strips as well the effects of overlay. Although not explicitly covered this technique also provides a method for determining the loss in the guided wave by determining the quality factor of modes at resonance.

4.1 Design of test jig.

The test jig used most accurately represents the ideal structure and is based on the design used by Heuven & Vlek [2]. The ground plane and sidewalls are constructed from a single block of brass which is chosen for its high conductivity and for practical reasons since it is easily machined. To complete the enclosure a removable lid is used which may be screwed firmly into place. The ends of the sections have been constructed to allow other units to be aligned accurately and fixed firmly and, further, allows for short circuit terminations and connection to coaxial cable.

Two sets of jigs have been constructed which are suitable for different types of substrate upon which any metallisation is fabricated. The first has a square cross section of dimension 34·0mm. and a maximum length of 200·0mm.. The lowest order waveguide mode of the empty guide appears at approximately 4·41 GHz.. The second set again has a square cross section but has smaller dimensions of 12·7mm. and a maximum length of 50·0mm.. The associated waveguide mode first appears at 11·81 GHz..

In order to be able to determine the propagation constant of the microstrip line by resonance methods the typical guide wavelength needs to be of the order of the maximum length. Secondly, for the more advanced experimental techniques to be used later it is important that this guide wavelength is kept as low as possible to ensure that different test pieces have identical electrical lengths. This makes the first set more suitable for lower dielectric substrate (ε_r = 2·33) the second set is more suitable for higher dielectric substrates (ε_r = 10·5).

4.2 Resonance techniques.

Before investigating the microstrip, the empty cavity formed by using two short circuits on the ends of a single test section, was tested by resonance. The short circuits used had small holes drilled in them through which small circular loops formed in the end of a piece of semi-rigid coaxial cable may be inserted in order to couple to the magnetic field in the guide. The frequencies at which the system resonates, as indicated by a peak in the transmission between the probes, are determined by the length of the jig such that at resonance the length 'l' is equal to an integer number 'n' of half guide wavelengths 'λ_g':-

$$l = \frac{1}{2}\left(n.\lambda_g \right) \quad \text{(at resonance)} \qquad (4.1)$$

which is necessary such that the boundary conditions at the short circuits are satisfied. In this way the tolerances of the dimensions of the jig may be tested, using the waveguide equation [1,1]:-

$$\frac{1}{\lambda^2} = \frac{1}{\lambda_c^2} + \frac{1}{\lambda_g^2} \qquad (4.2)$$

In practice the square cross section of the empty guide gives two peaks which are very close corresponding to the TE_{10} and TE_{01} modes. The two sets of data when analysed gave values for the height of 33·92mm. and for the width of 34·06mm. which is to within the tolerance of ±0·1mm. specified in the design. In the above the length of the resonator is taken to be exactly 200·0mm..

The test assumes the guide to be filled with air having ε_r = 1·0. By repeating the test with other homogeneous isotropic materials filling the cavity completely it is now possible to determine the permittivity of this new material. This is an important procedure which will be used later.

4.3 Application to shielded microstrip.

For microstrip measurements it is necessary to secure the substrate to the ground plane and alternative methods as to how this may be achieved have been investigated. First, the use of low-loss adhesive has been tested and although acceptable results were obtained it was clearly impractical to remove and led to damage of the substrate. The alternative method used a low-permittivity material tightly packed above the substrate so forcing the substrate onto the ground plane. Three materials have been considered:

1) foam

2) expanded polystyrene

3) radome material.

The foam, although it was clearly both low-loss and of low permittivity, was difficult to use because it was not sufficiently rigid. On the other hand, the radome material was not sufficiently pliable and was likely to distort after being used only a couple of times, further, its high relative permittivity ($\varepsilon_r = 1{\cdot}6$) meant that the higher order modes became propagating at lower frequencies.

The best (and the cheapest !) proved to be the expanded polystyrene: it has the lowest loss of any of the materials tested, was easy to cut and further the material could be re-used whilst providing adequate stabilty of the substrate. Before using this its material constants had to be determined; the permeability is assumed to be that of free space; the permittivity, however, had to be calculated by the resonance technique outlined earlier. When applied this test gave an average value for ε_r equal to 1·015.

4.4 Results for shielded microstrip.

The first tests performed were on symmetric strips using the smaller test jigs & the results for two different strip widths are shown in fig.(4.1) & fig.(4.2). The experimental points were determined by resonance of a 50·0mm. length of line terminated in short circuits. The design of these short circuits ensures good electrical contact to both the strip and the enclosure. For low frequencies & with the loop in the vertical plane the only resonances possible were for the fundamental mode. For higher frequencies the first higher order mode appears and because the probes couple to the magnetic field above the substrate these resonances are more significant than those of the fundamental mode which may no longer be traced. For still higher frequencies more higher order modes appear and with the exception of one or two points it no longer becomes possible to differentiate between the resonant peaks. By orientating the probes such that they couple to the odd modes of the guide the propagation constants of these modes may then be determined.

Comparing the narrow strip results of fig.(4.1) with those of the wider strip of fig.(4.2) the dramatic effect on the odd modes which was first identified by Yamashita[2,7] can be observed. Clearly there is very good agreement between the theoretical and experimental results for this test.

Agreement of experimental and theoretical data is also good for asymmetric strips. Although there is no longer a clear distinction between the odd and even modes which enables the procedure outlined above to be used it is, however, still possible to orientate the probes in such a way so as to couple preferentially to one set of modes and so again it is possible to determine propagation constants of some of the higher order modes as well as for the fundamental.

Example results for an asymmetric strip are shown in fig.(4.3) for a low permittivity substrate which have been determined from the resonances of a 200·0mm. length of line terminated in short circuits.

For the analysis of symmetric twin strips the odd and even modes may be determined quite simply by using the probes in either the vertical of the horizontal planes. Two results are given first for a low permittivity substrate 'fig.(4.4)' and secondly for a high permittivity substrate 'fig.(4.5)'. Although higher order modes could also be determined for these lines the results are not shown in the figures so as to allow the differences between the two basic modes to be highlighted. In both cases there is a clear distinction beween the two modes and the trends are correct. The apparent discrepancy between the theoretical curves and the experimental plots which is visible on this expanded scale is due to the end effect of the short circuits.

In order to make contact to the strips it is necessary to leave a tab protruding from the plane of the short circuit. This effects the performance of the short circuit and so leads to an error in the resonance tests. Further, there is a more significant effect with the open circuits which are used because of fringing fields. However, by modifying the test above it is possible to eliminate the error for these devices. Further, since these two devices are required for the calibration technique used later, it is also possible to characterise these devices directly.

The modified test requires two resonators of lengths l_1 and l_2 with one approximately twice the length of the other ($l_2 \cong 2l_1$). The effect of the short/open circuit is represented by an additional length of transmission line 'δl' which, it must be noted, is in general frequency dependent.

Thus resonance of the shorter section (frequency 'f_1') gives:-

$$l_1 + 2\delta l = \frac{1}{2}\left(n.\lambda_g\{f_1\} \right) = \frac{1}{2}\left[\frac{c.n}{f_1} \left(\frac{\lambda_g\{f_1\}}{\lambda_0\{f_1\}} \right) \right] \qquad (4.3)$$

whilst the longer section will resonate at approximately the same frequency 'f_2' but in this case the number of half wavelengths will be double that of the shorter resonator:-

$$l_2 + 2\delta l = \frac{1}{2}\left(2n.\lambda_g\{f_2\} \right) = \frac{c.n}{f_2} \left(\frac{\lambda_g\{f_2\}}{\lambda_0\{f_2\}} \right) \qquad (4.4)$$

Since the resonant frequencies are approximately the same, the normalised wavelength terms appearing in the above may be taken as being equal. Thus the two equations above may be solved:-

$$\frac{\lambda_0\{f_{1,2}\}}{\lambda_g\{f_{1,2}\}} = \frac{c.n}{l_2 - l_1} \left(\frac{1}{f_2} - \frac{1}{2f_1} \right) \qquad (4.5)$$

and the above is equal to the normalised propagation constant. The end effect 'δl' may also be expressed directly in terms of the measured values:-

$$\delta l = \frac{1}{2} \left(\frac{f_2 l_2 - f_1 l_1}{2f_1 - f_2} \right) \qquad (4.6)$$

In fig.(4.6) the experimental values for normalised propagation constant determined from short circuit resonators have been plotted using three different techniques; first using the results of the shorter length alone, secondly for the longer section alone and finally using the results of both line with correction for the end effect. Clearly the end effect is of greater significance for the shorter resonator and the corrected results are in very good

agreement with the theoretical curve. The results give a value for the equivalent end effect length which is almost independent of frequency. The value is negative which is expected from the physical considerations. A similar technique using open circuit resonators has been carried out and the results of these tests are shown in fig.(4.7). Again the end effect is most significant for the shorter resonator and again the corrected results are in close agreement with the theoretical data. In this case, however, the equivalent end effect length is positive which is a property of the fringing of the field at the open circuit which makes the line appear longer.

Note that the theoretical data for the previous examples has been computed using a value for the substrate permittivity which is slightly greater than the average value quoted for the material although remains well within the specified tolerance.

References.

[1]... Dahele, J.S. & Cullen, A.L.. "Electric Probe Measurements on Microstrip."
IEEE Trans. MTT-28, No. 7, July 1980, pp. 752-755.

[2]... Heuven van, J.H.C. & Vlek, T.H.A.M.. "Anisotropy in Alumina Substrates For Microstrip Circuits."
IEEE Trans. MTT-20, No.11, November 1972, pp. 775-777.

Figures. Page.

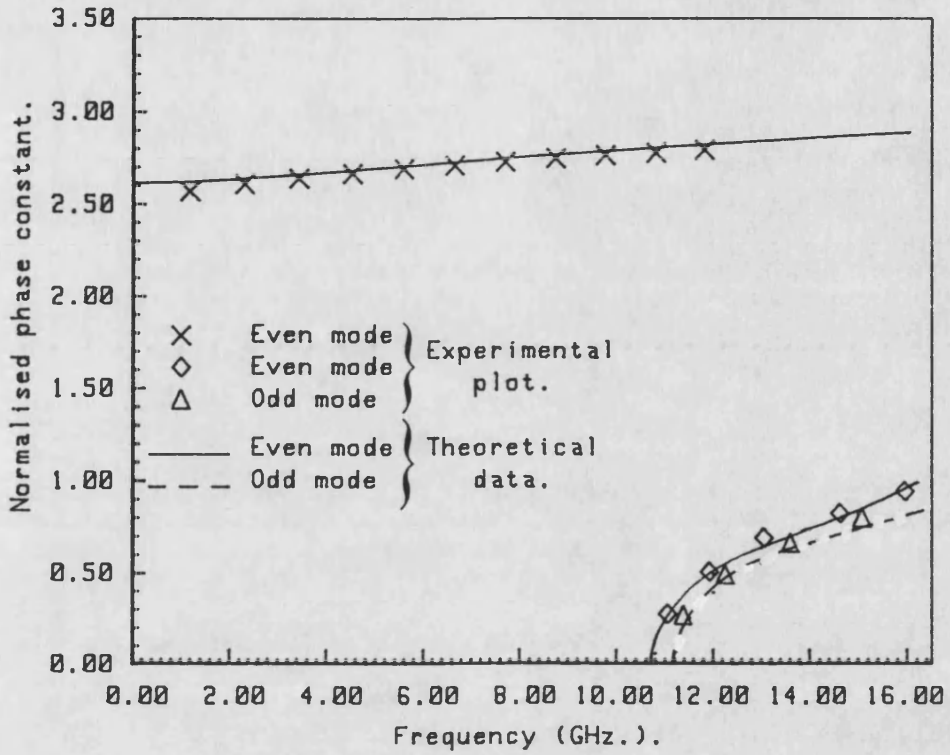

as = 12.700 mm. ws = 1.100 mm.
ha = 11.430 mm. ea = 1.015
hs = 1.270 mm. es = 10.500
symmetric strip

Comparison between experimental and theoretical results (symmetric strip).

Fig.(4.1)

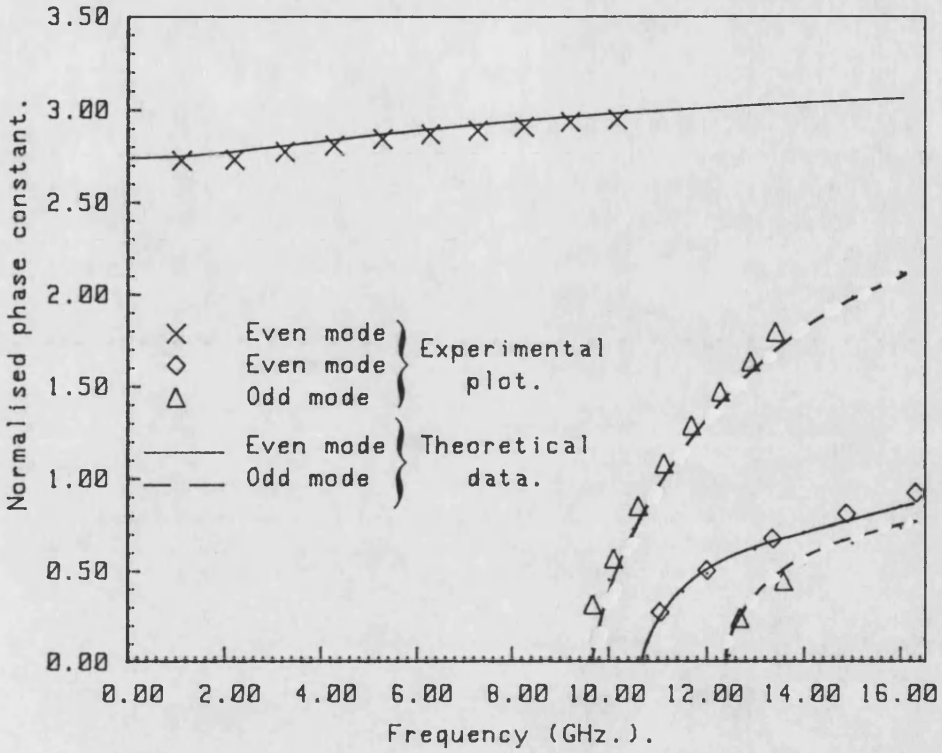

as = 12.700 mm. ws = 3.200 mm.
ha = 11.430 mm. ea = 1.015
hs = 1.270 mm. es = 10.500
symmetric strip

Comparison between experimental and theoretical results (symmetric strip).

Fig.(4.2)

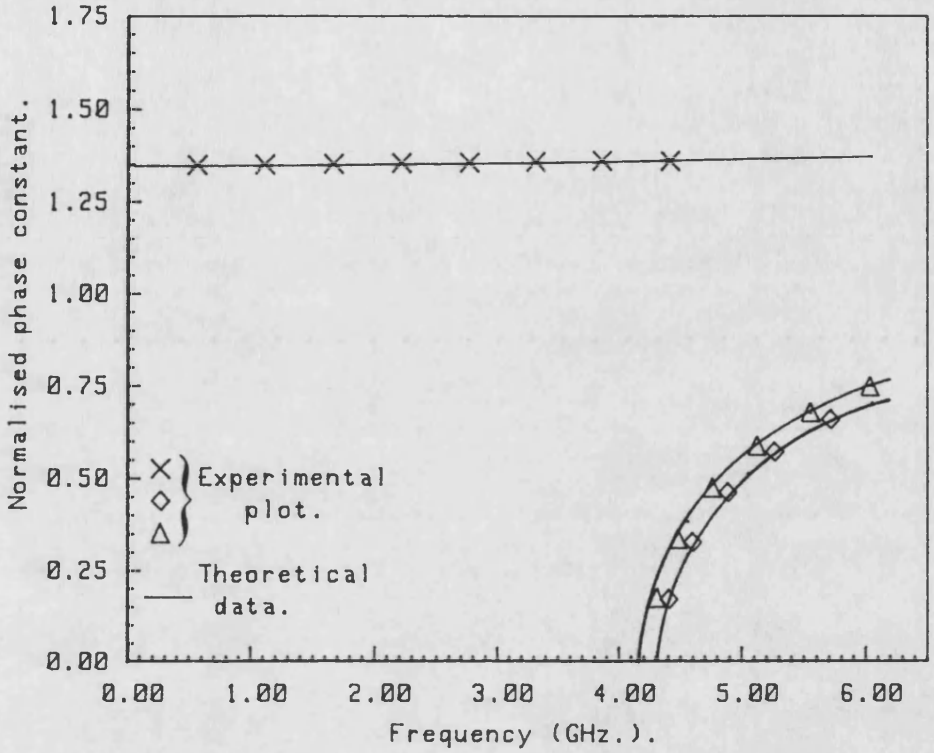

as = 34.000 mm. ws = 4.000 mm.
ha = 30.825 mm. ea = 1.015
hs = 3.175 mm. es = 2.330
offset from centre = 11.000 mm.

Comparison between experimental and theoretical results (asymmetric strip).

Fig.(4.3)

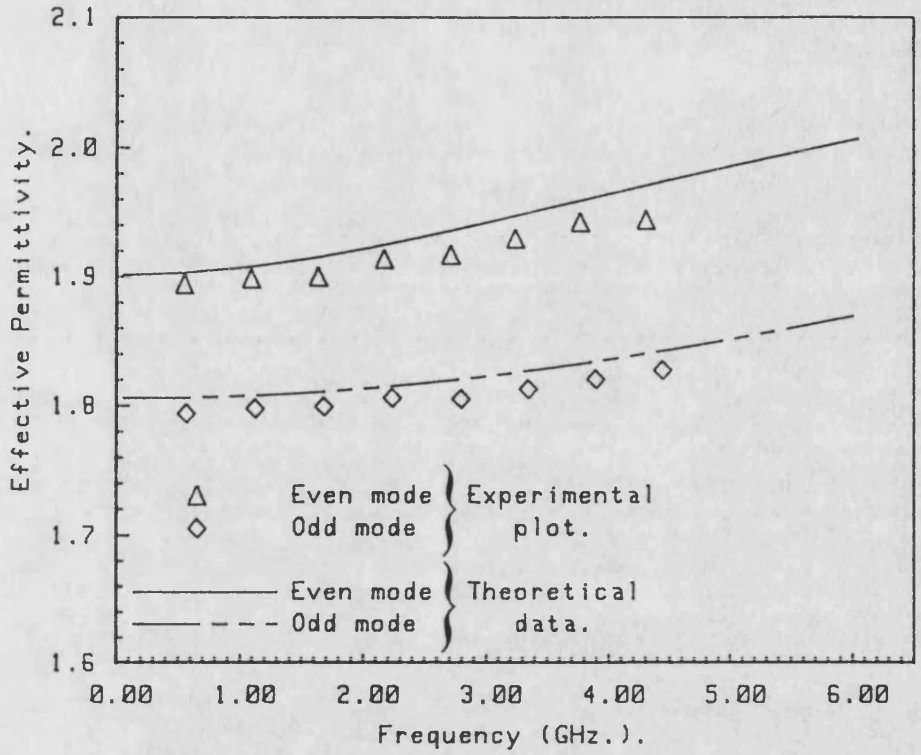

as = 34.000 mm. ws = 4.000 mm.
ha = 30.825 mm. ea = 1.015
hs = 3.175 mm. es = 2.330
strip separation = 8.000 mm.

Comparison between experimental and theoretical results (twin strips).

Fig.(4.4)

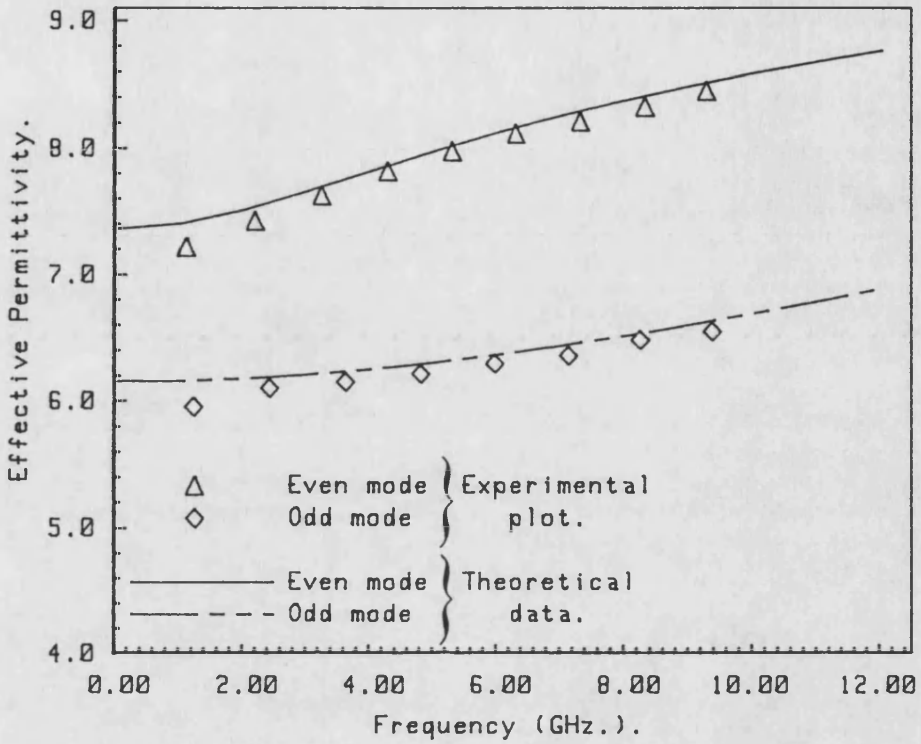

as = 12.700 mm. ws = 1.100 mm.
ha = 11.430 mm. ea = 1.015
hs = 1.270 mm. es = 10.500
strip separation = 1.100 mm.

Comparison between experimental and theoretical results (twin strips).

Fig.(4.5)

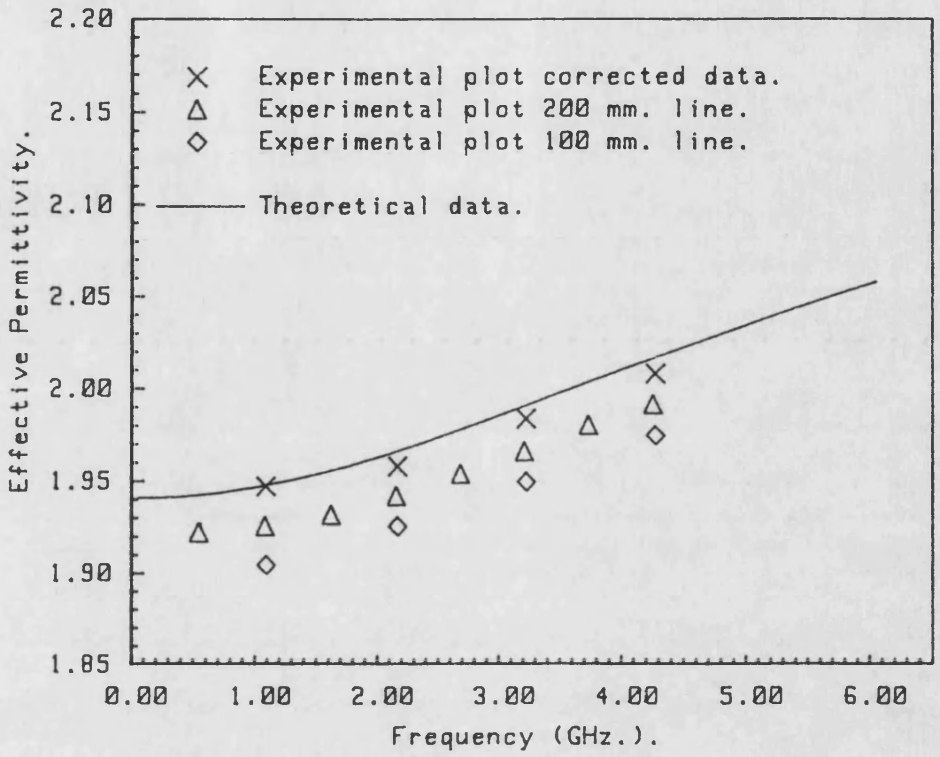

as = 34.000 mm. ws = 7.800 mm.
ha = 30.825 mm. ea = 1.015
hs = 3.175 mm. es = 2.350
symmetric strip

Effective permittivity determined by resonances of shorted lines.

Fig.(4.6)

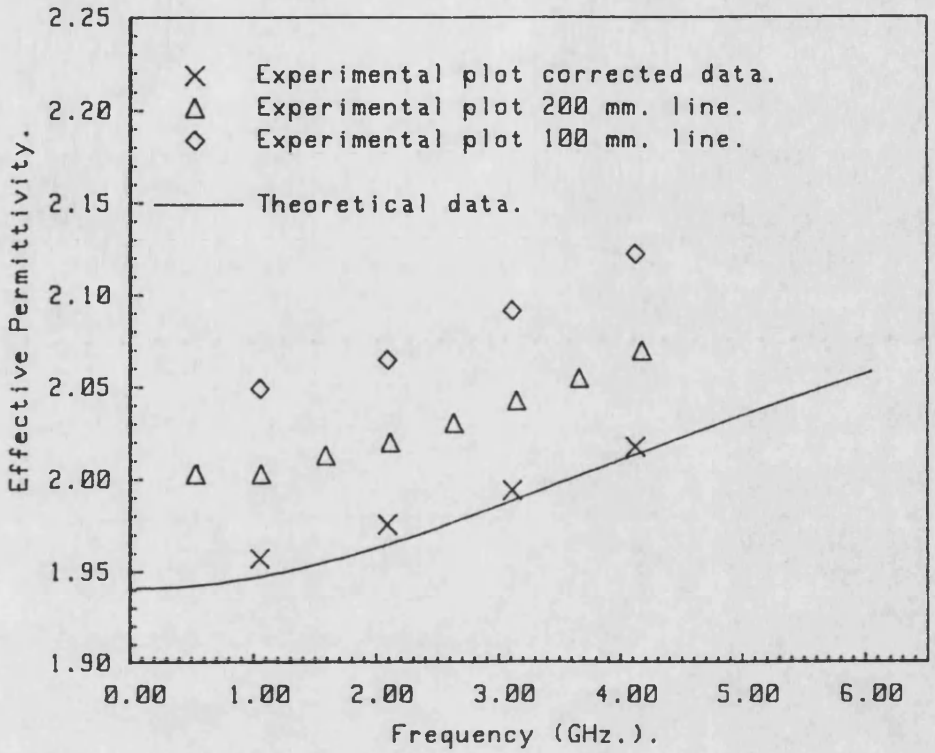

as = 34.000 mm. ws = 7.800 mm.
ha = 30.825 mm. ea = 1.015
hs = 3.175 mm. es = 2.350
symmetric strip

Effective permittivity determined by resonances of open ended lines.

Fig.(4.7)

CHAPTER FIVE

ANALYSIS OF THE STEP DISCONTINUITY

The requirement for an accurate understanding of the step and other related discontinuities has been outlined by Jansen & Koster [1]; it is expected to give the potential for more rapid growth and more efficient use of MIC's and MMIC's.

The simplest approaches possible, besides the static methods quoted frequently in CAD (see for example Gupta et al [2]), use the simplification of the magnetic wall waveguide equivalent of the microstrip line. The structure that results may be analysed using continuity of the transverse electromagnetic field in the plane of the discontinuity, which has been shown by Collin [1,1] to be both necessary and sufficient. The merits of two possible methods for the solution of this problem, the modified residue calculus method and the mode matching technique, have been discussed comprehensively by Chu & Itoh [3] and by Chu, Itoh & Shih [4] respectively.

The need for a full wave analysis taking account of the hybrid nature of the modes of the microstrip transmission line has been addressed by Jansen [5] and by Koster & Jansen [6] giving numerous results for different geometries. The method involves terminating the lines away from the discontinuity with short circuits and the location of these that cause the enclosure to resonate for a given frequency are then determined using an approximation to the current distribution at the metallisation interface. Extensive computation is required and it is not clear how the current is represented. Results presented compare well with the scattering parameter magnitudes and transmission phase angles of the magnetic wall waveguide model and the reflection phase angles of the common equivalent circuit model.

Meanwhile, the case of the finline step discontinuity has been investigated by Omar & Schünemann [7]. The method of solution is based on the mode matching technique similar to that used for the magnetic wall waveguide. However, the modes are considered as hybrid modes without any simplifications having been made. The methods for the matching of the modes are considered; the principle that the transverse electric and magnetic fields be equivalent at either side of the discontinuity is compared with the requirement for the continuity of the complex power flow.

A new technique, for microstrip, based on the variational approach has also been given by Railton & Rozzi [8]. The method uses an approximate expansion for the transverse electric field at the plane of the discontinuity and then a Galerkin's variational procedure to give the step parameters.

The mode matching method does seem to have some advantage over such a variational method; the number of modes required, before the parameters of the step converge, are reported to be of the order of 100 for the case of the variational method compared to the 40 reported for the mode matching case by Schmidt [10]. The mode matching method was later used by Uzunoglu, Capsalis & Chronopoulos [9]. In this contribution the modes of the continuous microstrip are determined by the formulation given by Mittra & Itoh [2,5]. This technique, it is noted, is capable of giving the complex modes, but is, however, restricted to the case of a symmetrically placed strip and the discontinuity analysis is thus also restricted to the case of symmetrically placed strips. Results are presented that suggest convergent answers may be achieved by taking as few as 10 modes of the input and output guides. This confidence in the technique is echoed by Xu, Webb & Mittra [11] and will be investigated first.

5.1 General Mode Matching Formulation.

First, the electromagnetic fields of the modes of the microstrip line may be written as the sum of a longitudinal field plus a transverse field vector. For the electric field:-

$$\underline{E}\,(x,y) \;=\; \underline{e}\,(x,y) \;+\; \underline{a}_z E_z \qquad (5.1)$$

whilst for the magnetic field:-

$$\underline{H}\,(x,y) \;=\; \underline{h}\,(x,y) \;+\; \underline{a}_z H_z \qquad (5.2)$$

For an incident mode 'i' say from strip 1 to the discontinuity at the plane $z = 0$ to strip 2, the requirement that the tangential field components be equivalent gives the following two identities:-

$$\underline{e}_i^{(s1)} \;+\; \sum_{p=0}^{\infty} A_p \;\underline{e}_p^{(s1)} \;=\; \sum_{q=0}^{\infty} B_q \;\underline{e}_q^{(s2)} \qquad (5.3)$$

for the electric field whilst for the magnetic field:-

$$\underline{h}_i^{(s1)} \;-\; \sum_{p=0}^{\infty} A_p \;\underline{h}_p^{(s1)} \;=\; \sum_{q=0}^{\infty} B_q \;\underline{h}_q^{(s2)} \qquad (5.4)$$

The constants A_p & B_q, which are in general complex, represent the scattered modes magnitudes & phases. The requirement is thus to solve for these constants.

Before explaining how this may be done it is necessary to define the following inner product:-

$$\langle\, \underline{e}_p \,,\, \underline{h}_q^{*} \,\rangle \;=\; \iint \left(\underline{e}_p \;\times\; \underline{h}_q^{*} \right) \cdot \underline{a}_z \; dS \qquad (5.5)$$

with S taken as the guiding cross section. For modes of the same strip this integral is proportional to the power flow in the direction of propagation (see (3.65)). For modes of different strips

the integral may be interpreted as the magnitude of the mode coupling 'C_{pq}'. In the latter case the integral may be determined in the same way as for the verification of mode orthogonality (section 3.5). The results of such an analysis are given in tables 5.1&2.

Considering these tables which are given for a 3·2mm./7·8mm. step it is clear that, whilst all the modes of one strip couple to all the modes of the other strip to varying degrees, the modes of the two strips are very similar with the diagonal terms of the table close to unity. This is, however, with the one exception of the fundamental mode for which the coefficient is of the order of 0·75. This is to be expected since for this mode the electromagnetic field is dominated by the presence of the strip whereas for the higher order modes the dominating effect is the shielding. For still higher order modes this no longer continues to be the case as for various strip widths some modes become complex and there is no longer a simple one-to-one correspondence between the modes.

Having defined the inner product the discontinuity may be analysed. A technique based on Galerkin's method is used by first taking the inner product, as defined by (5.5), of (5.3) with the complex conjugate of the transverse magnetic field of mode p' of strip 1:-

$$< \underline{e}_i^{(s1)} , \underline{h}_{p'}^{(s1)*} > + \sum_{p=0}^{\infty} A_p < \underline{e}_p^{(s1)} , \underline{h}_{p'}^{(s1)*} > = \sum_{q=0}^{\infty} B_q < \underline{e}_q^{(s2)} , \underline{h}_{p'}^{(s1)*} >$$

$$(p' = 0,1,..,\infty) \qquad (5.6)$$

Using the orthogonality of the modes & abbreviating (5.6) becomes:-

$$C_i^{(s1)} \delta_{ip'} + A_{p'} C_{p'}^{(s1)} = \sum_{q=0}^{\infty} B_q C_{qp'}^{(s2,s1)}$$

$$(p' = 0,1,..,\infty) \qquad (5.7)$$

Similarly, the complex conjugate of (5.4) is used taking its inner

product with the transverse electric field of mode q' of strip 2:-

$$< \underline{e}_{q'}^{(s2)}, \underline{h}_{i}^{(s1)*} > - \sum_{p=0}^{\infty} A_p^* < \underline{e}_{q'}^{(s2)}, \underline{h}_{p}^{(s1)*} > = \sum_{q=0}^{\infty} B_q^* < \underline{e}_{q'}^{(s2)}, \underline{h}_{q}^{(s2)*} >$$

$$(q' = 0,1,..,\infty) \qquad (5.8)$$

Using first the orthogonality of the modes and also abbreviating the inner products (5.8) becomes:-

$$c_{q'i}^{(s2,s1)} - \sum_{p=0}^{\infty} A_p^* \; c_{q'p}^{(s2,s1)} = B_{q'}^* \; c_{q'}^{(s2)}$$

$$(q' = 0,1,..,\infty) \qquad (5.9)$$

Note that q' is a dummy argument in the above identity so that rearranging the above gives the following:-

$$B_q^* = \frac{c_{qi}^{(s2,s1)}}{c_q^{(s2)}} - \frac{1}{c_q^{(s2)}} \sum_{p=0}^{\infty} A_p^* \; c_{qp}^{(s2,s1)} \qquad (5.10)$$

Taking the complex conjugate of the previous result:-

$$B_q = \frac{c_{qi}^{(s2,s1)*}}{c_q^{(s2)*}} - \frac{1}{c_q^{(s2)*}} \sum_{p=0}^{\infty} A_p \; c_{qp}^{(s2,s1)*} \qquad (5.11)$$

This identity may now be used by substituting for the unknown transmitted mode amplitudes/phase 'B_q' appearing in equation (5.7):-

$$c_i^{(s1)} \; \delta_{ip'} + A_{p'} \; c_{p'}^{(s1)} = \sum_{q=0}^{\infty} B_q \; c_{qp'}^{(s2,s1)}$$

$$= \sum_{q=0}^{\infty} \left(\frac{c_{qi}^{(s2,s1)*}}{c_q^{(s2)*}} - \frac{1}{c_q^{(s2)*}} \sum_{p=0}^{\infty} A_p \; c_{qp}^{(s2,s1)*} \right) c_{qp'}^{(s2,s1)}$$

$$(p' = 0,1,..,\infty) \qquad (5.12)$$

The order of summation in the above may now be changed.

The result is given as:-

$$A_{p'} C_{p'}^{(s1)} + \sum_{p=0}^{\infty} \left(A_p \sum_{q=0}^{\infty} \frac{C_{qp}^{(s2,s1)*} C_{qp'}^{(s2,s1)}}{C_q^{(s2)*}} \right)$$

$$= \sum_{q=0}^{\infty} \left(\frac{C_{qi}^{(s2,s1)*} C_{qp'}^{(s2,s1)}}{C_q^{(s2)*}} \right) - C_i^{(s1)} \delta_{ip'}$$

$$(p' = 0,1,..,\infty) \qquad (5.13)$$

By considering only a finite number of reflected modes and a finite number of transmitted modes equation (5.13) forms a system of linear equations in the reflected mode amplitudes/phases 'A_p' which may be determined by Gaussian elimination with back substitution. The transmitted mode amplitude/phases may now be determined by direct substitution of the unknowns in equation (5.11). Note that the number of reflected/trasnsmitted modes considered need not be the same although this will in general be assumed.

For the particular case when the incident mode is the fundamental mode 'i = 0' the scattering parameters of the step may be determined. The reflection coefficient is simply the reflected mode amplitude/phase of the fundamental mode:-

$$S_{11} = A_0 \qquad (5.14)$$

The transmission parameter must, however, be scaled:-

$$S_{21} = B_0 \sqrt{\left(\frac{C_0^{(s2)}}{C_0^{(s1)}} \right)} \qquad (5.15)$$

By applying the analysis in reverse all the scattering parameters for the discontinuity may be determined.

5.1.1 Results for the Mode Matching Method.

This technique has been put into practice for the example of a 3·2mm. to 7·8mm. step on a low permittivity substrate thickness 3·175mm.. The results for the magnitude and phase information show distinctly different characteristics.

The convergence of the magnitude of the reflection of the step for different frequencies is shown in fig.(5.1) and clearly the response converges very quickly and the actual value compares well with other published data. By considering the transmission parameters as well it is possible to do an independent check on the results by applying the condition for losslessness of the step:-

$$|S_{11}|^2 + |S_{21}|^2 = 1 \qquad (5.16)$$

This check has been made and is correct to 5 decimal places for even the lowest order expansions. This may be due to the observance of Omar [7] that the matching of the transverse electric and magnetic field is equivalent to the conservation of complex power.

The convergence of the phase as a function of the number of modes considered is shown in fig.(5.2) and shows that for the number of modes considered the answer differs from the expected value: the phase change for the ideal high/low impedance step is 180^0 and for the microstrip step under consideration a response $180^0 - \Delta\theta^0$ with $\Delta\theta$ being positive is expected whereas in this case $\Delta\theta$ is negative. Further, when reversing the step the phase change is still of the order of 180^0 which compares with the ideal case of a low/high impedance step the reflection phase of which should be 0^0.

Note that as an alternative to taking the expansion of equation (5.3) with the transverse magnetic field distribution of mode p' of strip 1 etc. it is possible to develop a similar formulation by

taking the expansion of equation (5.3) with the transverse magnetic field of mode q' of strip 2 etc.. This has been programmed and it is clear that for the case of a narrow strip to a wide strip then the original formulation is better giving answers which do not differ significantly from the expected value whereas for the case of a wide strip to a narrow strip the reverse is true. The difference in the results using the two formulations, which should by all accounts be equivalent, puts serious doubt on the suitability of the technique.

The observation in these cases is not surprising. Considering the results for which the mode matching formulation was originally proposed (the equivalent magnetic wall waveguide model) the problem in this case is comparatively simple first because the new equivalent geometry is uniform in the vertical 'y' direction and hence reduces to a one dimensional problem and secondly because the absence of singularities in the new structure make the principle of matching the fields on either side well conditioned. Even with these simplifications the number of modes that need be considered remains high (of the order of 20) to achieve convergence. Having considered this it is not surprising that the analysis of the shielded microstrip without any simplifications should be poorly conditioned.

An explanation of the apparently correct magnitude information can be achieved by comparing the result of this technique using only one mode for either guide and it can be shown that the result in this case is identical to that which is achieved using a corresponding simplification of the variational method which is presented later. The result accounts for the best choice of possible formulations since for the 'correct' case the expansion function in the variational technique satisfies the boundary conditions whilst for the alternative this is not true.

5.2 Variational Method.

A comprehensive discussion of the variational method for waveguide discontinuities is given in [1,1] and its application to microstrip has been given in [8]. A more rigorous treatment of the step discontinuity will be given which incorporates an analytic technique based on the experimental Weissfloch method in order to characterise the two port network completely.

The variational expression which is the basis of the technique will be determined for the general case; assuming the output guide to be terminated with a device having a reflection coefficient Γ. The device can be considered to be located at a distance of an integer number of half wavelengths away from the plane of the discontinuity such that only the fundamental mode is reflected with all higher order modes decaying to zero. The transverse electric field in the plane of the discontinuity '$\underline{\xi}(x,y)$' is related to the modes of the two lines on either side:-

$$\underline{\xi}(x,y) = (1+A_0)\ \underline{e}_0^{(s1)} + \sum_{p=1}^{\infty} A_p\ \underline{e}_p^{(s1)} = \sum_{q=1}^{\infty} B_q\ \underline{e}_q^{(s2)} + B_0(1+\Gamma)\ \underline{e}_0^{(s2)} \qquad (5.17)$$

Whilst the discontinuity magnetic field is not explicitly defined the equivalence of the magnetic field on either side of the discontinuity must still hold:-

$$(1-A_0)\ \underline{h}_0^{(s1)} - \sum_{p=1}^{\infty} A_p\ \underline{h}_p^{(s1)} = \sum_{q=1}^{\infty} B_q\ \underline{h}_q^{(s2)} + B_0(1-\Gamma)\ \underline{h}_0^{(s2)} \qquad (5.18)$$

It must be noted that the unknown reflected/transmitted mode amplitudes/phases 'A_p' and 'B_q' are dependant upon the reflection 'Γ' in this case. Using equation (5.17) it is possible to express 'A_p' and 'B_q' in terms of the assumed electric field distribution '$\underline{\xi}(x,y)$'

by taking the inner product of the fields with the transverse magnetic fields of each of the modes of the appropriate guide in turn. From orthogonality of this inner product the latter gives:-

$$(1+A_0) = \frac{< \underline{\xi}\ (x,y)\ ,\ \underline{h}_0^{(s1)} >}{< \underline{e}_0^{(s1)}\ ,\ \underline{h}_0^{(s1)} >} \qquad (5.19)$$

$$A_p = \frac{< \underline{\xi}\ (x,y)\ ,\ \underline{h}_p^{(s1)} >}{< \underline{e}_p^{(s1)}\ ,\ \underline{h}_p^{(s1)} >} \qquad (5.20)$$

$$B_0(1+\Gamma) = \frac{< \underline{\xi}\ (x,y)\ ,\ \underline{h}_0^{(s2)} >}{< \underline{e}_0^{(s2)}\ ,\ \underline{h}_0^{(s2)} >} \qquad (5.21)$$

$$B_q = \frac{< \underline{\xi}\ (x,y)\ ,\ \underline{h}_q^{(s2)} >}{< \underline{e}_q^{(s2)}\ ,\ \underline{h}_q^{(s2)} >} \qquad (5.22)$$

Equations (5.20) to (5.22) may be used to substitute directly for the unknown mode amplitudes/phases in (5.18) whilst (5.19) may be used to introduce the input admittance of the network 'Y_{in}':-

$$Y_{in} = \frac{1 - A_0}{1 + A_0} \qquad (5.23)$$

The resulting expression is given by the following:-

$$Y_{in}\ \frac{< \underline{\xi}\ ,\ \underline{h}_0^{(s1)} >\ \underline{h}_0^{(s1)}}{< \underline{e}_0^{(s1)}\ ,\ \underline{h}_0^{(s1)} >} =$$

$$\sum_{p=1}^{\infty} \frac{< \underline{\xi}\ ,\ \underline{h}_p^{(s1)} >\ \underline{h}_p^{(s1)}}{< \underline{e}_p^{(s1)}\ ,\ \underline{h}_p^{(s1)} >} + \sum_{q=1}^{\infty} \frac{< \underline{\xi}\ ,\ \underline{h}_q^{(s2)} >\ \underline{h}_q^{(s2)}}{< \underline{e}_q^{(s2)}\ ,\ \underline{h}_q^{(s2)} >}$$

$$+ \frac{1-\Gamma}{1+\Gamma} \frac{< \underline{\xi}\ ,\ \underline{h}_0^{(s2)} >\ \underline{h}_0^{(s2)}}{< \underline{e}_0^{(s2)}\ ,\ \underline{h}_0^{(s2)} >} \qquad (5.24)$$

The input admittance for the network may now be determined using an

approximation for the transverse electric field at the interface. That the analysis should be the optimum must now be determined.

Using equation (5.24) the inner product is taken throughout the expression with an arbitrary transverse vector function '$\underline{\xi}_1(x,y)$' of the transverse coordinates (this function may be of any form):-

$$Y_{in} \frac{< \underline{\xi} , \underline{h}_0^{(s1)} > < \underline{\xi}_1, \underline{h}_0^{(s1)} >}{< \underline{e}_0^{(s1)} , \underline{h}_0^{(s1)} >} = < \underline{\xi} \mid \underline{\underline{G}}(\Gamma) \mid \underline{\xi}_1 > \quad (5.25)$$

where the right hand side of the above is defined for this example:-

$$< \underline{\xi} \mid \underline{\underline{G}}(\Gamma) \mid \underline{\xi}_1 > =$$

$$\sum_{p=1}^{\infty} \frac{< \underline{\xi} , \underline{h}_p^{(s1)} > < \underline{\xi}_1, \underline{h}_p^{(s1)} >}{< \underline{e}_p^{(s1)} , \underline{h}_p^{(s1)} >} + \sum_{q=1}^{\infty} \frac{< \underline{\xi} , \underline{h}_q^{(s2)} > < \underline{\xi}_1, \underline{h}_q^{(s2)} >}{< \underline{e}_q^{(s2)} , \underline{h}_q^{(s2)} >}$$

$$+ \frac{1-\Gamma}{1+\Gamma} \frac{< \underline{\xi} , \underline{h}_0^{(s2)} > < \underline{\xi}_1, \underline{h}_0^{(s2)} >}{< \underline{e}_0^{(s2)} , \underline{h}_0^{(s2)} >} \quad (5.26)$$

It is now necessary to determine the first order variation in Y_{in} due to a first order change in the arbitrary vector function $\underline{\xi}_1$. To do this it is necessary to replace Y_{in} with $Y_{in} + \Delta Y_{in}$ and similarly $\underline{\xi}_1$ becomes $\underline{\xi}_1 + \Delta\underline{\xi}_1$. Now using the identities already derived we get $\Delta Y_{in} = 0$, which is to be expected since Y_{in} is independent of the arbitrary vector function!

The actual transverse electric field distribution in the plane of the discontinuity is, however, still unknown. Thus given that an approximation to this must be used the variation in Y_{in} for a variation in $\underline{\xi}$ must be determined. The analysis is identical to that used previously for the arbitrary vector function. In this case, however, in order to achieve zero first order variation there is a requirement that the arbitrary vector function $\underline{\xi}_1$ must be equal to

the actual transverse electric field $\underline{\xi}$. This result may be written:-

$$\lim_{\underline{\xi}_1 \to \underline{\xi}} \left\{ \Delta Y_{in} \right\} = 0 \qquad (5.27)$$

In order to obtain an approximation for Y_{in} the electric field '$\underline{\xi}$' is first expanded as a truncated set of basis functions:-

$$\underline{\xi}(x,y) = \sum_{l=0}^{M} c_l \, \underline{\Psi}_l(x,y) \qquad (5.28)$$

Here the coefficients c_l are scalar variables which are in general complex and the functions $\underline{\Psi}_l(x,y)$ are transverse vectors of the transverse coordinates which must be linearly independent. This expansion may now be substituted in equation (5.25):-

$$Y_{in} \sum_{l_1=0}^{M} \sum_{l_2=0}^{M} c_{l_1} c_{l_2} \frac{< \underline{\Psi}_{l_1} , \underline{h}_0^{(s1)} > < \underline{\Psi}_{l_2} , \underline{h}_0^{(s1)} >}{< \underline{e}_0^{(s1)} , \underline{h}_0^{(s1)} >} =$$

$$\sum_{l_1=0}^{M} \sum_{l_2=0}^{M} c_{l_1} c_{l_2} < \underline{\Psi}_{l_1} \mid \underline{\underline{G}}(\Gamma) \mid \underline{\Psi}_{l_2} > \qquad (5.29)$$

Note that the value of Y_{in} is independent of the absolute magnitude of the assumed field distribution and so the coefficient of the first term in the expansion could be taken as unity without any loss in generality.

It is now possible to solve for Y_{in} by applying the criteria for zero first order variation by taking partial derivatives of the above with respect to each of the parameters c_l in turn. The exact way in which the result is achieved will depend upon the choice of basis functions.

5.2.1 Scattering parameters of the step.

Use of the variational expression which has been determined above for the case $\Gamma = 0$ will give an immediate solution for the reflection of the fundamental mode 'S_{11}' for a mode incident from the source guide. The remaining parameters of the step may only be determined, however, by an analytic technique based on a modification of the experimental Weissfloch method the principles of which will now be covered.

First note that from (5.23) that the response of the network 'R' is related to its input admittance 'Y_{in}' via:-

$$R = \frac{1 - Y_{in}}{1 + Y_{in}} \qquad (5.30)$$

For the network comprising the step terminated in a device having a reflection coefficient Γ the response is given by the following:-

$$R = S_{11} + \frac{S_{12}\, S_{21}\, \Gamma}{1 - S_{22}\, \Gamma} \qquad (5.31)$$

Thus when the terminating device is a matched terminal load having a reflection $\Gamma = 0$ the result for S_{11} is given directly:-

$$R\ (\ \Gamma = 0\ ) = S_{11} \qquad (5.32)$$

The remaining parameters that describe the step discontinuity must be determined from data for two different values of Γ: this is equivalent to physically connecting two different devices to the output guide and is very similar to the calibration procedure used in the experimental determination of the step parameters to be covered later.

The two different 'devices' have reflection coefficients Γ_1 & Γ_2 and the corresponding measured responses will be denoted R_1 & R_2. Thus assuming that S_{11} has already been determined, these two equations may be solved for the unknown scattering parameters:-

$$S_{22} = \frac{\Gamma_1 \left[R_2 - S_{11} \right] - \Gamma_2 \left[R_1 - S_{11} \right]}{\Gamma_2 \Gamma_1 \left[R_2 - R_1 \right]} \qquad (5.33)$$

$$S_{12}S_{21} = \frac{\left[\Gamma_2 - \Gamma_1 \right] \left[R_1 - S_{11} \right] \left[R_2 - S_{11} \right]}{\Gamma_2 \Gamma_1 \left[R_2 - R_1 \right]} \qquad (5.34)$$

Although the standards could be arbitrary, the choice must address the numerical problems involved: it is clear that,for standards which are similar, the terms in the above equations will become small and accuracy will be lost. Further, the individual values for the reflection standards must be high in order that the terms $R - S_{11}$ remain sufficiently large again to maintain numerical precision. Finally, from equation (5.24) it can be seen that there are numerical problems should the reflection standards be given by $\Gamma = \pm 1\angle 0^0$. The best solution possible would seem to be given by $\Gamma = \pm 1\angle 90^0$, which appear to satisfy all of the above criteria.

The parameters of the step may thus be determined. Note that in order to separate the term $S_{12}S_{21}$ it is necessary to use the reciprocal nature of the network which infers that '$S_{12} = S_{21}$'.

5.2.2 Method 1.

A suitable choice for the basis functions of the discontinuity field may be taken as the transverse part of the electric fields of the modes of the wider line - which will be assumed to be strip 1. These functions satisfy the boundary conditions and, furthermore, for this choice, (5.29) simplifies:-

$$Y_{in} = \frac{1}{< \underline{e}_0^{(s1)} , \underline{h}_0^{(s1)} >} \sum_{l_1=0}^{M} \sum_{l_2=0}^{M} c_{l_1} c_{l_2} < \underline{e}_{l_1}^{(s1)} | \underline{\underline{G}}(\Gamma) | \underline{e}_{l_2}^{(s1)} > \qquad (5.35)$$

where the coefficient c_0 is taken equal to unity.

The equation above may now be differentiated with respect to each of the remaining coefficients in turn:-

$$\frac{\partial Y_{in}}{\partial c_{l'}} = \frac{2}{< \underline{e}_0^{(s1)} , \underline{h}_0^{(s1)} >} \sum_{l=0}^{M} c_l < \underline{e}_l^{(s1)} | \underline{\underline{G}}(\Gamma) | \underline{e}_{l'}^{(s1)} > \qquad (l' = 1,2,..,M) \qquad (5.36)$$

The previous result forms a system of linear equations in the unknown coefficients c_l which may be determined by Gaussian elimination with back substitution. By using these coefficients in expression (5.35) a variational approximation to the input admittance Y_{in} may now be determined. Note that for this choice of basis functions it is only necessary to determine a fixed number of modes of the wider line because of mode orthogonality.

5.2.3 Results for variational method 1.

This method has been used for the 7·8mm./3·2mm. step for the standard low permittivity substrate of thickness 3·175mm. enclosed in a box having the same dimensions as the experimental jig described in chapter 4. The magnitude of the reflection from the wider line 'S_{11}' is plotted in fig.(5.3) and the corresponding phase in fig.(5.4). For the magnitude response the results converge very quickly and the result plotted are those obtained using 50 modes of the narrower line and two basis functions (i.e. two modes of the wider line), however, the shown phase is that projected from results considering up to the first 50 modes of the narrow line (convergence not having been fully achieved), and are typical of other published results.

The magnitude of the transmission parameter 'S_{12}' is such that the requirement for losslessness given by (5.16) hold to 6 decimal places and the magnitude of the reflection parameter of the narrow line 'S_{22}' is numerically equal to $|S_{11}|$ again to 6 decimal places which is expected from reciprocity. However, the numerically sensitive phase, on the other hand, is in general unreliable, giving a value for the transmission phase angles which oscillates about 0^0 this being the expected phase angle neglecting the parasitics of the step. Further, the reflection phase angle for the narrower line which ignoring the parasitics of the step would be expected to give a value around 180^0 shows a small variation in the wrong sense i.e. the phase increases with frequency instead of decreasing. That the results should be more accurate for the reflection of the wider line is to be expected since modes of the wider line may be directly related to the discontinuity field whereas the modes on the narrower line must take account of the weak mode coupling to this field.

5.2.4 Method 2.

To improve the answers given by the previous method it is noted that the choice of expansion functions must be considered to be somewhat restrictive. Therefore, a method of analysis will be presented which enables arbitrary expanding functions to be used and later physical conditions which could be used to develop a more exact set of expanding functions will be discussed.

For arbitrary expanding functions which do not give rise to any simplifications as before, equation (5.29) must be differentiated directly with respect to each of the coefficients c_l in turn and the derivatives of Y_{in} equated to zero. Following a similar approach used in [1,1] it is possible to write the expression for Y_{in} as:-

$$Y_{in} = \frac{Num}{Den} \tag{5.37}$$

Taking partial derivatives of the above gives:-

$$\frac{\partial Y_{in}}{\partial c_{l'}} = \frac{1}{Den}\left(\frac{\partial\ Num}{\partial c_{l'}} - Y_{in}\ \frac{\partial\ Den}{\partial c_{l'}}\right)$$

$$= 0 \qquad (l' = 0,1,..M) \tag{5.38}$$

This procedure gives a set of simultaneous equations in the unknown basis function coefficients 'c_l' and the unknown input admittance:-

$$2\sum_{l=0}^{M} c_l \ < \underline{\Psi}_{l'} \ | \ \underline{\underline{G}}(\Gamma) \ | \ \underline{\Psi}_l \ >$$

$$- 2\ Y_{in} \sum_{l=0}^{M} c_l \ \frac{< \underline{\Psi}_{l'} \ , \ \underline{h}_0^{(s1)} > < \underline{\Psi}_l \ , \ \underline{h}_0^{(s1)} >}{< \underline{e}_0^{(s1)} \ , \ \underline{h}_0^{(s1)} >} = 0$$

$$(l' = 0,1,..,M) \tag{5.39}$$

Note that this set of equations could have been obtained by applying Galerkin's method to equation (5.24). Further, for the case when the

basis functions are given by the transverse electric fields of the the modes of the wider line then (5.36) may be obtained as a special case of (5.39) as anticipated. Without this simplification the set of equations (5.39) forms a set of homogeneous equations from which Y_{in} may be determined by searching for a non-trivial solution by requiring the determinant of the matrix of coefficients be zero.

Although this appears to give a polynomial in Y_{in} of degree 'M+1' the resulting matrix may be simplified considerably. First note that the matrix equation may be written as:-

$$\begin{bmatrix} Z_{in}G_{00} - F_{00} & Z_{in}G_{01} - F_{01} & \cdots\cdots & Z_{in}G_{0M} - F_{0M} \\ Z_{in}G_{10} - F_{10} & Z_{in}G_{11} - F_{11} & \cdots\cdots & Z_{in}G_{0M} - F_{0M} \\ Z_{in}G_{20} - F_{20} & Z_{in}G_{21} - F_{21} & \cdots\cdots & Z_{in}G_{0M} - F_{0M} \\ \cdots\cdots & \cdots\cdots & \cdots\cdots & \cdots\cdots \\ Z_{in}G_{M0} - F_{M0} & Z_{in}G_{M1} - F_{M1} & \cdots\cdots & Z_{in}G_{MM} - F_{MM} \end{bmatrix} \begin{bmatrix} c_0 \\ c_1 \\ : \\ : \\ c_M \end{bmatrix} = \begin{bmatrix} 0 \\ 0 \\ 0 \\ : \\ 0 \end{bmatrix} \qquad (5.40)$$

where Z_{in} is merely the reciprocal of Y_{in}. The elements of the matrix F 'F_{ij}' may be written as a product $f_i f_j$ by inspection from (5.39) and this simplification gives the following result for a non-trivial solution of the above:-

$$Z_{in} = \frac{1}{DET\ (G)} \sum_{l=0}^{M} DET\ (\ G\{\text{row } l \text{ replaced by row } l \text{ of } F\}\ ) \qquad (5.41)$$

Thus the result may be determined directly.

Although this method increases the computational requirement compared to method 1 since the simplification of orthogonality cannot be used, it must be noted that the basis functions may be expressed as x and y components separately with a corresponding reduction in computation per basis function.

5.2.5 Results for variational method 2.

For this method of analysis the transverse electric fields of the modes of the wider line may again be used but the transverse components may be separated:-

$$\Psi_{2l} = c_{2l}\left[\underline{a}_x E_{xl}^{(s1)}(x,y)\right] \qquad (l=0,1,..M)$$
$$\Psi_{2l+1} = c_{2l+1}\left[\underline{a}_y E_{yl}^{(s1)}(x,y)\right] \qquad (l=0,1,..M) \qquad (5.42)$$

The components will still satisfy the boundary conditions but will not individually be orthogonal to the modes of the wider line and thus this choice will allow all modes of the wider line to be incorporated into the analysis. Further, when using the modes of the wider line for the basis functions the result for the inner product with the y directed component of one mode may be determined directly from the result for the inner product of the x directed component of the same mode as a consequence of mode orthogonality.

This technique has once again been used for the standard 7·8mm./3·2mm. step considered earlier and the results are almost identical to those obtained in method 1 using 50 modes for the input and output lines with the 'best' results being obtained for the reflection of the wider line.

Note that for this method it is not necessary to use the calibration technique to determine the reflection off the narrower line but the step may be reversed and the analysis programmed using the narrow line as the source line. Results using this technique are in complete agreement with those obtained using the more involved numerical calibration method.

That the results are not completely satisfactory is due to the failure of the technique to accurately account for the discontinuity field. The actual field at the discontinuity is expected to contain

very stong singularities particularly at the 90^0 corner for which the field are expected to have a singularity as a function of the radial distance of -0.703 [12]. Further, there will be a singularity all the way along the end of the wider line for which the narrow line does not overlap and a further different order singularity at the 270^0 corner. Ideally the set of expanding functions used to describe this field should take account of all of these effects.

However, as a simple test to investigate ways of more correctly expanding this discontinuity field it may be noted that the y component of the modes of the narrow line also satisfy the required boundary conditions and may be incorporated into the analysis. One problem which becomes immediately apparent from using these terms is that the results for the discontinuity analysis do not converge even considering the 50 modes for each of the input and output lines.

This is a fundamental restriction of the use of this variational method. On the one hand it is necessary to provide a reasonable trial field function such that only a limited number of terms in the expansion need be considered which will keep the matrices involved small and hence numerical accuracy high whilst on the other hand it is necessary to be able to program the resulting algorithm accurately which is not possible if the products in (5.26) converge slowly.

From the observations it seems clear that the approximations made by using the simpler technique 'method 1' do provide the more realisable algorithm since the the terms in (5.26) do converge rapidly as a consequence of mode orthogonality and the small coupling terms for the modes of the other line 'see tables 5.1/2', whereas the use of a more accurate trial field seems thwarted by poor convergence of the expression in (5.26).

5.2.6 Cascaded steps.

For cascaded steps which are considered to be so close that the higher order modes which are scattered at one of the steps are still appreciably high at adjacent steps so as to cause a distortion of the electromagnetic field, then these must be taken into account.

Although no results will be presented for this problem the following scheme demonstrates how the techniques proposed may be extended to analyse these structures. The principle by which the higher order modes may be calculated is identical to the method already used for the fundamental mode: the reflection standards may be considered to be mode selective such that they only have an effect on any one specific mode and furthermore they may be considered to be connected to the input guide as well as the output guide. The complete parameters for the model of fig.(5.5) may be determined by systematically considering each input line in turn to be the source and each one of the output lines and the remaining input lines to have the variable load. This may appear to be a laborious method of determining these parameters but it must be noted that the main time consuming portion of the program is the computation of the coefficients to be used in the variational expressions and these coefficients are common for all of the lines to be considered and the technique can, therefore, be very efficient.

References.

[1]... Jansen, R.H. & Koster, N.H.L.. "A Unified CAD Basis for the frequency dependent characterization of Strip, Slot and Coplanar MIC Components."
Proc. 11th European Microwave Conference, 1981, pp. 682-687.

[2]... Gupta, K.C., Garg, R. & Chadha, R.. "Computer Aided Design of Microwave Circuits."
Dedham M.A. Artech House 1981.

[3]... Chu, T.S. & Itoh, T.. "Analysis of Microstrip Step Discontinuity by the Modified Residue Calculus Technique."
IEEE Trans. MTT-33, No.10, October 1985, pp. 1024-1028.

[4]... Chu, T.S., Itoh, T. & Shih, Y-C.. "Comparative Study of Mode-Matching Formulations for Microstrip Discontinuity Problems."
IEEE Trans. MTT-33, No.10, October 1985, pp. 1018-1023.

[5]... Jansen, R.H.. "Hybrid mode analysis of end effects of planar microwave and millimetrewave transmission lines."
IRE Proc., Vol.128, Pt.H, No. 2, April 1981.

[6]... Koster, N.H.L. & Jansen, R.H.. "The Microstrip Step Discontinuity: A Revised Description."
IEEE Trans. MTT-34, No. 2, February 1986, pp. 213-223.

[7]... Omar, A.S. & Schünemann, K.. "Transmission Matrix Representation of Finline Discontinuities."
IEEE Trans. MTT-33, No. 9, September 1985, pp. 765-770.

[8]... Railton, C. & Rozzi, T.. "The Rigorous Analysis of Cascaded Step Discontinuities in Microstrip."
IEEE Trans. MTT-36, No. 7, July 1988, pp. 1177-1185.

[9]... Uzunoglu, N.K., Capsalis, C.N. & Chronopoulos, C.P..
"Frequency-Dependent Analysis of a Shielded Microstrip Step Discontinuity Using an Efficient Mode-Matching Technique."
IEEE Trans. MTT-36, No. 6, June 1988, pp. 976-984.

[10].. Schmidt, L.P.. "Rigorous Computation of the Frequency Dependant Properties of Filters and Coupled Resonators Composed from Transverse Microstrip Discontinuities."
Proc. 10th European Microwave Conference, 1980, pp. 436-440.

[11].. Xu, Q., Webb, K.J. & Mittra, R.. "Study of Modal Solution Procedures for Microstrip Step Discontinuities."
IEEE Trans MTT-37, No. 2, February 1989. pp. 381-387.

[12].. Marchetti, S. & Rozzi, T..
Private communication.

TABLE 5.1

Magnitude of the coupling coefficients for the modes of 3.2 & 7.8 mm. lines.

Mode	Electric Field (3.2 mm. strip) 0	1	2	3	4	5	6	7	8	9	10
Magnetic Field (7.8 mm. strip) 0	0.757936	0.005823	0.033135	0.070532	0.025282	0.119753	0.009462	0.008949	0.011850	0.002729	0.160388
1	0.004966	1.002113	0.006361	0.012091	0.002577	0.011607	0.000815	0.000767	0.001014	0.000253	0.015280
2	0.010410	0.001229	1.007406	0.094702	0.004710	0.019637	0.001232	0.001176	0.001653	0.000454	0.020053
3	0.006369	0.001655	0.079312	0.988448	0.009924	0.042543	0.002623	0.002425	0.003093	0.000647	0.040477
4	0.022068	0.000463	0.000536	0.000673	1.001880	0.046663	0.001264	0.001689	0.002171	0.000613	0.016822
5	0.004653	0.000399	0.003894	0.009024	0.034107	0.981966	0.004689	0.003889	0.004968	0.001062	0.057374
6	0.009899	0.000139	0.000205	0.001096	0.000684	0.000182	1.000137	0.005550	0.003338	0.000807	0.011040
7	0.043831	0.000564	0.001385	0.005892	0.001401	0.008452	0.006003	0.976497	0.210936	0.012197	0.029077
8	0.017619	0.000238	0.000504	0.002265	0.000689	0.002737	0.001848	0.211088	0.977968	0.007724	0.018781
9	0.002821	0.000031	0.000121	0.000444	0.000006	0.000976	0.000882	0.014496	0.004024	1.000008	0.003315
10	0.005424	0.000190	0.001155	0.002393	0.003167	0.016641	0.005173	0.010016	0.013100	0.003227	0.976888

TABLE 5.2

Magnitude of the coupling coefficients for the modes of 3.2 & 7.8 mm. lines.

Mode	Electric Field (7.8 mm. strip) 0	1	2	3	4	5	6	7	8	9	10
Magnetic Field (3.2 mm. strip). 0	0.786348	0.006317	0.006735	0.003381	0.011593	0.002086	0.003790	0.016564	0.006590	0.001076	0.000702
1	0.026089	0.997941	0.003747	0.006352	0.001352	0.002753	0.000366	0.001158	0.000508	0.000045	0.001605
2	0.040807	0.001400	1.002839	0.086994	0.003440	0.008498	0.000791	0.002236	0.001020	0.000063	0.004281
3	0.080037	0.001952	0.085028	1.004021	0.006251	0.018544	0.001379	0.003484	0.001657	0.000054	0.009017
4	0.016124	0.000305	0.002279	0.005575	1.000362	0.036982	0.001203	0.003194	0.001454	0.000089	0.005202
5	0.070657	0.000540	0.007325	0.022126	0.037174	0.995792	0.003340	0.004868	0.002867	0.000289	0.026790
6	0.004326	0.000088	0.000459	0.001056	0.000922	0.003621	0.999995	0.006325	0.001932	0.000948	0.005912
7	0.003988	0.000189	0.000641	0.000956	0.001850	0.002923	0.005616	0.977168	0.210735	0.014529	0.010616
8	0.005081	0.000081	0.000535	0.001166	0.001351	0.003599	0.003087	0.209951	0.977484	0.004037	0.014132
9	0.001072	0.000063	0.000019	0.000217	0.000123	0.000701	0.001034	0.013393	0.007108	1.000054	0.003592
10	0.063872	0.000271	0.004576	0.014123	0.004719	0.038493	0.006513	0.012091	0.011550	0.004126	0.991185

Figures. Page.

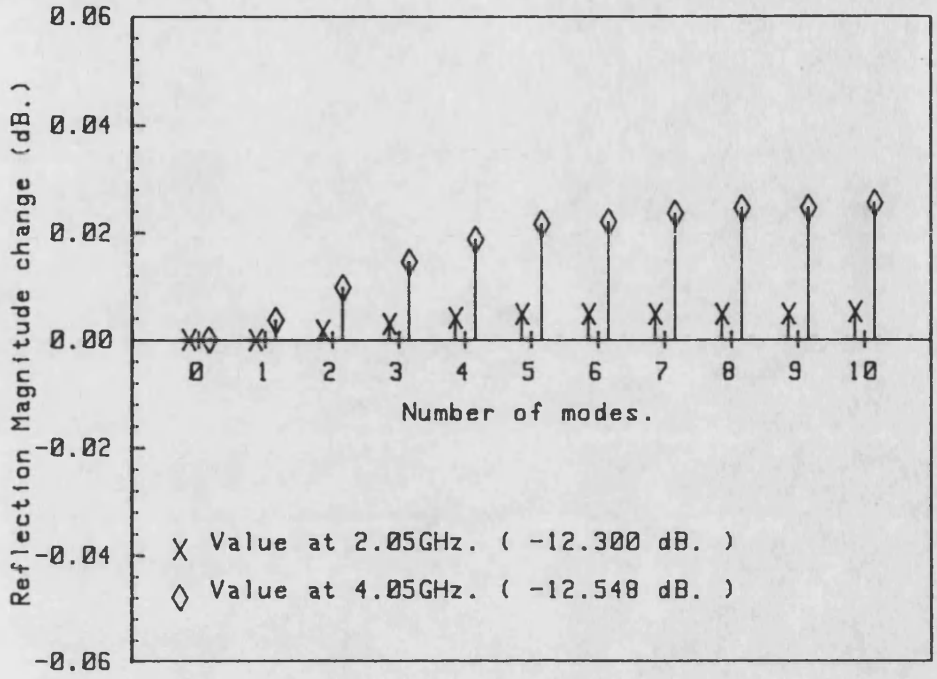

as = 34.000 mm.
ha = 30.825 mm. ea = 1.015
hs = 3.175 mm. es = 2.350
Impedance step 3.2mm./7.8mm.

Magnitude of reflection parameter determined by mode matching technique.

Fig.(5.1)

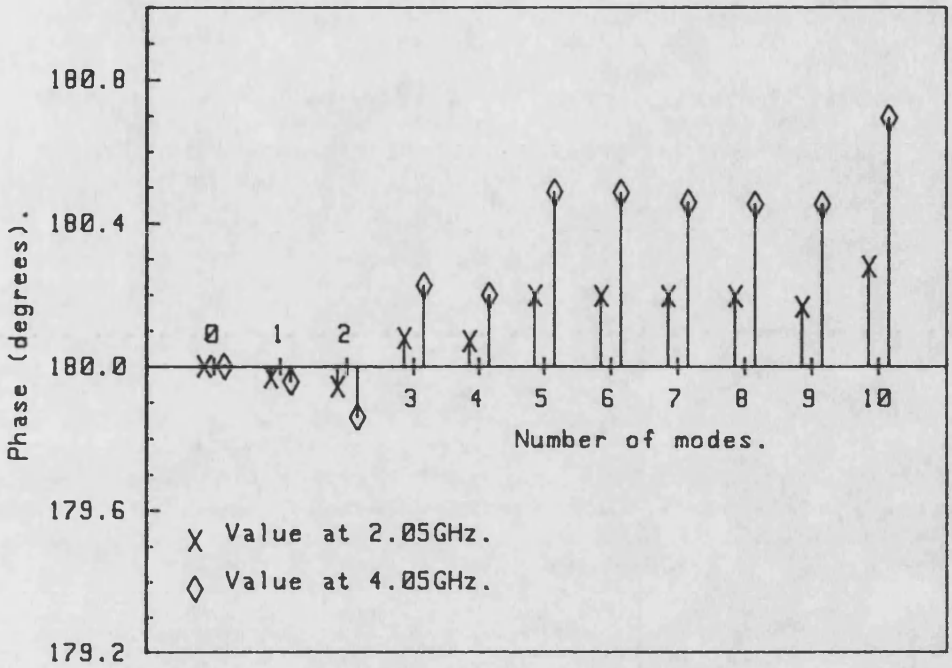

as = 34.000 mm.
ha = 30.825 mm. ea = 1.015
hs = 3.175 mm. es = 2.350
Impedance step 3.2mm./7.8mm.

Phase of reflection parameter determined by mode matching technique.

Fig.(5.2)

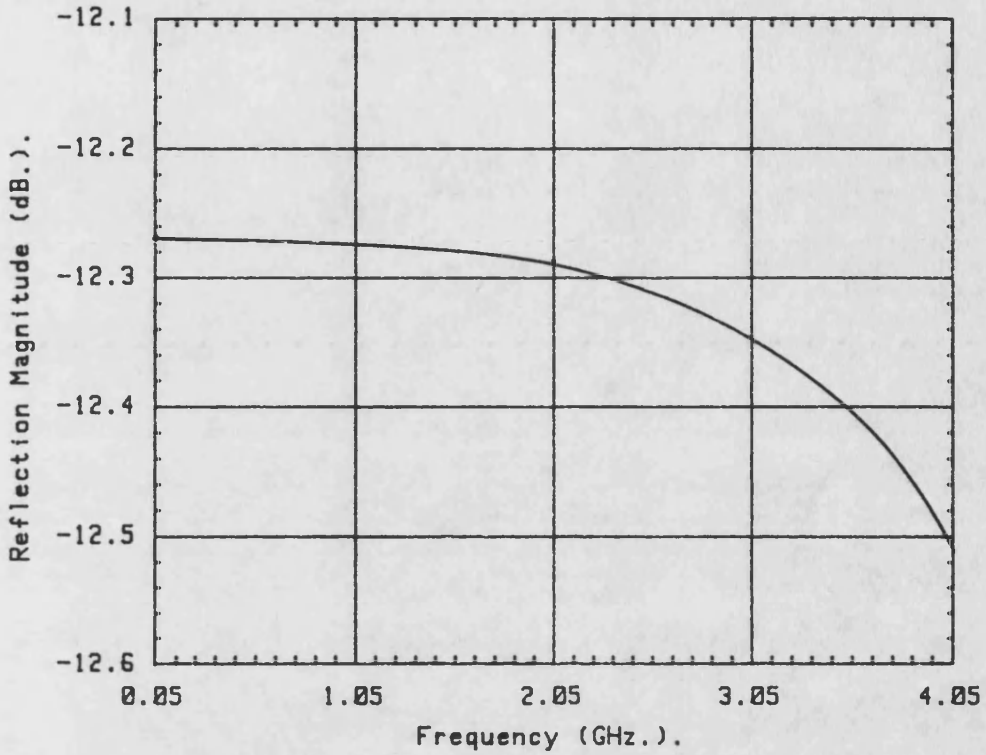

as = 34.000 mm.
ha = 30.825 mm. ea = 1.015
hs = 3.175 mm. es = 2.330
Impedance Step 7.8mm./3.2mm.

Theoretical magnitude of the shielded microstrip impedance step.

Fig.(5.3)

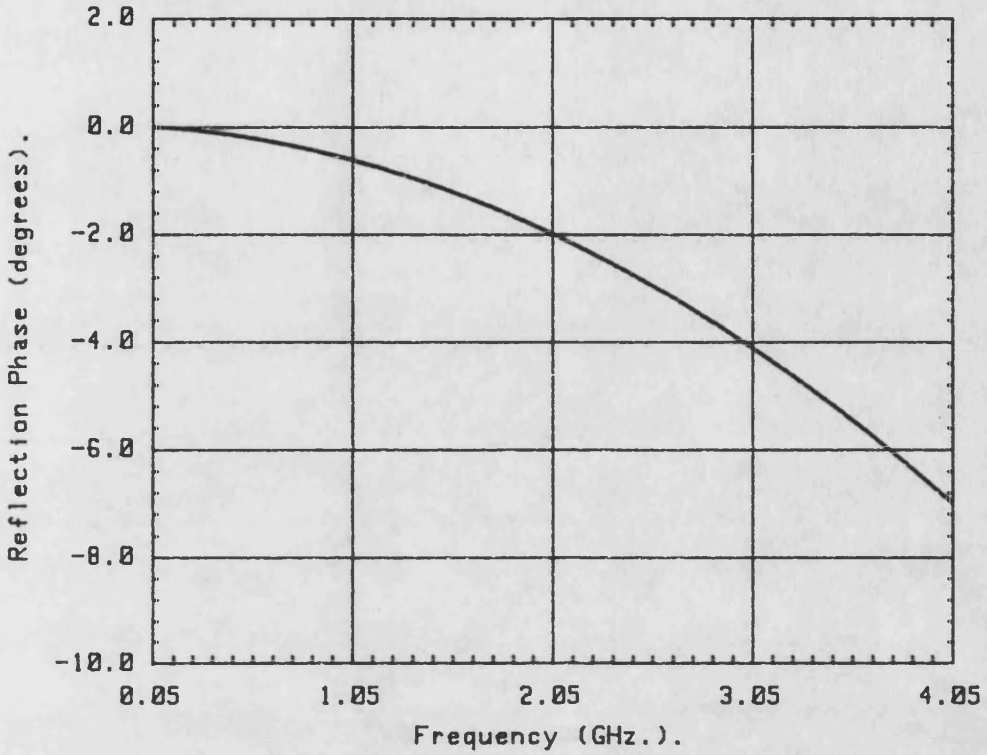

as = 34.000 mm.
ha = 30.825 mm. ea = 1.015
hs = 3.175 mm. es = 2.330
Impedance Step 7.8mm./3.2mm.

Theoretical phase response of the shielded microstrip impedance step.

Fig.(5.4)

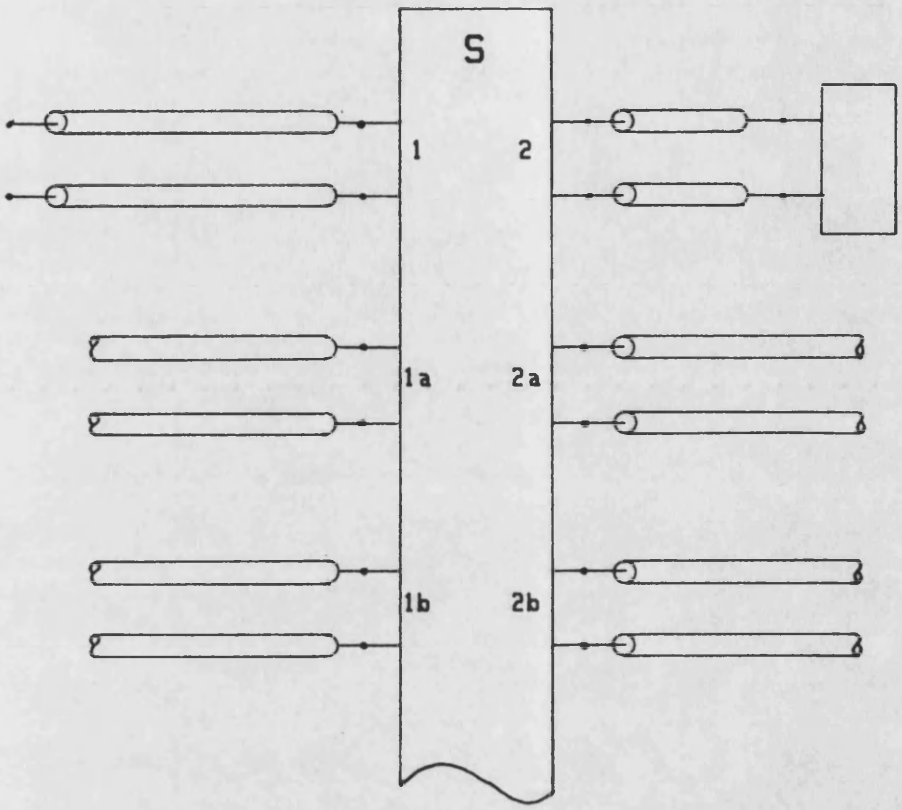

Scattering parameter model of shielded microstrip step discontinuity.

Fig.(5.5)

CHAPTER SIX

ADVANCED EXPERIMENTAL TECHNIQUES

Although considerable attention has been paid to the theoretical analysis of the microstrip step discontinuity, the experimental characterisation of this structure has lagged behind. Chu & Itoh, for example, have given the theoretical results for a cascaded and an offset step [1], however, experimental comparison has only been made for the case of the cascaded step and even then only the magnitude of the reflection coefficient has been considered.

The main problems with experimental techniques are first the need to de-embed the data to account for change in reference planes and secondly, the need for calibration to eliminate systematic errors arising from non-ideal connections etc.. Calibration for experimental work is exactly the same as for the theoretical technique presented for the variational method (see chapter 5). Experimental use of this technique for microwaves dates back to 1968 [2],[3]. All of the original work was developed for measurement equipment having coaxial connections (ports) for which suitable calibration standards, which are required to characterise the unknowns of the measurement equipment, are readily available and, further, connectors of the coaxial lines can be manufactured to a high degree of tolerance making their electrical properties almost identical.

For microstrip, no such calibration standards exist. In particular, it is difficult to achieve a matched load over a wide bandwidth, as a consequence of the dispersive nature of microstrip. Other standards commonly used are the short and open circuits, however, if these are not available it is possible to characterise approximations to them which may be used instead (see chapter 4).

Techniques have been developed to use whatever standards are available, for example Scalzi [4] has used offset short circuits in a similar way to the waveguide calibration [5]. Recently, Dunleavy & Katehi [6] have used through-short-delay (TSD) to characterise the effects of microstrip gaps and coupled-line filters.

The scope of this section will be to cover the investigation of calibration techniques for microstrip starting with a brief review of the basic principles involved and a simulation is used to demonstrate the technique. The availability of suitable short and open circuits which may be characterised using the methods of chapter 4 is assumed. The existence of a matched terminal load which is of paramount importance to the technique is not taken for granted and a method based on time domain analysis is proposed to overcome this problem. This technique is quite general and may be used for other forms of transmission lines for which the dispersion of the fundamental mode is low so that pulses may propagate along the line without being significantly 'spread out'. To check the validity of this approach a calibration of a theoretical model closely related to the actual microstrip step has been simulated using a standard circuit modelling program and data from this and the simulated calibration standards is used. The results, although showing deviation from the theoretical data at the higher frequencies, do enhance the measurements. A similar approach has been recently reported by Gronau & Wolff [7].

Finally, the effect of connector repeatabilty is investigated leading to the choice of the calibration method adopted. Having done this it is found that the main stumbling block to the accuracy of the technique remains the connectors although results are presented for the reflection coefficients of a shielded microstrip impedance step which agree largely with the theoretical results presented earlier.

6.1 Principles of Calibration.

Given any practical piece of measurement equipment it is necessary to calibrate to enable the elimination of systemtic errors that may exist so that, when it is used in practice, any readings taken may be adjusted to give a true representation of the parameters of the device under test (DUT). It is advantageous to assume that the equipment may be separated into two; the first part being an ideal measurement instrument and the second part being an arbitrarily defined 'error' network. The theory of calibration is thus mainly concerned with the best way in which the elements of this network may be found.

For the experimental network arrangement of fig.(6.1) it is thus necessary to determine the scattering parameters of the error network. To do this readings are taken when different loads are connected to its port. The reading 'R' of the automatic network analyser (ANA) is then given by:-

$$R = S_{11} + \frac{S_{12}\, S_{21}\, \Gamma}{1 - S_{22}\, \Gamma} \qquad (6.1)$$

First, with a matched terminal load connected having a reflection coefficient '$\Gamma = 0$' the response of the ANA 'R_{load}' is:-

$$R_{load} = S_{11} + \frac{S_{12}\, S_{21}\, 0}{1 - S_{22}\, 0} \qquad (6.2)$$

This gives the first parameter of the network straight away:-

$$S_{11} = R_{load} \qquad (6.3)$$

To determine the other parameters of the network two other independent standards are required. The normal standards for a two

conductor system are the short and open circuits for reasons that will be explained later.

The method of determining the parameters may be investigated assuming non-ideal devices 'Γ_1' & 'Γ_2' having responses R_1 & R_2 respectively:-

$$R_{1,2} = S_{11} + \frac{S_{12} S_{21} \Gamma_{1,2}}{1 - S_{22} \Gamma_{1,2}} \qquad (6.4)$$

The above form a pair of simultaneous equations in the error terms 'S_{22}' & '$S_{12}S_{21}$'. Note that the second expression appears as a product. This expression cannot be separated but this is not a problem since it will always appear in this form. The values of these error terms are given from the above:-

$$S_{22} = \frac{\Gamma_1 [R_2 - S_{11}] - \Gamma_2 [R_1 - S_{11}]}{\Gamma_2 \Gamma_1 [R_2 - R_1]} \qquad (6.5)$$

$$S_{12}S_{21} = \frac{[\Gamma_2 - \Gamma_1] [R_1 - S_{11}] [R_2 - S_{11}]}{\Gamma_2 \Gamma_1 [R_2 - R_1]} \qquad (6.6)$$

using the value already obtained for S_{11}.

Problems may arise in the above if the standards are not ideal, because it is possible that the reflection coefficients could be equal or could at least be so similar that the errors involved in the above equations would become significant. The requirement is thus for maximum phase separation of the standards to ensure that the data input is unique. In particular, care must be taken when using offset short or open circuits due to the change in reflection phase as a function of frequency. Thus the ideal standards are the perfect short circuit and perfect open circuit.

Although the technique of calibration is quite standard it will be demonstrated by considering an example. Although the technique could be demonstrated by considering a passive error circuit the more general case for which the scattering parameters may be independently defined will be considered. This situation arises in the network analyser as a consequence of three separate sources of measurement error: the directivity error which is due to the couplers on the ports, the source match error which is due to non-ideal conectors on the test ports and the reflection signal path tracking error arising from error in the reference signals which are used. Thus these terms may be arbitrarily defined and the following may be simulated using a circuit modelling program; the response of an open circuit, the response of a short circuit and the response of a matched load. These measurements enable the error terms to be evaluated. To demonstrate this a further simulation has been made: the response of a length of transmission line having characteristic impedance Z_{01} terminated in a load of value Z_{01}. Thus using the error terms which have been computed it is possible to calibrate to remove these errors. The readings taken with & without calibration are shown in fig.(6.2) & fig.(6.3). The theoretical response of this step is given simply by:-

$$\Gamma = \frac{Z_{01} - Z_0}{Z_{01} + Z_0} \qquad (6.7)$$

For the given example with '$Z_{01} = 75\Omega$' & '$Z_0 = 50\Omega$' the theoretical response is, therefore:-

$$|\Gamma| = -13.979 \text{ dB.} \qquad (6.8a)$$

$$\arg(\Gamma) = 0 \qquad (6.8b)$$

and clearly the calibrated response is as expected.

6.2 Principles of Time Domain Analysis.

It is imperative that, for the calibration technique presented, there is available a matched terminal load. However, this is not possible for the case of microstrip first because of the dispersive nature of the line giving rise to a frequency dependent Z_0 and secondly because of the hybrid nature of the electromagnetic field which prevents any simple design of attenuator. As a method of overcoming this problem, time domain analysis has been investigated.

The response of any linear network may be expressed in one of two ways; either in the frequency domain given as its response in magnitude and phase to sinusoidal inputs; or in the time domain in terms of its impulse or step response. The two domains are related to each other by the Fourier transform.

Data from the ANA is available for discrete values of frequency. A Fourier series analogy of the above thus enables the response of a periodic set of pulses/steps to be determined by direct numerical computation. It must be noted, that in practice the input is assumed to be bandlimited so that it has only frequency components in the range of operation of the ANA at any one time (this subject is very involved and a more comprehensive discussion may be found in [5]). For a device having discontinuities which are separated by a length of transmission line the response to this set of pulses/steps will be of the form of a group of scaled pulses/steps which may be separated by virtue of the time delay between the discontinuities. By isolating the response for a given discontinuity its frequency response may thus be determined by transforming the data back to the frequency domain. Note that it is only possible to accurately account for the first response in time as subsequent responses also include transmission terms of previous discontinuities.

Note that the example of calibration considered in the previous section may not be handled using the time domain analysis since the error terms need not represent a physically realisable system.

Thus the test circuit of fig.(6.4) has been used. This circuit, which represents the measurement of a microstrip impedance step, uses a simple RCL circuit to model the effect of a coaxial to microstrip transition and a reactive 'T' network to represent the parasitics of the microstrip impedance step.

To calibrate to the plane of the microstrip step it is first necessary to measure the short and open circuits and also the matched terminal load. In this case, however, it is assumed that a matched load is unavailable and it is only possible to use a coaxial load having first used a microstrip to coaxial transition. It is now necessary to use time domain analysis to obtain the data that would have been obtained for an ideal load. The pulse response of this arrangement is shown in fig.(6.5). The first pulse is due to the elements which appear in the error network and the second due to the load mismatch. By 'gating out' this second response the result is an approximation to that which would have been obtained had a matched load been used. Using this data for the calibration instead of that from an ideal terminal load the calibration procedure outlined earlier may be repeated. Using the test circuit with the second microstrip line the effects of the connectors may now be eliminated using the calibration data that has been determined. When measuring the microstrip step, however, it is necessary to use time domain again since there will not be a suitable load for this second microstrip line. The results, shown in fig.(6.6) & fig.(6.7) together with the the theoretical value which may also be determined using the circuit modelling program, show excellent agreement over much of the

frequency range.

As an alternative to the pulse response the time domain analysis may proceed by using the response to a unit step. The time domain response of the approximte load is once again considered and is shown in fig.(6.8). The calibration procedure continues as for the impulse response and the magnitude and phase responses of the microstrip step measured using this technique are shown in fig.(6.9) and fig.(6.10) respectively. It is clear that there is little difference between the techniques using either impulse or step response.

There are many factors which affect the performance of the examples cited above such as the exact time at which the 'gate' starts/stops and also the 'gate' characteristics but in general all of the results become meaningless at the higher frequencies.

6.3 Measurement of the Shielded microstrip step.

It is necessary to design a measurement system that will use to full effect the techniques which have been outlined. This has been done using the experimental rig already used for propagation measurements described in chapter 4.

The initial design investigated, used an in line microstrip calibration to which various devices could then be connected using some form of butt connection and the parameters of the device de-embedded to account for any length of transmission line between the calibrated plane and the plane of the discontinuity. Although calibration of the microstrip line could be achieved using the approximations to the short and open circuits and further using the time domain procedure for the simulation of the matched terminal load the technique is subject to significant errors arising as a consequence of the poor connection between two microstrip lines and hence the measurement of any device. Further, the need to de-embed the data also presented problems.

To overcome these difficulties an alternative method has been proposed. In this method, the calibration is again made to the microstrip plane as above but instead of attempting to connect a device in line, a second longer microstrip test jig was substituted for that for which the calbration was performed with the discontinuity to be characterised appearing at the calibrated plane. This technique is by no means ideal; it does negate the requirement for an in-line connection and any de-embedding but it is clear that the electrical properties of the test jig used for calibration and that used for the measurement would not be identical.

This technique has been used to investigate a 7·8mm./3·2mm. step for the the low permittivity jigs introduced in chapter 4.

The 10cm. jig with a uniform 7·8mm. line is used to obtain the calibration data using the non ideal short and open circuits the effect of which must be included and further since the 7·8mm. line has a Z_0 of approximately 50Ω a coaxial load may be used after first using a coaxial to microstrip transition.

Having obtained sufficient data to be able to calibrate, the 10cm. section is then replaced with the longer 20cm. section which is fitted with the microstrip impedance step which is placed centrally i.e. at the calibrated plane. The second line has a Z_0 of approximately 90Ω and an approximation to a matched termination may be obtained using chip resistors mounted on the microstrip line and the line then grounded. Data for the reflection of the step may then be obtained by calibrating the raw data and then applying the time domain procedure to account for the approximate 90Ω load. Magnitude and phase information of the response determined using this technique is plotted in figs.(6.11) and (6.12) respectively. The main source of error in these results arises from the time domain procedures such that the data is only valid for low frequencies upto about 3.0 GHZ.. Oscillation of the traces arises as a consequence of the difference between the coax. to microstrip transition used for the calibration and that used for the measurement of the step itself. The other major source of measurement error is undoubtedly the difference in the physical location of the reference planes: a difference of 0·1 mm. in the reference planes can give rise to a phase error of 0.35^{0} / GHz..

The procedure used above may be repeated for the reversal of the step this time using the appropriate load as described above for the calibration stage and the measurement of the step. The results for this test are shown in figs.(6.13) and (6.14) for magnitude and phase respectively.

References.

[1]... Chu, T. & Itoh, T.. "Generalized Scattering Matrix Method for Analysis of Cascaded and Offset Microstrip Discontinuities." IEEE Trans. MTT-34, No. 2, February 1986, pp. 280-284.

[2]... Hackborn. "An Automatic Network Analyser System." Microwave Journal, Vol.11, May 1968, pp. 45-52.

[3]... Kruppa, W. & Sodomsky, K.F.. "An Explicit Solution for the Scattering Parameters of a Linear Two-Port Measured with an Imperfect Test Set." IEEE Trans. MTT-19, No. 1, January 1971, pp. 122-123.

[4]... Scalzi, G.. "Network Analyser Calibration Using Offset Shorts." IEEE Trans. MTT-36, No. 6, June 1988, pp. 1097-1100.

[5]... "Instrument training manual for HP8510." Hewlett Packard.

[6]... Dunleavy, L.P. & Katehi, P.B.. "Shielding Effects in Microstrip Discontinuities." IEEE Trans. MTT-36, No.12, December 1988, pp. 1767-1774.

[7]... Gronau, G. & Wolff, I.. "A Simple Broad-Band Device De-embedding Method Using an Automatic Network Analyser with Time-Domain Option." IEEE Trans. MTT-37, No. 3, March 1989, pp. 479-483.

Figures. Page.

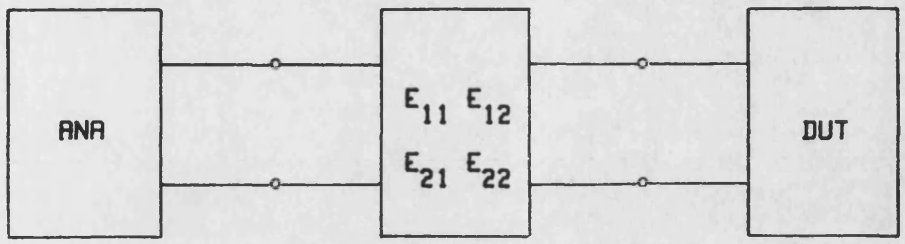

E_{11} E_{12} } Scattering Parametrs of
E_{21} E_{22} } Representative error network.

ANA Automatic Network Analyser.

DUT Device Under Test.

Schematic representation of microwave measurement system (one port).

Fig.(6.1)

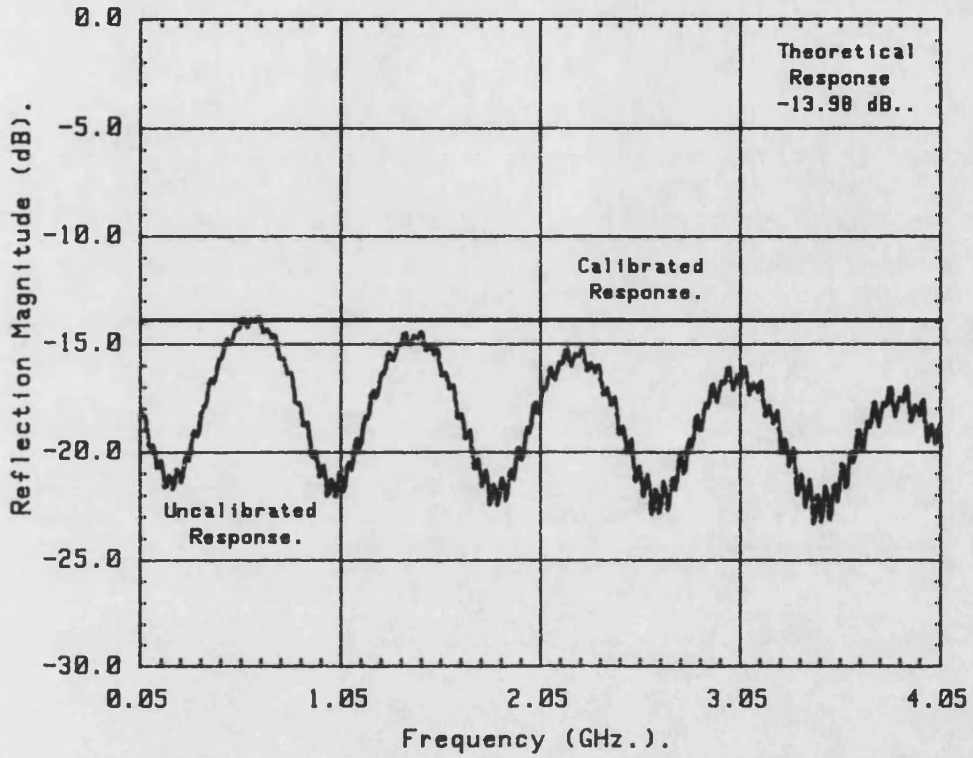

Effect of calibration on the 50/75 Ohm impedance step.

Fig.(6.2)

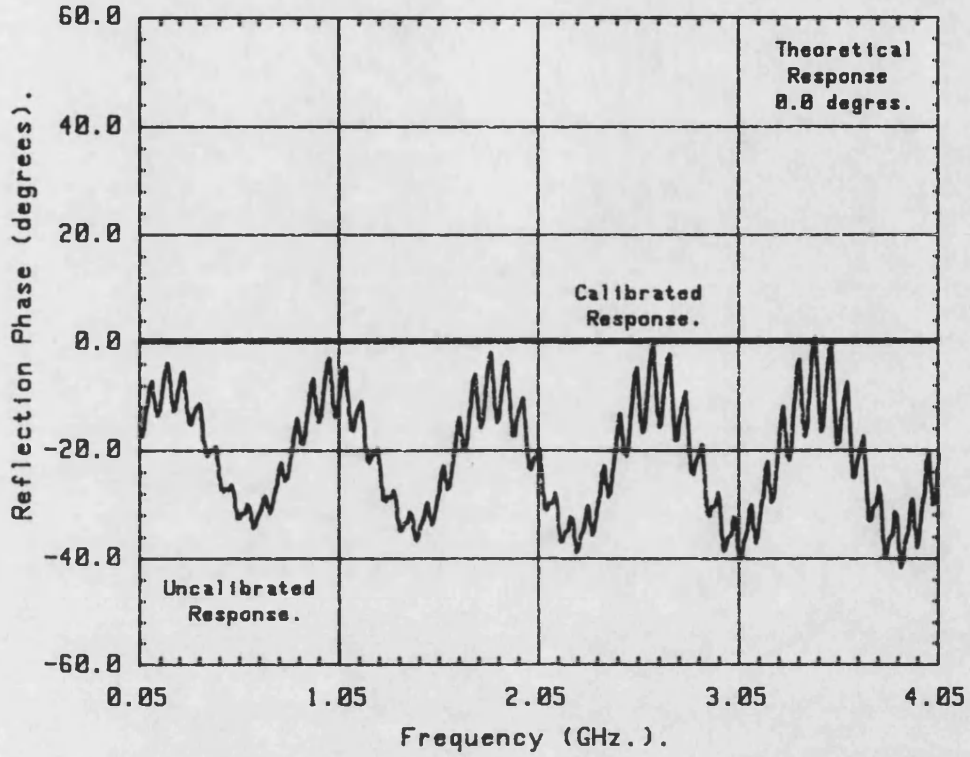

Effect of calibration on the 50/75 Ohm impedance step (Phase Response).

Fig.(6.3)

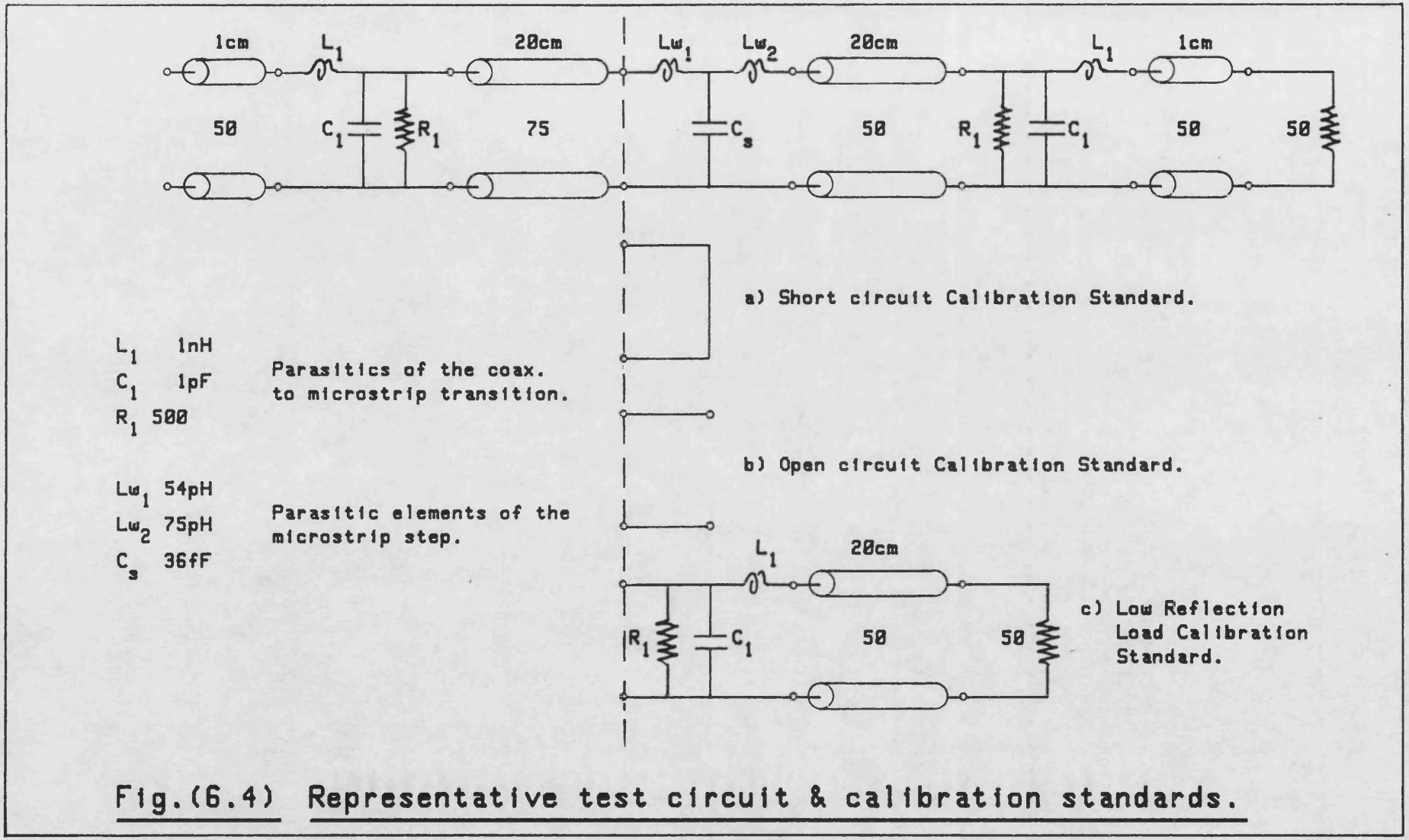

Fig.(6.4) Representative test circuit & calibration standards.

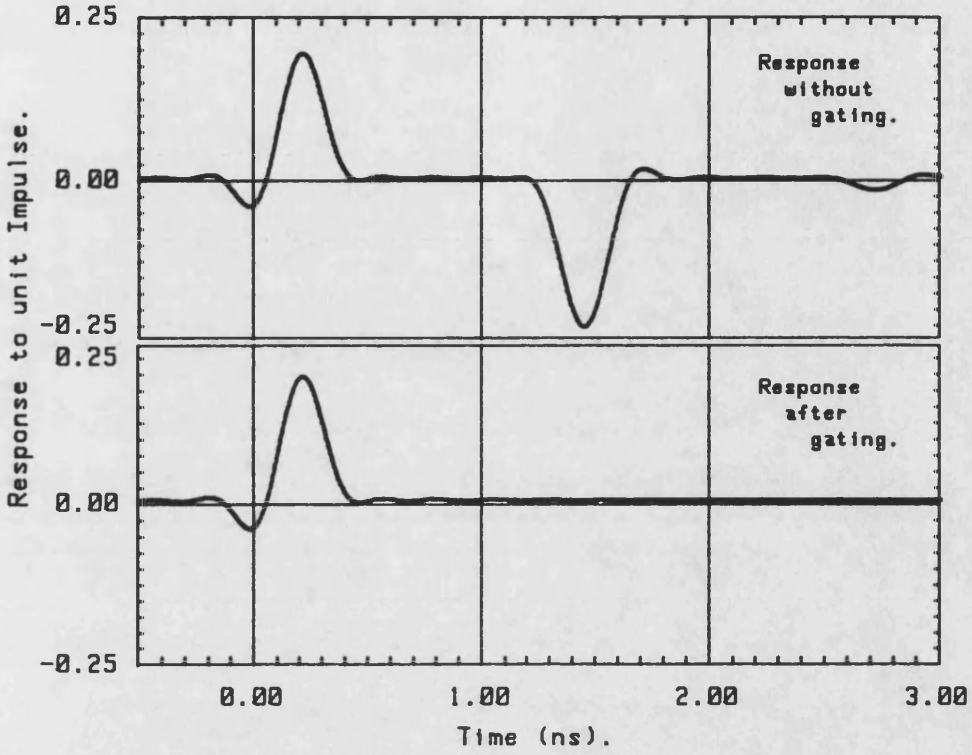

Time Domain - Impulse Response.

Simulated impedance step
as in Fig.(6.4).

Impulse response of the simulated test section with/without gating.

Fig.(6.5)

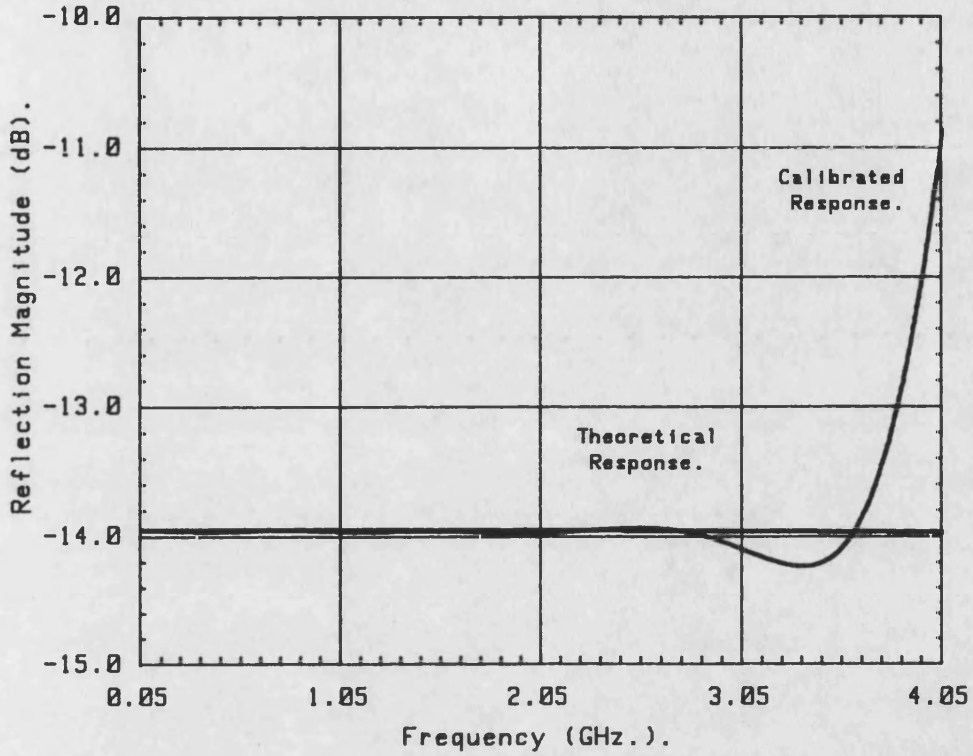

Time Domain - Impulse Response.

Simulated impedance step
as in Fig.(6.4).

Magnitude of the simulated impedance step using time domain calibration.

Fig.(6.6)

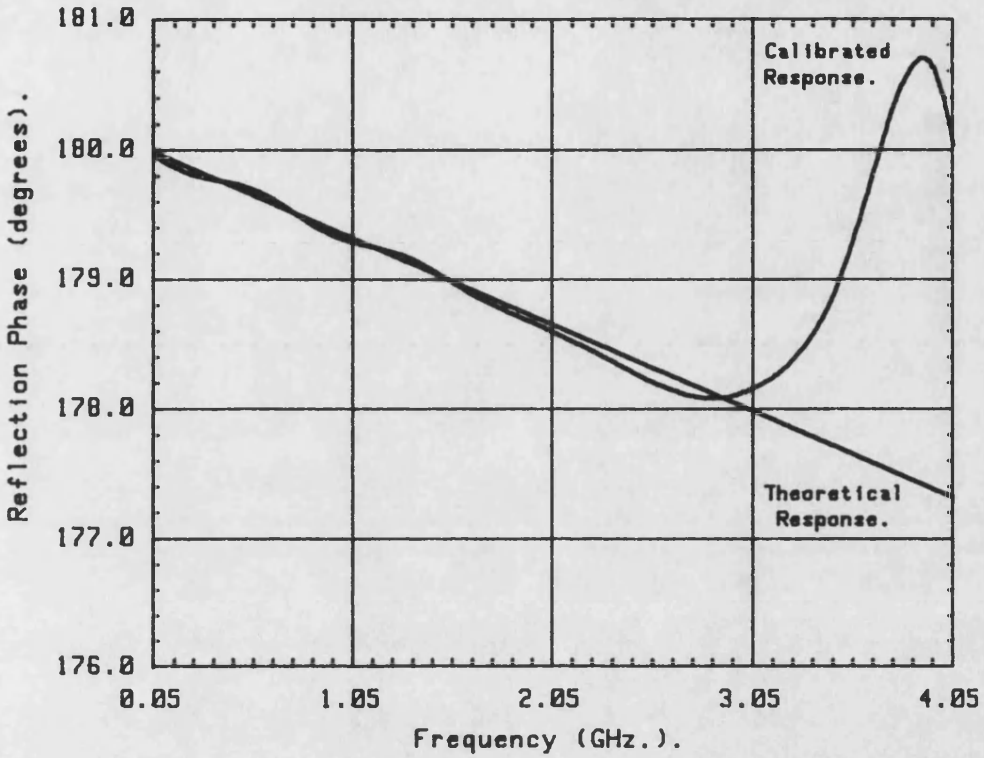

Time Domain - Impulse Response.

Simulated impedance step
as in Fig.(6.4).

Phase of the simulated impedance step using time domain calibration.

Fig.(6.7)

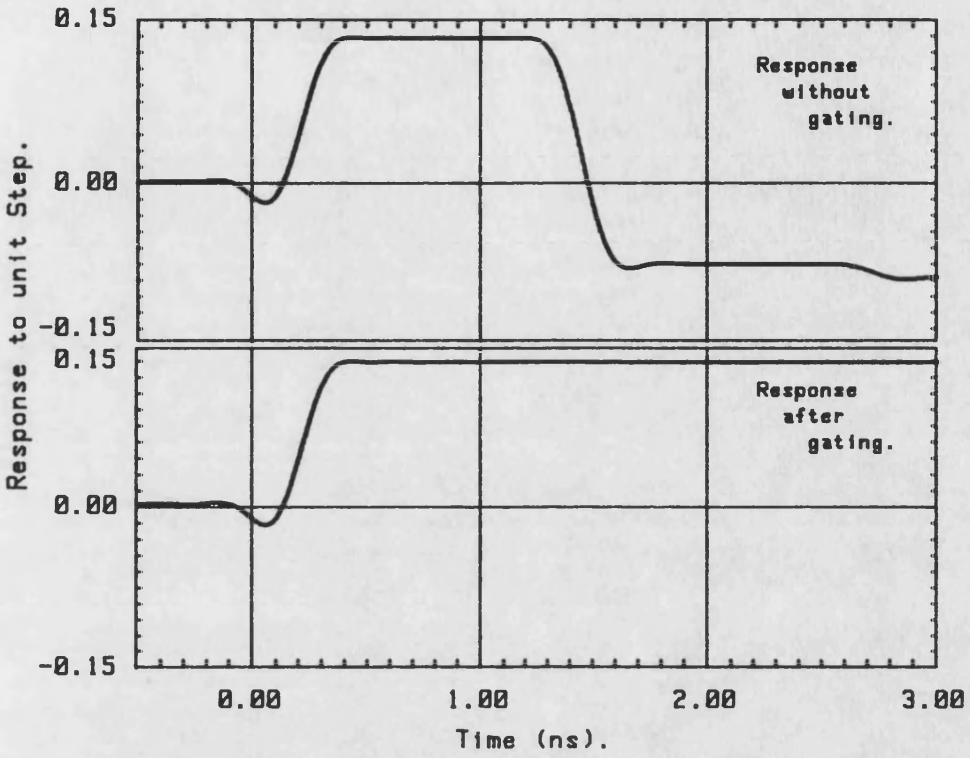

Time Domain - Step Response.

Simulated impedance step
as in Fig.(6.4).

Step response of the simulated test section with/without gating.

Fig.(6.8)

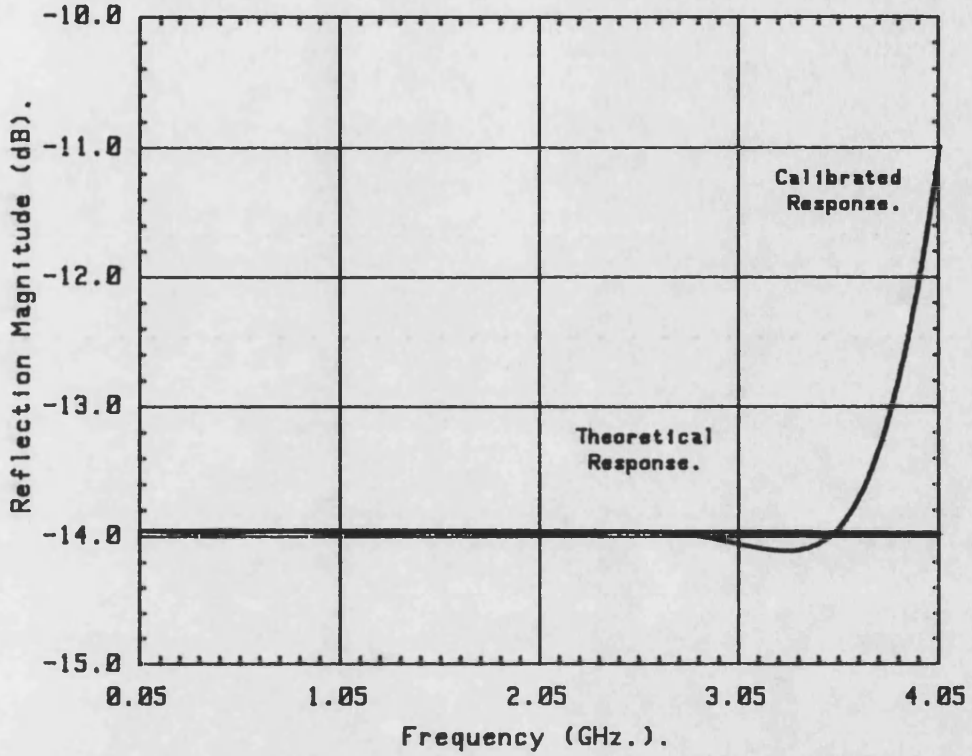

Time Domain - Step Response.

Simulated impedance step
as in Fig.(6.4).

Magnitude of the simulated impedance step using time domain calibration.

Fig.(6.9)

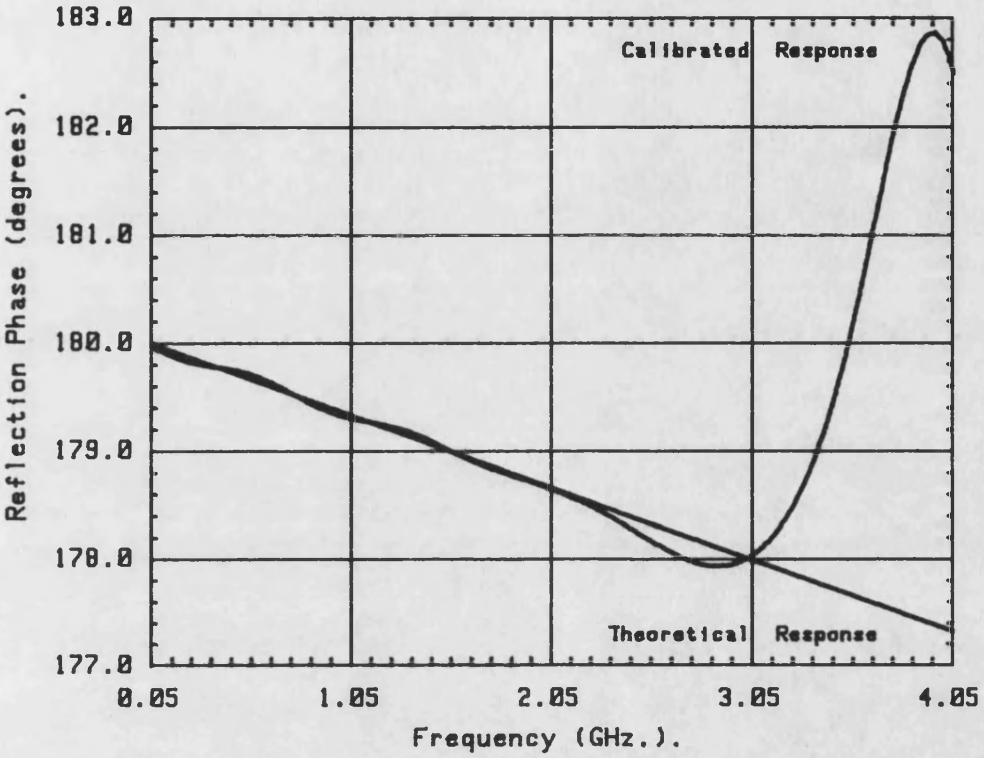

Time Domain - Step Response.

Simulated impedance step
as in Fig.(6.4).

Phase of the simulated impedance step using time domain calibration.

Fig.(6.10)

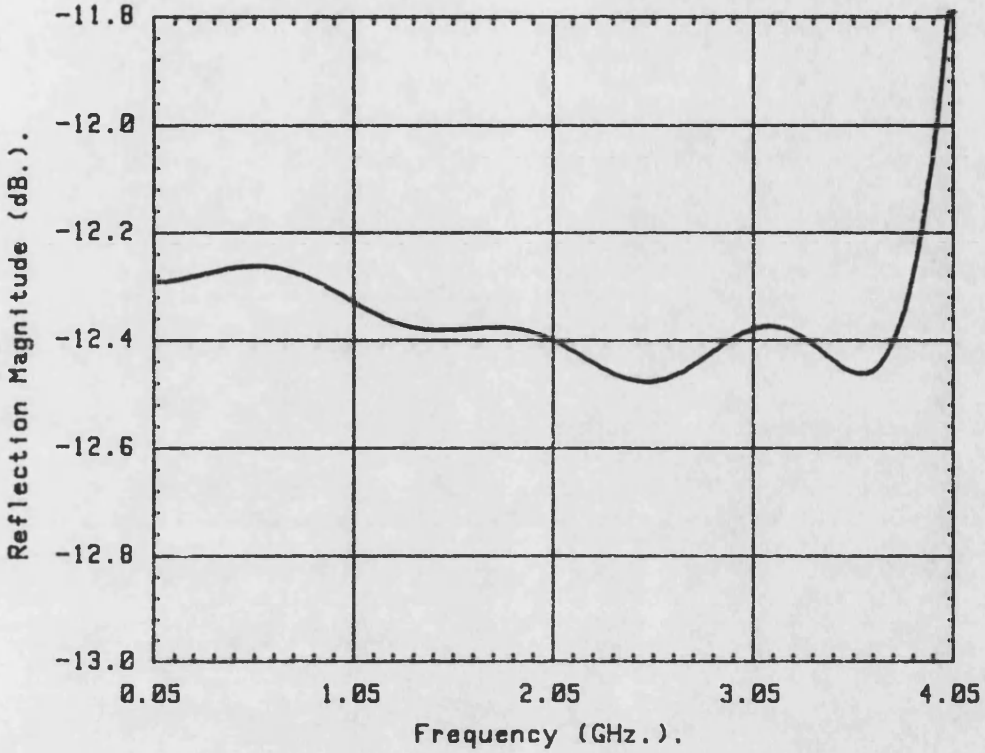

as = 34.000 mm.
ha = 30.825 mm. ea = 1.015
hs = 3.175 mm. es = 2.330
Impedance Step 7.8mm./3.2mm.

Experimental results for reflection magnitude of microstrip step in width.

Fig.(6.11)

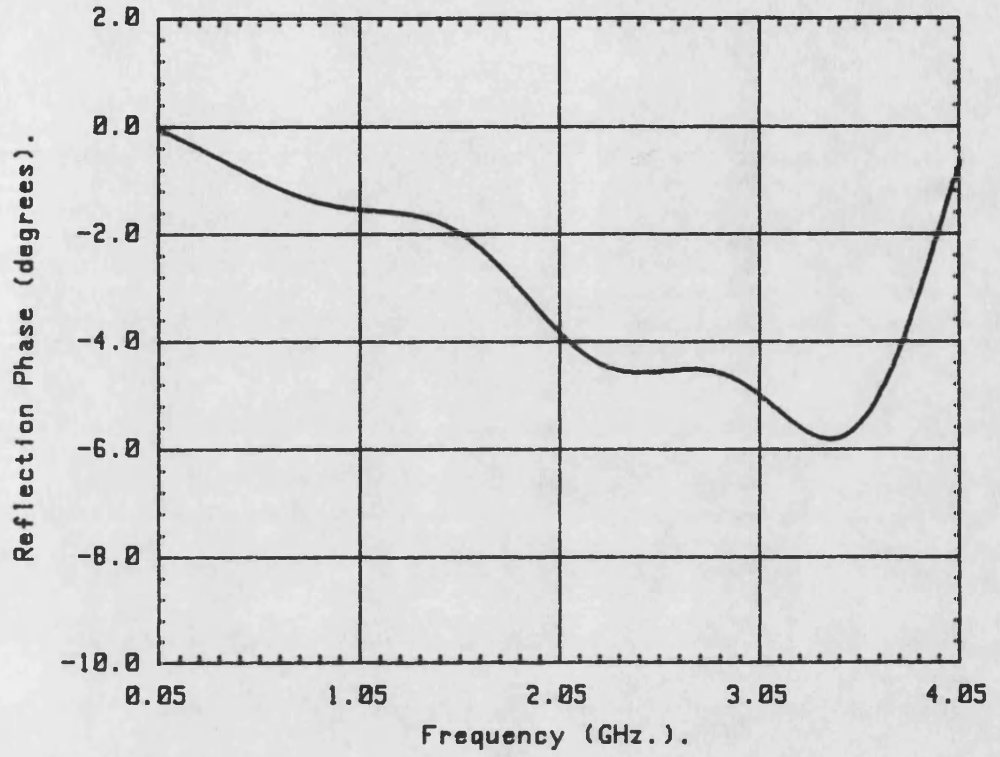

as = 34.000 mm.
ha = 30.825 mm. ea = 1.015
hs = 3.175 mm. es = 2.330
Impedance Step 7.8mm./3.2mm.

Experimental results for reflection phase of microstrip step in width.

Fig.(6.12)

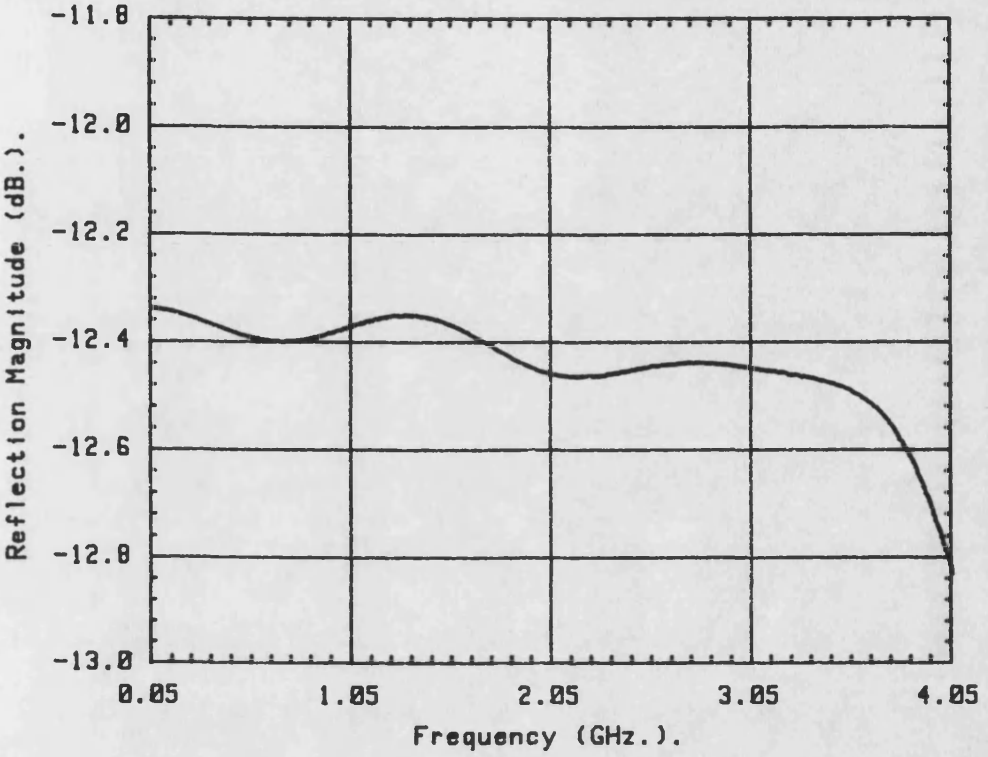

as = 34.000 mm.
ha = 30.825 mm. ea = 1.015
hs = 3.175 mm. es = 2.330
Impedance Step 3.2mm./7.8mm.

Experimental results for reflection magnitude of microstrip step in width.

Fig.(6.13)

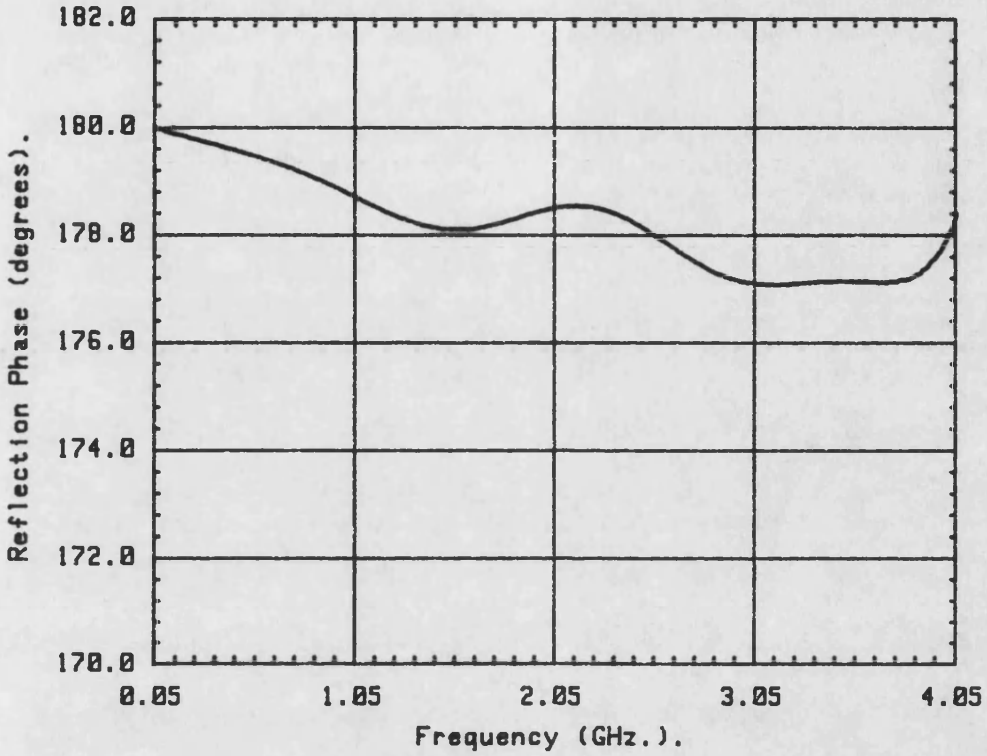

as = 34.000 mm.
ha = 30.825 mm. ea = 1.015
hs = 3.175 mm. es = 2.330
Impedance Step 3.2mm./7.8mm.

Experimental results for reflection phase of microstrip step in width.

Fig.(6.14)

CONCLUSIONS

The parameters of the continuous shielded microstrip transmission line have been determined by a variational technique and results have been verified by comparison with other theoretical work and experiments. The variational technique has been shown to be equivalent to the extensively used Galerkin's method although the new technique gives greater physical insight into properties of the higher order modes. The analysis has been extended to cover both symmetric twin strips and further the effect of using dielectric overlay has been investigated and extensive results have been presented. Although finite strip thickness has not been discussed a simple method for inclusion of loss arising as a consequence of finite conductivity in the microstrip may be achieved directly by considering the equivalent TE and TM transmission line models which have already been used to great effect for considering the effects of dielectric overlay.

For the discontinuity analysis, a variational technique has been investigated which is easily programmable albeit numerically laborious. The presented data shows considerable deviation from the static results for the step discontinuity which is in keeping with other publised data. New experimental techniques have been developed, checked using simulated data and then applied to the shielded microstrip step. These experimental techniques may be readily applied to other types of discontinuity and other forms of transmission line provided that the restrictions which have been discussed in the relevant sections are not violated.

The theoretical techniques presented have, it has to be said, been largely inconclusive. Whilst it is clear that the techniques are

reliable in themselves it seems clear that the application to the shielded microstrip step in width suffers from the absence of a closed form expression for the higher order modes whilst convergence of the finite sums which must therefore be considered is in general very poor. Further, the need to identify these modes alone raises serious questions on the practicality of any technique requiring the evaluation of large numbers of higher order modes.

It would be interesting to see the variational method presented in this thesis applied to the equivalent magnetic wall waveguide model which would be a compromise between accuracy and practicality with the potential of being sufficiently compact to be incorporated into computer aided design software.

31st July '89.